

UNIVERSITY  
OF MICHIGAN

JAN 26 1954

ENGINEERING  
LIBRARY

THE QUARTERLY JOURNAL OF  
MECHANICS AND  
APPLIED  
MATHEMATICS

VOLUME VI PART 4

DECEMBER 1953

OXFORD  
AT THE CLARENDON PRESS  
1953

*Price 15s. net*

PRINTED IN GREAT BRITAIN BY CHARLES BATEY AT THE UNIVERSITY PRESS, OXFORD

# THE QUARTERLY JOURNAL OF MECHANICS AND APPLIED MATHEMATICS

## Editorial Board

S. GOLDSTEIN  
G. I. TAYLOR

R. V. SOUTHWELL  
G. TEMPLE

together with

A. C. AITKEN  
S. CHAPMAN  
A. R. COLLAR  
T. G. COWLING  
C. G. DARWIN  
W. J. DUNCAN  
A. E. GREEN  
A. A. HALL  
D. R. HARTREE  
L. HOWARTH  
WILLIS JACKSON

J. R. WOMERSLEY

H. JEFFREYS  
J. E. LENNARD-JONES  
M. J. LIGHTHILL  
G. C. MCWITTIE  
N. F. MOTT  
W. G. PENNEY  
A. G. PUGSLEY  
L. ROSENHEAD  
O. G. SUTTON  
ALEXANDER THOM  
A. H. WILSON

## Executive Editors

V. C. A. FERRARO

D. M. A. LEGGETT

THE QUARTERLY JOURNAL OF MECHANICS AND APPLIED MATHEMATICS is published at 15s. net for a single number with an annual subscription (for four numbers) of 50s. post free.

## NOTICE TO CONTRIBUTORS

1. *Communication.* Papers should be communicated to one or other of the Executive Editors, by name, at King's College, Strand, London, W.C. 2.
2. *Presentation.* Manuscripts should preferably be typewritten, and each paper should be preceded by a summary not exceeding 300 words in length. References to literature should be given in standard order, *author, title of journal, volume number, date, page.* These should be placed at the end of the paper and arranged according to the order of reference in the paper.
3. *Diagrams.* The number of diagrams should be kept to the minimum consistent with clarity. The lines of the figures should be drawn in ink either on draughtsman's paper or on good quality white paper. Each individual line in the figure should bear reducing to one-half of the size of the original, and great care should be exercised to see that the lines are regular in thickness, especially where they meet. Lettering of the figure should be in pencil and should be sufficient to define clearly the lines and curves in it. The writing of formulae or of explanations on the diagram itself should be avoided. All explanations of symbols, etc., should be given in underline. Contributors should indicate on their manuscripts where figures should be inserted.
4. *Tables.* Tables should preferably be arranged so that they can be printed with the columns parallel to the longer edge of the page.
5. *Notation.* All single letters used to denote vectors in the manuscript should be marked by underlining with a wavy line. Scalar and vector products should be denoted by  $\underline{a} \cdot \underline{b}$  and  $\underline{a} \wedge \underline{b}$  respectively. Real and imaginary parts of complex quantities should be denoted by  $\text{re}$  and  $\text{im}$  respectively.
6. *Offprints.* Authors of papers will be entitled to 25 free offprints. This number is available for sharing between authors of joint papers.
7. All correspondence other than that dealing with contributions should be addressed to the Publisher:

GEOFFREY CUMBERLEGE  
OXFORD UNIVERSITY PRESS  
AMEN HOUSE, LONDON, E.C. 4

ICS

s is  
for

ive

uld  
ure  
ge.  
of

ith  
er  
ng  
he  
ld  
he  
All  
ld

ne

be  
d  
d

is  
d

For  
theor  
gener  
tend  
for a  
which  
by cl

1. In  
THE  
theor  
witho  
in sp  
is sat  
with  
‘two-  
poten  
infini  
is of  
case,

If i  
v to b

for so  
howe

† A  
 $g(r, \theta, \dots)$

‡ W  
to any

[Qua  
5092.

# A NOTE ON UNIQUENESS PROOFS FOR BOUNDARY- VALUE PROBLEMS IN POTENTIAL THEORY AND STEADY HEAT CONDUCTION

By M. E. RAYNER (*Westfield College, London*)

[Received 22 May 1952]

## SUMMARY

For boundary-value problems in an infinite region in two-dimensional potential theory and steady heat conduction, the logarithmic singularities of solutions, in general, prevent our proving uniqueness. If, however, we allow the boundary to tend to infinity in two directions, and consider the problem in a semi-infinite region, for a very wide class of boundary conditions, we can find additional information which enables us to prove uniqueness (except possibly for an arbitrary constant) by classical methods.

## 1. Introduction

The classical uniqueness proof for boundary-value problems in potential theory is based on the Green identity (1). The argument can be applied without difficulty to finite regions, and it can be extended to infinite regions in space provided that the potential is regular at infinity.<sup>†</sup> This condition is satisfied for fields due to point sources, but it fails to be satisfied for fields with plane symmetry due to line sources, which give rise to problems of 'two-dimensional' potential theory. For these problems the elementary potential is of the form  $A \log r$ , and thus tends to infinity as  $r$  tends to infinity, while in the three-dimensional problem the elementary potential is of the form  $A/r$ , and thus tends to zero as  $r$  tends to infinity. In either case, the constant  $A$  is determined by the source strength.

If in the two-dimensional case, at large distances, we subject the potential  $v$  to be of the form

$$v = A \log r + f(\theta) + g(r, \theta)$$

for some undetermined constant  $A$  and functions  $f(\theta)$  and  $g(r, \theta)$ , where, however,  $g(r, \theta)$  is regular at infinity, and prescribe either

- (i) its value,
- (ii) the value of  $\frac{\partial}{\partial n} v$ ,
- (iii) the value of  $\frac{\partial}{\partial n} v + hv \quad (h > 0)$

<sup>†</sup> A function  $g(r, \theta, \dots)$ , where all the  $\theta$ 's are angles, is said to be regular at infinity if  $g(r, \theta, \dots) = O(1/r)$ , and  $(\partial/\partial r)g(r, \theta, \dots) = O(1/r^2)$  as  $r \rightarrow \infty$ .

<sup>‡</sup> We adopt the convention that  $\partial/\partial n$  denotes differentiation along the outward normal to any region.

on a closed curve  $C$ , this being the interior boundary of an infinite region, then in cases (i) and (iii)  $v$  is not always uniquely determined. In fact, suppose that  $C$  is the circle  $r = 1$ , and that  $v^*$ , supposed to be the difference between two solutions with prescribed values on  $C$ , is given by  $v^* = \log r$ . Then  $v^* = 0$  on  $C$ , and satisfies the condition at infinity, but it does not vanish identically. Hence the first boundary-value problem is not unique. Again, suppose that  $C$  is the circle  $r = a$ , where  $a (> 1)$  is the unique solution of the equation

$$a \log a = 1/h,$$

and let  $v^* = \log r$ . Then

$$\frac{\partial}{\partial n} v^* + h v^* = -1/r + h \log r$$

vanishes for  $r = a$ , but it does not vanish identically, and hence the third boundary-value problem is not unique.

In case (ii) the proof of the uniqueness of  $v$  requires an additional argument involving Gauss's theorem. It should be noted that the appeal to this theorem is not necessary in the corresponding three-dimensional uniqueness proof.

In a similar manner it may be shown that the boundary-value problem for composite regions separated by a closed curve, such as the case of two dielectrics, or that of steady heat flow in two media with or without contact resistance at the boundary, have unique solutions except for arbitrary constants.

This note is primarily concerned with the uniqueness proof for semi-infinite regions. The question seems to deserve some attention for two reasons. First, despite what has been said above, uniqueness (except possibly for an arbitrary constant) can be proved for semi-infinite regions for all the usual boundary conditions. Secondly, in the literature on potential theory, a uniqueness proof for semi-infinite regions is usually omitted,† although one of the simplest examples for which the boundary-value problem can be solved analytically is the half-plane bounded by a straight line. I believe that the present note therefore fills a gap.

In addition, the proof provides information about the total source strength of the so-called 'image systems' for general semi-infinite regions. This information is also of interest in the three-dimensional problem, although in this case it is not required for the uniqueness proof.

We first treat the very simple cases of the first and second boundary-value problems, which are closely related to the image methods of electrical conductor problems and hydrodynamical problems of irrotational flow of an

† But see, however, H. and B. S. Jeffreys, *Methods of Mathematical Physics* (Cambridge, 1950), section 6.074.

inviscid fluid. Afterwards we deal with the rather general problem of steady heat flow in a composite region with contact resistance. The proof of the uniqueness of the solution of the third boundary-value problem or the dielectric case can be constructed on similar lines.

## 2. Notation

We shall suppose throughout that the whole plane is divided into two semi-infinite regions  $G_1$  and  $G_2$  by a regular curve  $\Gamma$  which goes to infinity in two directions.<sup>†</sup> If  $O$  is any point in  $G_1$ , and  $P_1$  and  $P_2$  are points on  $\Gamma$ , let  $\omega$  be the angle  $P_1OP_2$ . As  $P_1$  and  $P_2$  go to infinity in different directions, suppose the limit of the angle  $\omega$  is  $\omega_2$ . Then  $\omega_1 = 2\pi - \omega_2$ .

## 3. First boundary-value problem

Suppose  $v'$  and  $v''$  are two solutions of Laplace's equation in  $G_1$ , which assume a given value on  $\Gamma$ . We will suppose that, at large distances,  $v'$  and  $v''$  are of the form  $A'\log r + f'(\theta) + g'(r, \theta)$  and  $A''\log r + f''(\theta) + g''(r, \theta)$ , respectively, where  $g'(r, \theta)$  and  $g''(r, \theta)$  are regular at infinity. Then  $v' - v'' = 0$  on  $\Gamma$ , so that as  $r \rightarrow \infty$  on  $\Gamma$ ,

$$(A' - A'')\log r + (f'(\theta) - f''(\theta)) = O(1/r).$$

Therefore  $A' = A''$ . Thus any two solutions can differ only by a term which is  $O(1)$  as  $r \rightarrow \infty$ , and by the classical uniqueness theorem it can be shown that these solutions can, in fact, differ only by a constant; but since the solutions take prescribed values on  $\Gamma$ , the solutions are identical, and so the first boundary-value problem has a unique solution.

We can look at this problem in a slightly different way. Suppose that there is an electric field with potential  $v_0$  due to charges which are all in a finite sub-region of  $G_1$ . If we now introduce a conducting, infinitely long sheet along  $\Gamma$ , how will the field be altered? If the perturbing potential is  $u$ , then the modified potential is  $v_0 + u$  and so  $u = -v_0$  on  $\Gamma$ , from which it follows that for large values of  $r$ ,  $u = -A_0\log r + O(1)$  if  $v_0 = A_0\log r + O(1)$  as  $r \rightarrow \infty$ . If we now interpret the perturbing potential  $u$  as due to a system of image sources situated in  $G_2$ , we have the result that the algebraic sum of these sources is equal in magnitude but opposite in sign to the sum of the sources of  $v_0$ .

It is evident, by the same argument, that this result also holds in three dimensions, where all the sources of  $v_0$  lie to one side of an infinite open regular surface.

<sup>†</sup> Thus excluding, for instance, the case of the curve formed by the two spirals  $r = \theta$  and  $r = \theta + \alpha$ , where  $0 < \alpha < 2\pi$ .

#### 4. Second boundary-value problem

Suppose that the normal derivative of the potential is prescribed on  $\Gamma$ , and that  $v'$  and  $v''$  are two solutions of Laplace's equation in  $G_1$ , which at large distances behave like

$$A' \log r + f'(\theta) + g'(r, \theta) \quad \text{and} \quad A'' \log r + f''(\theta) + g''(r, \theta)$$

respectively. It is assumed that in  $G_1$ ,  $g'(r, \theta)$  and  $g''(r, \theta)$  are regular at infinity.

By Gauss's theorem,

$$\int_{\Gamma(R)} \frac{\partial}{\partial n} (v' - v'') ds + \int_{S_1(R)} \frac{\partial}{\partial n} (v' - v'') ds = 0, \quad (1)$$

where  $S_1(R)$  is the arc in  $G_1$  of a circle  $S(R)$ , radius  $R$ , and  $\Gamma(R)$  is the finite arc cut by  $S(R)$ .

Then as  $R \rightarrow \infty$ , since  $(\partial/\partial n)(v' - v'') = 0$  on  $\Gamma$ , from (1),

$$\omega_1(A' - A'') \rightarrow 0,$$

i.e.

$$A' = A''.$$

With this information the solution can be shown to be unique except for a constant.

Also, we may consider the hydrodynamical problem when  $v_0$  is the velocity potential of a flow due to a given system of sources in  $G_1$ . To find the effect of introducing a wall along  $\Gamma$ , we define the perturbing potential  $u$ , so that

$$\frac{\partial}{\partial n} (v_0 + u) = 0$$

on  $\Gamma$ . Suppose that  $v_0$  behaves like  $A_0 \log r + f_0(\theta) + g_0(r, \theta)$ , and  $u$  like  $B \log r + f_1(\theta) + g_1(r, \theta)$ , at large distances, where  $g_0(r, \theta)$  and  $g_1(r, \theta)$  are regular at infinity in  $G_1$ ;  $u$  can be interpreted as the velocity potential due to a system of image sources in  $G_2$ .

If we assume that all the sources in  $G_1$  lie in some finite region, it is possible to find an  $R$  such that, by Gauss's theorem,

$$\oint_{\Gamma(R) + S_1(R)} \frac{\partial}{\partial n} (v_0 + u) ds = \int_{S_1(R)} \frac{\partial}{\partial n} (v_0 + u) ds = 2\pi A_0. \quad (2)$$

Since

$$\lim_{R \rightarrow \infty} \int_{S_1(R)} \frac{\partial}{\partial n} (v_0 + u) ds = \omega_1(A_0 + B),$$

from (2)

$$B = \frac{(2\pi - \omega_1)}{\omega_1} A_0 = \frac{\omega_2}{\omega_1} A_0. \quad (3)$$

Thus the ratio of the algebraic sum of the image sources to the sum of the sources in  $G_1$  is  $\omega_2/\omega_1$ .

A completely analogous argument in three dimensions shows that the algebraic sum of the source systems are related by (3), but in this case  $\omega_1$  and  $\omega_2$  must be interpreted in terms of solid angles.

### 5. Steady heat conduction in a composite region with contact resistance

Let  $v_1$  and  $v_2$  be the temperature distributions in  $G_1$  and  $G_2$  respectively, then  $v_1$  and  $v_2$  are solutions of Laplace's equation except at those points at which heat sources are situated; on  $\Gamma$  they satisfy the conditions:

$$C_1 \frac{\partial v_1}{\partial \nu} = H(v_2 - v_1), \quad (4)$$

$$C_2 \frac{\partial v_2}{\partial \nu} = H(v_2 - v_1), \quad (5)$$

where  $C_1$ ,  $C_2$ , and  $H$  are positive constants, and  $\partial/\partial\nu$  denotes differentiation along the normal to  $\Gamma$  from  $G_1$  to  $G_2$ .

Suppose  $v_0$  is the temperature distribution due to a given distribution of sources which lie within some finite region of  $G_1$ . To find the effect of introducing the boundary  $\Gamma$ , we define perturbing temperature distributions  $u_1$  and  $u_2$  so that

$$v_1 = v_0 + u_1, \quad v_2 = v_0 + u_2.$$

$u_1$  and  $u_2$  will have no singularities in  $G_1$  and  $G_2$  respectively.

We assume that, for large  $r$ ,  $v_0$  has the form  $A_0 \log r + f_0(\theta) + g_0(r, \theta)$ ,  $u_1$  the form  $B \log r + f_1(\theta) + g_1(r, \theta)$ , and  $u_2$  the form  $B \log r + f_2(\theta) + g_2(r, \theta)$ , where  $g_0(r, \theta)$  and  $g_1(r, \theta)$  are regular at infinity in  $G_1$  and  $g_0(r, \theta)$  and  $g_2(r, \theta)$  are regular at infinity in  $G_2$ .

It is possible to find an  $R$  so that  $S(R)$  contains all the singularities of  $v_0$ , whence from Gauss's theorem,

$$\int_{S_1(R)} \frac{\partial}{\partial n} (v_0 + u_1) ds + \int_{\Gamma(R)} \frac{\partial}{\partial n} (v_0 + u_1) ds = 2\pi A_0. \quad (6)$$

In the same way, if  $S_2(R)$  is the arc of  $S(R)$  lying in  $G_2$ ,

$$\int_{S_2(R)} \frac{\partial}{\partial n} (v_0 + u_2) ds + \int_{\Gamma(R)} \frac{\partial}{\partial n} (v_0 + u_2) ds = 0. \quad (7)$$

Using (4) and (5), from (6) and (7) it follows that

$$C_1 \int_{S_1(R)} \frac{\partial}{\partial n} (v_0 + u_1) ds + C_2 \int_{S_2(R)} \frac{\partial}{\partial n} (v_0 + u_2) ds = 2\pi C_1 A_0. \quad (8)$$

When  $R \rightarrow \infty$ , the left-hand side of (8) tends to

$$C_1 \omega_1 (A_0 + B_1) + C_2 \omega_2 (A_0 + B_2),$$

while the right-hand side is constant. Therefore

$$(C_2 - C_1) \omega_2 A_0 + C_1 \omega_1 B_1 + C_2 \omega_2 B_2 = 0. \quad (9)$$

Reverting to (7), and using (5),

$$\int_{S_2(R)} \frac{\partial}{\partial n} (v_0 + u_2) \, ds + \frac{H}{C_2} \int_{\Gamma(R)} (u_1 - u_2) \, ds = 0. \quad (10)$$

In the limit as  $R \rightarrow \infty$ , the first term on the left-hand side of (10) converges to  $(A_0 + B_2) \omega_2$ , therefore the second term converges. This implies that as  $R \rightarrow \infty$ , along  $\Gamma$ ,

$$u_1 - u_2 \rightarrow 0;$$

thus

$$B_1 = B_2; \quad (11)$$

and from (9) and (11), we have

$$B_1 = B_2 = \frac{\omega_2 (C_1 - C_2)}{\omega_1 C_1 + \omega_2 C_2} A_0. \quad (12)$$

From (12) it follows that for the given conditions on an infinite boundary, and a given distribution of singularities, the perturbing temperature distributions can be proved to be unique except for an arbitrary constant.

For a straight-line boundary,  $\omega_1 = \omega_2 = \pi$ , and so

$$B_1 = B_2 = \frac{(C_1 - C_2)}{C_1 + C_2} A_0.$$

In three dimensions, when  $v_0$  has the form  $A_0/r + g(r, \theta, \phi)$  where

$$g(r, \theta, \phi) = O(1/r^2) \quad \text{and} \quad \frac{\partial}{\partial r} g(r, \theta, \phi) = O(1/r^3)$$

as  $r \rightarrow \infty$ , and with corresponding forms for  $u_1$  and  $u_2$ , it can be shown, by an analogous argument, that (12) remains true when  $\omega_1$  and  $\omega_2$  are interpreted in terms of solid angles.

#### REFERENCE

1. O. D. KELLOGG, *Foundations of Potential Theory* (Berlin, 1929), 211–15.

(9)

# NOTE ON LIN'S ITERATION PROCESS FOR THE EXTRACTION OF COMPLEX ROOTS OF ALGEBRAIC EQUATIONS

(10) *By J. MORRIS† and J. W. HEAD‡*

[Received 8 May 1952]

## SUMMARY

A simple iterative procedure for the extraction of factors of algebraic polynomials has been given by Lin (1). The rational basis of this procedure and the conditions for its convergence are here discussed.

### Introduction

(11) AMONG many possible methods of determining quadratic factors of algebraic polynomials, that due to Lin (1) has been found particularly useful by one of the authors in the solution of practical problems connected with servo-mechanisms. The weakness of Lin's method is the lack of specific criteria for its convergence.

(12) The rational basis of Lin's process is here investigated, and clear-cut criteria for its convergence are given. These criteria are for the most part qualitative, because the appropriate analytical expressions contain the 'unknowns' being sought and the criteria found are only truly rigorous in the immediate vicinity of the roots.

The extraction of a quadratic factor from a quartic equation and the simplest case of extracting a linear factor are discussed in detail; the general case of extracting a factor of degree  $r$  from an equation of degree  $n$  is briefly considered.

### 1. Description of the process

As an illustration of the procedure consider the quartic

$$F(x) = x^4 + 2x^3 + 8x^2 + 10x + 7.$$

In the absence of any indication of an appropriate approximation to a quadratic factor, we take the last three terms of the quartic, viz.

$$8x^2 + 10x + 7,$$

divide this coarsely by the coefficient of  $x^2$  and thus make  $x^2 + 1.25x + 1$ , for example, a starting factor. Then we proceed as follows:

$$\begin{array}{r} x^2 + 1.25x + 1)x^4 + 2x^3 + 8x^2 + 10x + 7(x^2 + 0.75x \\ \underline{x^4 + 1.25x^3 + x^2} \\ 0.75x^3 + 7x^2 + 10x \\ \underline{0.75x^3 + 0.94x^2 + 0.75x} \\ 6.06x^2 + 9.25x + 7 \end{array}$$

† Research Consultant.

‡ B.B.C. Research Department.

and thereby obtain the quadratic remainder

$$6.06x^2 + 9.25x + 7 = 6.06(x^2 + 1.538x + 1.155).$$

Then we take the factor  $x^2 + 1.538x + 1.155$  for the next approximation and repeat the process with the original quartic; and so on.<sup>†</sup> Thus we obtain in succession

$$F(x) = (x^2 + 1.538x + 1.155)(x^2 + 0.462x) + 6.129(x^2 + 1.544x + 1.142),$$

$$F(x) = (x^2 + 1.544x + 1.142)(x^2 + 0.456x) + 6.154(x^2 + 1.540x + 1.137),$$

$$F(x) = (x^2 + 1.540x + 1.137)(x^2 + 0.460x) + 6.156(x^2 + 1.540x + 1.137).$$

Hence after four iterations we derive the quadratic factor

$$x^2 + 1.540x + 1.137$$

and, in the course of the procedure, the remaining factor

$$x^2 + 0.460x + 6.156,$$

both computed to four figures. As a check we notice that

$$(x^2 + 1.540x + 1.137)(x^2 + 0.460x + 6.156) \\ = x^4 + 2x^3 + 8.001x^2 + 9.998x + 6.999.$$

It may be remarked that in the early stages, and until the factor we are trying to extract appears to have become stabilized, it is unnecessary to work to any but superficial 'accuracy' for the reason that in a fully iterative process errors are only of transitory effect until the final stages, when we must have regard for arithmetical accuracy to the required number of significant figures.

## 2. Convergence of the process

We notice in the numerical example given in the preceding section that, for the particular quartic considered, the successive approximation process for the extraction of a quadratic factor was operated rapidly, but such quick convergence will not necessarily occur in other cases. As in all iterative processes, criteria specifying the conditions for convergence become of paramount importance if the process is to be of practical value in actual arithmetical computation.

Reverting to the particular numerical example worked out, we observe that for a root  $x$  of the equation  $F(x) = 0$

$$(x^2 + 1.25x + 1)(x^2 + 0.75x) = -6.06(x^2 + 1.538x + 1.155),$$

$$(x^2 + 1.538x + 1.155)(x^2 + 0.462x) = -6.129(x^2 + 1.544x + 1.142),$$

$$(x^2 + 1.544x + 1.142)(x^2 + 0.456x) = -6.154(x^2 + 1.540x + 1.137).$$

<sup>†</sup> In Lin's original paper the process by which the successive divisors are obtained is described somewhat differently, but the successive divisors themselves are identical with those given here.

Hence

$$x^2 + 1.540x + 1.137 \\ = (-1)^3 \frac{(x^2 + 0.75x)}{6.06} \frac{(x^2 + 0.462x)}{6.129} \frac{(x^2 + 0.456x)}{6.154} (x^2 + 1.125x + 1).$$

Thus the convergence of the process in this case depends on the successive ratios

$$R_1 = \frac{x(x+0.75)}{6.06}, \quad R_2 = \frac{x(x+0.462)}{6.129}, \quad R_3 = \frac{x(x+0.456)}{6.154},$$

and so on, becoming numerically less than unity; and the smaller these ratios the more rapid the convergence towards the specific quadratic factor being sought.

It seems therefore that starting with a more or less arbitrary quadratic factor there will eventually emerge from the process that factor, if any, for whose roots the foregoing ratios  $R_i$  tend to become numerically smaller than unity. Otherwise the process will be divergent and in consequence abortive so far as producing a quadratic factor is concerned.

To rationalize the process for the quartic in general let

$$F(x) = x^4 + a_3 x^3 + a_2 x^2 + a_1 x + a_0; \quad (1)$$

and let this be written

$$F(x) = (x^2 + p_r x + q_r)(x^2 + P_r x) + \frac{a_0}{q_{r+1}} (x^2 + p_{r+1} x + q_{r+1}). \quad (2)$$

Equating corresponding coefficients we must have

$$p_r + P_r = a_3, \quad (3)$$

$$p_r P_r + q_r = a_2 - a_0 \frac{1}{q_{r+1}}, \quad (4)$$

$$q_r P_r = a_1 - a_0 \frac{p_{r+1}}{q_{r+1}}. \quad (5)$$

Let the quadratic factor to emerge from the application of the process (assumed convergent for that factor) be  $x^2 + px + q$ , so that

$$F(x) = (x^2 + px + q)(x^2 + Px) + \frac{a_0}{q} (x^2 + px + q). \quad (6)$$

Also let us write

$$p_r = p + \xi_r, \quad q_r = q + \eta_r, \quad P_r = P + X_r,$$

where  $\xi_r, \eta_r, X_r$  are assumed to be small quantities of the first order.

Substituting these in (3), (4), (5), and neglecting quantities of higher order than the first, we find

$$\xi_r + X_r = 0, \quad (7)$$

$$\xi_r P + X_r p + \eta_r = \frac{a_0}{q^2} \eta_{r+1}, \quad (8)$$

$$X_r q + \eta_r P = -\frac{a_0}{q} \xi_{r+1} + \frac{a_0 p}{q^2} \eta_{r+1}. \quad (9)$$

It must again be pointed out that (7), (8), and (9) are only rigorously true in the immediate neighbourhood of the roots, and that this neighbourhood is unknown initially.

In view of the relation  $P = a_3 - p$  we obtain from the relations (7), (8), (9) the two equations in  $\xi_r$ ,  $\eta_r$  as follows:

$$[p(a_3 - 2p) + q]\xi_r - (a_3 - 2p)\eta_r = \frac{a_0}{q}\xi_{r+1}, \quad (10)$$

$$(a_3 - 2p)\xi_r + \eta_r = \frac{a_0}{q^2}\eta_{r+1}. \quad (11)$$

Now let

$$\xi_r = \bar{\xi}\lambda^r, \quad \eta_r = \bar{\eta}\lambda^r, \quad (12)$$

where  $\lambda$  is a parameter and  $\bar{\xi}$ ,  $\bar{\eta}$  are appropriate constants.

Substituting these expressions for  $\xi_r$ ,  $\eta_r$  in the equations (10) and (11), we derive two latent root equations in  $\lambda$  as follows:

$$\left[ p(a_3 - 2p) + q - \frac{a_0}{q}\lambda \right] \bar{\xi} - (a_3 - 2p)\bar{\eta} = 0, \quad (13)$$

$$(a_3 - 2p)\bar{\xi} + \left( 1 - \frac{a_0}{q^2}\lambda \right) \bar{\eta} = 0. \quad (14)$$

The corresponding characteristic equation in  $\lambda$  is thus the quadratic

$$\frac{a_0^2}{q^3}\lambda^2 - \frac{a_0}{q} \left[ 2 + \frac{p(a_3 - 2p)}{q} \right] \lambda + [(a_3 - p)(a_3 - 2p) + q] = 0; \quad (15)$$

and for the convergence of the iteration process under consideration as applied to the quartic (1) both roots of (15) in  $\lambda$  must have modulus less than unity.<sup>†</sup> For the quartic of section 1, we have  $a_3 = 2$ ,  $a_0 = 7$ , and for the factor  $x^2 + 1.540x + 1.137$ , we have also  $p = 1.540$ ;  $q = 1.137$ . In this case (15) reduces to

$$33.34\lambda^2 - 3.307\lambda + 0.6402 = 0. \quad (16)$$

The roots of this quadratic are complex and have modulus

$$(0.6402/33.34)^{\frac{1}{2}} = 0.139.$$

This gives the rational explanation for the rapidity of the convergence of the process in the particular case considered.

For the other factor, viz.  $x^2 + 0.460x + 6.156$ , we find that the modulus of the roots is 6.10 and thus this factor could not be found primarily by the process in the ordinary way.

<sup>†</sup> If we eliminate  $x$  between the equations  $x^2 + px + q = 0$  and  $x^2 + Px + (\lambda a_0/q) = 0$ , we obtain (15). It follows that if  $x_1$  and  $x_2$  are the roots of  $x^2 + px + q = 0$ , the roots of (15) are  $-q(x_1^2 + Px_1)/a_0$  and  $-q(x_2^2 + Px_2)/a_0$ . The significance of the ratios called  $R_i$  in section 1 is thus explained.

We notice that the solution of the iteration equations (13), (14) above is

$$\xi_r = \bar{\xi}_1 \lambda_1^r + \bar{\xi}_2 \lambda_2^r, \quad (17)$$

$$\eta_r = \bar{\eta}_1 \lambda_1^r + \bar{\eta}_2 \lambda_2^r, \quad (18)$$

where  $\lambda_1, \lambda_2$  are the two roots in  $\lambda$  of the quadratic equation (15) and  $\bar{\xi}_1, \bar{\eta}_1; \bar{\xi}_2, \bar{\eta}_2$  are appropriate constants.

Lin (1) suggested that when his process was not convergent the given equation should be transformed, either by squaring the roots or by increasing or decreasing them all equally. He gave examples for which such transformations did produce convergence. In other cases, however, the convergence may be retarded; for example if the roots of the equation discussed in section 1 are squared, the equation becomes

$$y^4 + 12y^3 + 38y^2 + 12y + 49 = 0 \quad (19)$$

and the convergence is retarded.

If as a result of any transformation (1) becomes

$$G(y) = y^4 + b_3 y^3 + b_2 y^2 + b_1 y + b_0, \quad (20)$$

an approximate equation corresponding to (15) can be formed by replacing in (15)  $a_0$  by  $b_0$ ;  $a_3$  by  $b_3$ ;  $p$  by  $(b_1/b_2)$ ;  $q$  by  $(b_0/b_2)$ .

Unless the roots of this approximate equation have moduli appreciably less than unity, the right transformation has not been found. If better approximations to  $p, q$  than  $(b_1/b_2)$  and  $(b_0/b_2)$  are known, they should clearly be used.

### 3. The general case

Although our discussion here is limited to the extraction of a quadratic factor from a quartic, Lin's method can be used (when convergent) to obtain a factor of degree  $r$  from an equation of degree  $n$  ( $r < n$ ). If the  $n$ -ic is

$$x^n + a_{n-1} x^{n-1} + \dots + a_2 x^2 + a_1 x + a_0 = 0 \quad (21)$$

our first divisor is, in effect,

$$(x/a_r)(a_r x^r + a_{r-1} x^{r-1} + \dots + a_1 x + a_0); \quad (22)$$

and if the remainder after this division is

$$B(x) \equiv b_r x^r + b_{r-1} x^{r-1} + \dots + b_1 x + b_0, \quad (23)$$

the second divisor is  $xB(x)/b_r$ , and so on.

Criteria for convergence are obtained as for the quartic, but the equation corresponding to (15) becomes increasingly complicated as  $r$  and  $n$  increase, and for convergence all its roots, whether real or complex, must have modulus less than 1.

#### 4. The special case of a linear factor

The extraction of a *linear* factor has interesting special features. Consider, for example, the simple cubic

$$F(x) = x^3 + 6x^2 + 11x + 6. \quad (24)$$

We obtain in succession

$$\begin{aligned} F(x) &= (x+2.5)(x^2+3.5x)+2.25(x+2.67), \\ F(x) &= (x+2.67)(x^2+3.33x)+2.11(x+2.84), \\ F(x) &= (x+2.84)(x^2+3.16x)+2.03(x+2.96), \\ F(x) &= (x+2.96)(x^2+3.04x)+2.00(x+3). \end{aligned} \quad (25)$$

Now

$$F(x) = (x+1)(x+2)(x+3), \quad (26)$$

and it will be found that the process is convergent for the factors  $(x+1)$  and  $(x+3)$  but not for the factor  $(x+2)$ .

In general let  $F(x)$  represent a polynomial of any degree and let

$$F(x) = (x-p_r)xP_r(x) - \frac{a_0}{p_{r+1}}(x-p_{r+1}). \quad (27)$$

Then

$$F(p_r) = -\frac{a_0}{p_{r+1}}(p_r-p_{r+1}), \quad (28)$$

or

$$\frac{a_0}{p_{r+1}} = \frac{a_0 - F(p_r)}{p_r}, \quad (29)$$

which is the symbolical representation of Lin's iterative process applied to the case of a linear factor.

For the derivation of a convergence criterion let  $p_r = p + \xi_r$ , where  $p$  is a root of  $F(x) = 0$ , and  $\xi$  is assumed to be a small quantity of the first order.

$$\text{We thus find that } \xi_{r+1} = \left[ 1 + \frac{pF'(p)}{a_0} \right] \xi_r, \quad (30)$$

the corresponding  $\lambda$  equation being

$$\lambda = 1 + \frac{pF'(p)}{a_0}, \quad (31)$$

where

$$\xi_r = \bar{\xi}\lambda^r \quad (32)$$

is the solution of the 'difference' equation (7).

Clearly the convergence will depend on the numerical value of  $\lambda$  being less than unity and the  $\xi_r$  will comprise a pure geometrical progression. In particular, if

$$F(x) \equiv (x+p_1)(x+p_2)\dots(x+p_n) \quad (33)$$

for the factor  $(x+p_1)$ , the appropriate value of  $\lambda$  obtained from (31) becomes

$$\lambda(p_1) = 1 - \frac{(p_2-p_1)(p_3-p_1)\dots(p_n-p_1)}{p_2 p_3 \dots p_n}. \quad (34)$$

If therefore  $F(x)$  is transformed by increasing each root by  $\alpha$ ,  $\lambda(p_1)$  will have to be replaced by

$$\mu(p_1) = 1 - \frac{(p_2-p_1)(p_3-p_1)\dots(p_n-p_1)}{(p_2+\alpha)(p_3+\alpha)\dots(p_n+\alpha)} \quad (35)$$

and as  $\alpha$  varies,  $\mu$  can vary over a wide range of values.

### 5. Conclusions

We have obtained definite convergence criteria for Lin's process when a quadratic factor is extracted from a quartic, and the way in which a root is reached when a linear factor is extracted by the process has been examined for an equation of general degree whose factors are known. If the equation is transformed, the criteria can be applied to the transformed equation, but any particular transformation, such as squaring or increasing the roots, can either improve or retard the convergence. The effect of any transformation on convergence in a particular case can be roughly gauged by applying the convergence criteria to the transformed equation, with the unknown roots involved in those convergence criteria replaced by the best available approximations to them.

### REFERENCE

1. SHIH-NGE LIN, 'A method of successive approximations of evaluating the real and complex roots of cubic and higher order equations', *J. Math. and Phys.* **20** (1941), 231-42.

# THEORETICAL CONSIDERATIONS ON FREE CONVECTION IN TUBES

By M. J. Lighthill

(*Department of Mathematics, The University, Manchester*)

[Received 2 July 1952]

## SUMMARY

Methods are developed for predicting the flow and heat transfer due to free convection in heated vertical tubes, closed at the bottom and opening into a reservoir of cool fluid at the top. These include methods of predicting whether the flow is laminar or turbulent, and whether the boundary layer of heated fluid fills or does not fill the tube, or fills it with a stagnant region near the closed end; and six methods of analysis are needed for the various combinations of these cases. The flow found depends on a certain modified Grashof number  $G_a$  (see List of symbols) and on the length-radius ratio  $l/a$ . For laminar flow, indeed, it depends only on the quotient of these quantities (Fig. 7), but laminar flow becomes hard to achieve for large  $G_a$ . For large entry disturbances turbulence is expected for  $G_a$  greater than about  $10^4$ , and then the shape of the heat-transfer curve changes with  $l/a$ . The theory of the turbulent flow, which is based on an assumption relating the exchange coefficient to its value for ordinary pipe flow, indicates that turbulence decreases heat transfer when the boundary layer fills the tube and increases it otherwise. This leads to a peculiar 'bucket' in the heat-transfer curves (Fig. 9).

The Grashof number at which the heat transfer becomes most effective rises steeply with  $l/a$  (Fig. 10).

The theory is extended to apply to a tube closed at both ends, part heated and part cooled. There is some discussion of a mechanical engineering application in which the external force is not gravity but centrifugal. The whole theory is tentative only, and a critical evaluation is postponed until a larger body of experimental information is available, but some reference to experiment is included in a 'Note added in proof' at the end of the paper.

## CONTENTS

	Page
1. Introduction . . . . .	400
2. Laminar flow: the three régimes . . . . .	404
3. The equations of the laminar flow . . . . .	406
4. Flow with laminar boundary layer not filling the tube . . . . .	409
5. The similarity régime (laminar flow) . . . . .	411
6. Laminar flow filling the tube without similarity . . . . .	415
7. Synopsis of the laminar flow régimes . . . . .	417
8. Turbulent flow: general considerations . . . . .	419
9. Hypothesis concerning exchange coefficients in confined turbulence . . . . .	423
10. The similarity régime (turbulent flow) . . . . .	427
11. Turbulent flow filling the tube without similarity . . . . .	430
12. Synopsis of the turbulent and laminar flow régimes . . . . .	433
13. Flow in a completely closed tube, part heated and part cooled . . . . .	436

## List of symbols

<i>g</i>	acceleration due to gravity
<i>f</i>	externally produced acceleration (may or may not be <i>g</i> )
$\alpha$	coefficient of cubic expansion
<i>T</i>	temperature
<i>T<sub>0</sub></i>	temperature at walls
<i>T<sub>1</sub></i>	temperature on the axis at the orifice
<i>l</i>	length of tube
<i>a</i>	radius of tube
<i>v</i>	kinematic viscosity = $\mu/\rho$
$\kappa$	thermal diffusivity = $k/\rho c_p$
$\rho$	density
<i>c<sub>p</sub></i>	specific heat at constant pressure
$\mu$	viscosity
<i>k</i>	thermal conductivity
<i>G<sub>t</sub></i>	modified Grashof number (or 'Rayleigh number') based on length = $\frac{\alpha(T_0 - T_1)fl^3}{\nu\kappa}$
<i>G<sub>a</sub></i>	modified Grashof number based on radius = $\frac{\alpha(T_0 - T_1)fa^3}{\nu\kappa}$
$\sigma$	Prandtl number = $\nu/\kappa = \mu c_p/k$
<i>X</i>	distance from closed end
<i>R</i>	distance from axis of tube
<i>U</i>	axial velocity (i.e. in <i>X</i> -direction)
<i>V</i>	radial velocity (i.e. in <i>R</i> -direction)
<i>p</i>	pressure
<i>u</i>	non-dimensional axial velocity = $a^2 U / \kappa l$ in laminar flow and = $K a U / \nu$ in turbulent flow
<i>v</i>	non-dimensional radial velocity = $a V / \kappa$ (in laminar flow only)
<i>t</i>	non-dimensional temperature = $\alpha f a^4 (T_0 - T) / \nu \kappa l$ in laminar flow and = $\alpha f a^3 (T_0 - T) / \nu^2$ in turbulent flow
<i>r</i>	non-dimensional distance from axis = $R/a$
<i>x</i>	non-dimensional distance from closed end = $X/l$ for laminar flow and = $K^2 X/a$ for turbulent flow
<i>t<sub>1</sub></i>	value of <i>t</i> (laminar flow) on axis at orifice = $(a/l)G_a = (a/l)^4 G_t$
<i>Q</i>	total rate of heat transfer from tube
<i>N<sub>a</sub></i>	Nusselt number based on radius = $Q/2\pi lk(T_0 - T_1)$
<i>N<sub>t</sub></i>	Nusselt number based on length = $Q/2\pi ak(T_0 - T_1)$
$\beta$	a function of <i>x</i> (with different significances in sections 4, 5, and 6)
$\gamma, \delta$	functions of <i>x</i> (section 4)

$q$	mean rate of inward radial heat flow per unit area per unit time, divided by $\rho c_p$
$q_0$	value of $q$ at the wall
$\tau$	mean shearing stress retarding upward flow from inside, divided by $\rho$
$\tau_0$	skin friction divided by $\rho$ , i.e. minus the value of $\tau$ at the wall
$T_m$	average temperature over a cross-section
$\lambda$	logarithmic decrement of turbulent similarity solution
$\epsilon$	exchange coefficient (eddy kinematic viscosity)
$\overline{u'v'}$	turbulent shearing stress (divided by $\rho$ ) = $\epsilon \partial U / \partial R$
$K, A$	constants in empirical equation for mean velocity in turbulent pipe flow
$R$	Reynolds number based on skin friction = $a\sqrt{\tau_0/\nu}$
$Q$	non-dimensional form of local heat transfer rate = $\frac{\alpha f a^3 q_0}{K \nu^2 \sqrt{\tau_0}}$
$B, C, D$	functions of $x$ (sections 10, 11)
$T_c, t_c$	temperatures (actual and non-dimensional) on the axis
$N_X$	Nusselt number based on heat transfer from a length $X$ of tube measured from the closed end, and on the length $X$ ,
	$= \left( \int_0^X q_0 dX \right) / \kappa \{ T_0 - T_c(X) \}$
$B_T$	value of $B$ where turbulence disappears
$H$	suffix denoting heated portion of tube
$C$	suffix denoting cooled portion of tube

## 1. Introduction

THE subject of this paper is the effect of confining walls (and floors) on laminar or turbulent free convection flow. But the author's interest in this general subject arose through consideration of a specific practical problem.

One would hardly have expected heat transfer by free convection currents to be useful in mechanical engineering, largely because the appropriate scales of length and time are too small for the acceleration due to gravity to have much effect. But free convection can take place in any external force field, and in particular the centrifugal accelerations (which in rotary machinery may be of the order of  $10^4 g$ ) can produce very rapid free convection currents, causing extremely effective heat transfer.

E. Schmidt first proposed to use these for cooling turbine blades, and a turbine incorporating his ideas was constructed in Germany during the war. Each blade contained a number of thin cylindrical cavities pointing radially outwards from a reservoir of cool fluid in the hub. The effect of the

centrifugal force field was to cause the fluid heated at the circumference of each cavity to move towards the hub and be replaced by cool fluid moving outwards down the centre. Schmidt has recently written an account (1) of this and later work.

The parameter of greatest significance in heat transfer by free convection is the modified Grashof number† (sometimes called Rayleigh number)

$$G = \frac{\alpha(T_0 - T_1)fl^3}{\nu\kappa}. \quad (1)$$

Here  $\alpha$  is the coefficient of cubic expansion,  $T_0 - T_1$  the temperature difference,  $f$  the external acceleration (usually  $g$ , but in the present application centrifugal and many times  $g$ ),  $l$  a typical length,  $\nu$  the kinematic viscosity, and  $\kappa$  the thermal diffusivity. (We shall sometimes base the modified Grashof number on the length  $l$  of the tube and call it  $G_l$ , and sometimes on the radius  $a$  and call it  $G_a$ .) The Nusselt number

$$N = \frac{Q}{kS(T_0 - T_1)/d}, \quad (2)$$

where  $Q$  is the rate of heat transfer across area  $S$ ,  $k$  is the thermal conductivity of the fluid, and  $d$  is a typical length, is found to increase as  $G$  increases. For example, for heat transfer from a vertical flat plate with laminar flow  $N \propto G^{\frac{1}{4}}$  (Pohlhausen quoted in (4)) and the increase appears to be rather more rapid when turbulent flow occurs, namely for  $G$  greater than about  $10^9$  (Saunders (2)).

An important feature of Schmidt's proposals was to maximize  $G$  not only by using a large value of the acceleration  $f$  but also by adjusting the pressure and temperature of the cooling fluid as closely as possible to the critical condition, in which the viscosity is a minimum and the coefficient of expansion is very large.‡ By these means it is expected to obtain modified Grashof numbers  $G_l$  (based on the length of the cavities) of the order of  $10^{14}$ .

A serious difficulty in the original system proposed by Schmidt is that sediment may accumulate at the ends of the cavities as a result of centrifugal separation. This is hard to avoid because the fluid in the cavities forms part of a large volume of fluid circulating between the turbine and a heat exchanger outside it. Therefore an alternative arrangement has been proposed (Cohen (1)) in which the cavities are completely enclosed; they stretch into, and are immersed in, a secondary circulating fluid in the hub

† The ordinary Grashof number is the same but with  $\nu^2$  instead of  $\nu\kappa$  in the denominator. Saunders (2) and McAdams (3, p. 248) showed that the influence of  $\nu$  and  $\kappa$  on free convection flow is about equally important and that dynamic similarity between flows is much more accurately achieved if the modified Grashof numbers are identical than if the Grashof numbers proper are identical.

‡ The specific heat is also great in this condition, causing  $k$  to be large although the thermometric conductivity  $\kappa$  is small like  $\nu$ .

(Fig. 1). These concealed cavities then act like streaks of very highly conducting material within the blades, transferring heat from the blades to the cooling fluid.

As a result of the conclusion of hostilities Schmidt's turbine was abandoned before it had been successfully run, although preliminary experiments had indicated that it was a workable proposition. However, the problem of constructing a practical gas turbine incorporating the idea is still being actively tackled.

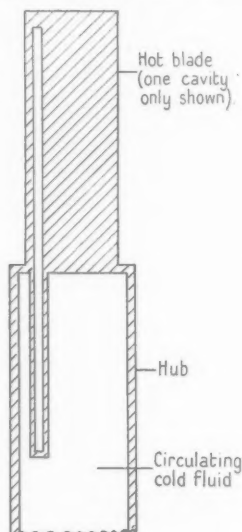


FIG. 1. Arrangement proposed by Cohen.

technique, by reducing one at least of the many uncertainties in the way of progress.

It is also hoped that they may be of interest to scientists as illuminating a rather unusual kind of fluid motion, whose essential difference from problems of free convection which have been studied theoretically is in the effect of the constraining walls.

The case of laminar flow is treated below at considerable length, before that of turbulent flow. From a scientific point of view this is natural since both subjects are equally interesting. From an engineering point of view it is equally desirable, even though in the practical application the flow will always be turbulent. For study of the corresponding laminar flow, being more reliable, is essential to bring out certain broad qualitative details of what happens,† and also to give lower limiting conditions into

† Thus it will be found that there are three geometrically different régimes of flow, depending on the range of values in which the ratio of tube length to tube radius lies.

which the turbulent flow must subside at the Grashof number of transition. Further, it is quite possible that the laminar flow may have practical importance in problems of ordinary free convection under gravity.

As the basic problem for throwing light on the subject we consider fluid in a cylindrical cavity, closed at one end and opening into a reservoir of cool fluid at the other end, as in Schmidt's original proposal. The external acceleration  $f$  acts axially towards the closed end, and the solid boundaries are maintained at a given temperature  $T_0$ . The fluid entering the tube along the axis at the open end is supposed to have the temperature  $T_1$  of the reservoir. The laminar flow is studied by means of the equations of motion in boundary layers. Approximate methods of solution are used in which the equations for momentum and energy transfer across a cross-section play a part. Such a procedure, based on the Kármán-Pohlhausen method (5, ch. 4) in ordinary boundary layer theory, was first applied to free convection problems by Squire (5, p. 641). The calculation of the turbulent case is made possible by assumptions concerning the eddy viscosity, based on recent work by Reichardt (6) and by Townsend (7, 8).

The basic problem just described will take up almost the whole paper, but it may be remarked at once that knowledge concerning *this* flow can be applied directly to predict conditions in the more complicated flow of Fig. 1. Here the hot fluid at the circumference of the cavities in the blade moves towards the hub and comes into head-on collision with the cold fluid, also at the circumference (where it is in contact with the coolant), which is moving outwards. We may suppose that the two mix perfectly and are forced in towards the centre. The temperature of the mixture, say  $T_1$ , will depend on the temperatures  $T_{0H}$  and  $T_{0C}$  of the blades and the coolant and on the ratio of the quantities of fluid colliding. Also this ratio will be equal to the ratio of the quantity of mixed fluid which moves out down the blade (along the axis of the cavity) to that which moves towards the hub. The flow in the heated part of the tube, on these assumptions, is identical with that in the 'basic problem' described above, if  $l$  signifies now the length of the heated part. That in the cooled part is the same with  $T_{0C}$  replacing  $T_{0H}$  and a new value for  $l$ . Finally the temperature  $T_1$  must be determined from the condition that it could be produced by mixing in the ratio in which the hot and cold fluid do mix at the join (which will itself depend on  $T_1$ ).<sup>†</sup> For example, if the two lengths were equal and the constants of the flow (including the external acceleration  $f$ ) were uniform,  $T_1$  would, by

<sup>†</sup> We shall see that to join the solutions up it is sufficient to apply the conditions that the rate of heat transfer across a cross-section, and also the central temperature, are continuous at the join; all other discontinuities being taken care of by the mixing process described above.

symmetry, be equal to  $\frac{1}{2}(T_{0H} + T_{0C})$ . A more realistic case is considered at the end of the paper, and the above considerations applied in detail to it.

The author expresses his gratitude to Mr. H. Cohen for introducing him to the problem and for assistance with it at all stages of the work.

## 2. Laminar flow: the three régimes

The characteristic non-dimensional parameters of the problem are the length-radius ratio  $l/a$  of the cylindrical cavity, the modified Grashof number  $G_l$  or  $G_a$  (it will appear that  $G_a$  plays a slightly more important role; in any case  $G_l = (l/a)^3 G_a$ ), and the Prandtl number  $\sigma = \nu/\kappa$  (the ratio of diffusivities of shear and heat). It is not contemplated that fluids of Prandtl number differing markedly from 1 be used in the practical problem; this restriction will be used to simplify the calculations in the turbulent case, but the laminar flow calculations will be valid for all values of  $\sigma$  except the very small ones typical only of liquid metals.

When  $l/a$  is sufficiently small (for a given  $G_a$ , say) the flow up the sides of the cavity may approximate to the free convection flow up a vertical plate. This is a flow of boundary layer type, which was calculated in the laminar case by Pohlhausen. The experiments of Schmidt and Beckmann (4), and also of Saunders (2), gave excellent agreement with the calculations. For flow inside a circular cylinder it is known that the curvature of the wall as such does not affect the form or validity of the boundary layer approximation. On the other hand, the solution would take no account of the confined space in which the motion occurs, which makes it necessary that the flux upwards at the walls be balanced by an equal flux downwards at the centre. In fact the Pohlhausen solution supposes no vertical velocity outside the boundary layer, the fluid entrained into the boundary layer being assumed to approach it horizontally. Hence the solution will be valid only when the cross-sectional area of the boundary layer is small compared with that of the whole cavity. This condition restricts greatly the length-radius ratio  $l/a$  for a given  $G_a$ .

However, the solution in question is extended in section 4 by permitting a vertical flow outside the boundary layer in the centre of the cavity, as illustrated in Fig. 2. This yields the first of the three flow régimes. One might at first expect it to be valid up to a value of  $l/a$  for which the boundary layer first fills the whole tube. Actually, however, it should break down for a rather smaller value of  $l/a$ , roughly that at which there is no longer a maximum in the volume flow of unheated fluid (i.e. of fluid outside the boundary layer) at the orifice cross-section. For it is only possible that unheated fluid be drawn into the boundary layer to become partially heated fluid, not vice versa.

When  $l/a$  exceeds this critical value the boundary layer mixes with the central flow and, when a steady state is reached, fills the whole tube. The nature of the resulting flow is a little difficult to perceive intuitively, but an extreme case, with much larger  $l/a$ , can be visualized. This is one in which all tendency for the boundary layer to thicken with distance from the closed end has disappeared. Then the distributions of velocity and

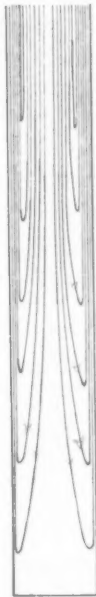


FIG. 2. Flow with boundary layer not filling tube.

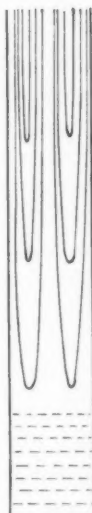


FIG. 3. Similarity régime with stagnant portion.

temperature are similar at each section of the tube, only their scale increasing as the orifice is approached. It will be found that under these circumstances the scales of both the temperature and (axial) velocity profiles increase linearly along the tube. The condition that the central temperature should rise from its value  $T_1$  at the orifice to the value  $T_0$  at the bottom then determines the length-radius ratio  $l/a$  for this particular flow as a certain multiple of  $G_a$  (section 5).

This is the largest value of  $l/a$  for which there is motion all along the tube. For greater values still (which we may regard as achieved by extending the tube beyond the closed end) the additional length is filled with fluid at rest at the temperature of the walls, the 'similarity flow' in the remainder being

unchanged. This third régime of flow, which occurs when  $l/a$  exceeds the second critical value described above, is illustrated in Fig. 3.

But a factor of order 10 separates the first critical value of  $l/a$  (corresponding to the breakdown of the boundary layer solution) from the second (corresponding to the onset of the similarity solution). The intermediate range must be filled by a solution which permits variation down the tube of velocity and temperature profiles which nevertheless fill the whole tube. Such a solution is obtained in section 6. The similarity profiles are attained near the orifice and more crimped profiles near the closed end, where the fluid rises in the middle as well as at the sides, falling only in an annulus between these two regions.

The calculations for laminar flow are simplified by letting the Prandtl number  $\sigma$  tend to infinity. Physically this corresponds to neglecting the inertia of the fluid compared with the forces due to its viscosity and the external acceleration  $f$ . It is known that this is a good approximation, even if  $\sigma$  is really about 1, in the problem of free convection from a vertical plate, which is one extreme case of the present problem. The other extreme case (the similarity solution) is also worked out below for general  $\sigma$ , and when  $\sigma \rightarrow \infty$ , and the difference found to be small when  $\sigma$  is near 1. It is reasonable to conclude that the simplified calculations obtained in the limit as  $\sigma \rightarrow \infty$  are also a good approximation in all the intermediate cases, and, in these, only the simplified calculations are actually carried out below.

### 3. The equations of the laminar flow

The equations of motion of the problem are similar to the ordinary equations of free convection flow except that the pressure no longer takes its hydrostatic value.

In all cases one is justified in simplifying the equations by the boundary layer approximation, in other words, neglecting the gradient of a quantity along the tube compared with its gradient along a radius. For in all cases either the flow is of boundary layer type (as in the extreme case of free convection from a vertical plate, for which the solutions of the boundary layer equations are known to be in excellent agreement with experiment) or else (when the boundary layer fills the whole tube) the length-radius ratio is large.

With this approximation the equations of conservation of mass, heat and momentum respectively, in steady axisymmetrical flow, are

$$\frac{\partial U}{\partial X} + \frac{\partial V}{\partial R} + \frac{V}{R} = 0, \quad U \frac{\partial T}{\partial X} + V \frac{\partial T}{\partial R} = \kappa \left( \frac{\partial^2 T}{\partial R^2} + \frac{1}{R} \frac{\partial T}{\partial R} \right), \quad (3)$$

$$U \frac{\partial U}{\partial X} + V \frac{\partial U}{\partial R} = -f - \frac{1}{\rho} \frac{\partial p}{\partial X} + \nu \left( \frac{\partial^2 U}{\partial R^2} + \frac{1}{R} \frac{\partial U}{\partial R} \right), \quad \frac{\partial p}{\partial R} = 0. \quad (4)$$

Here  $X$  is measured along the tube from an origin at the closed end, and  $R$  radially outwards from the axis; the corresponding velocity components are  $U$  and  $V$ .  $T$  is the temperature,  $\kappa$  the thermal diffusivity (thermometric conductivity),  $\rho$  the density, and  $p$  the pressure.

In the momentum equation it is necessary to take into account the fact that  $\rho^{-1}$  varies with temperature according to the equation

$$\rho^{-1} = \rho_0^{-1}[1 + \alpha(T - T_0)], \quad (5)$$

where suffix 0 signifies conditions at the wall  $R = a$  and  $\alpha$  is the coefficient of cubic expansion. By this means the thermal buoyancy force is made apparent. For by (4), with  $R = a$  (where  $U = V = 0$ ),

$$0 = -f - \frac{1}{\rho_0} \frac{dp}{dX} + v_0 \left( \frac{\partial^2 U}{\partial R^2} + \frac{1}{R} \frac{\partial U}{\partial R} \right)_{R=a}, \quad (6)$$

and hence, substituting for  $dp/dX$  from (6) in (4) and using (5),

$$U \frac{\partial U}{\partial X} + V \frac{\partial U}{\partial R} = \alpha f(T - T_0) + \nu \left[ \frac{\partial^2 U}{\partial R^2} + \frac{1}{R} \frac{\partial U}{\partial R} \right]_a^R. \quad (7)$$

Equations (3) and (7) are three equations for  $U$ ,  $V$ , and  $T$  to be solved under the boundary conditions at the walls

$$U = V = 0 \text{ and } T = T_0, \text{ for } R = a \text{ and for } X = 0, \quad (8)$$

and subject also to the condition that  $T = T_1$  at the orifice on the axis ( $X = l$ ,  $R = 0$ ).

The substitutions necessary to reduce simultaneously the equations of motion and the boundary conditions to non-dimensional forms, in which the minimum of parameters is retained, are

$$U = \frac{\kappa l}{a^2} u, \quad V = \frac{\kappa}{a} v, \quad T = T_0 - \frac{\nu \kappa l}{\alpha f a^4} t, \quad R = ar, \quad X = lx. \quad (9)$$

Then equations (3) and (7) become

$$\frac{\partial u}{\partial x} + \frac{\partial v}{\partial r} + \frac{v}{r} = 0, \quad u \frac{\partial t}{\partial x} + v \frac{\partial t}{\partial r} = \frac{\partial^2 t}{\partial r^2} + \frac{1}{r} \frac{\partial t}{\partial r}, \quad (10)$$

$$\frac{1}{\sigma} \left( u \frac{\partial u}{\partial x} + v \frac{\partial u}{\partial r} \right) = -t + \left[ \frac{\partial^2 u}{\partial r^2} + \frac{1}{r} \frac{\partial u}{\partial r} \right]_1^r, \quad (11)$$

while conditions (8) become

$$u = v = t = 0 \quad \text{for } r = 1 \text{ and for } x = 0, \quad (12)$$

and the condition at the orifice becomes

$$(t)_{x=1, r=0} = t_1 = \frac{\alpha f a^4 (T_0 - T_1)}{\nu \kappa l} = \frac{a}{l} G_a = \left( \frac{a}{l} \right)^4 G_l. \quad (13)$$

Thus (for a given  $\sigma$ ) the one parameter affecting the laminar flow régime is the parameter  $t_1$  defined in (13) as the quotient

$$\frac{\text{modified Grashof number based on radius}}{\text{length-radius ratio}} = \frac{\alpha f a^3 (T_0 - T_1) / \nu \kappa}{l/a}. \quad (14)$$

This parameter determines which flow among the sequence described in section 2 actually occurs.

Note also from equation (11) the simplification (section 2) achieved by allowing  $\sigma$  to tend to infinity, and its physical significance as the neglect of inertia forces compared with buoyancy and viscous forces.

Now the most important result of any calculation on the above equations will be the value of the total heat transfer rate, suitably put into non-dimensional form. For this purpose we use normally the Nusselt number based on wall area and tube radius,

$$N_a = \frac{Q}{k(T_0 - T_1)2\pi la/a} = \frac{a}{(T_0 - T_1)l} \int_0^l \left( \frac{\partial T}{\partial R} \right)_{R=a} dX \quad (15)$$

$$= \frac{1}{t_1} \int_0^1 \left( - \frac{\partial t}{\partial r} \right)_{r=1} dx, \quad (16)$$

and occasionally that based on the tube length, namely  $N_l = (l/a)N_a$ . The former, however, is a function of  $t_1$  alone, and so the main results of the calculations will be graphs of  $N_a$  against  $t_1$ . But the distribution of heat transfer rate along the tube needs to be considered also.

No attempt will be made below to solve equations (10) and (11) throughout the fluid, but only at the walls and on the axis and in the forms obtained by integrating them over each cross-sectional area, namely

$$\int_0^1 ru dr = 0, \quad \frac{\partial}{\partial x} \int_0^1 rut dr = \left( \frac{\partial t}{\partial r} \right)_{r=1}, \quad (17)$$

$$\frac{1}{\sigma} \frac{\partial}{\partial x} \int_0^1 ru^2 dr = - \int_0^1 rt dr + \frac{1}{2} \left( \frac{\partial u}{\partial r} - \frac{\partial^2 u}{\partial r^2} \right)_{r=1}. \quad (18)$$

These integrated forms express conservation of mass, heat and momentum respectively for the fluid filling any cross-section of the tube. The forms of equations (10) and (11) at the walls and on the axis are

$$\begin{aligned} \left( \frac{\partial^2 t}{\partial r^2} + \frac{1}{r} \frac{\partial t}{\partial r} \right)_{r=1} &= 0, & \left( u \frac{\partial t}{\partial x} \right)_{r=0} &= \left( \frac{\partial^2 t}{\partial r^2} + \frac{1}{r} \frac{\partial t}{\partial r} \right)_{r=0}, \\ \frac{1}{\sigma} \left( u \frac{\partial u}{\partial x} \right)_{r=0} &= - (t)_{r=0} + \left[ \frac{\partial^2 u}{\partial r^2} + \frac{1}{r} \frac{\partial u}{\partial r} \right]_1^0. \end{aligned} \quad (19)$$

Here the equations which would involve  $v$  are omitted, since by (17) and (18) a solution for  $t$  and  $u$  alone is sufficient. The omitted equations result from the equation of continuity, which is fully taken account of by the first of equations (17).

In sections 5 and 6 solutions of (17), (18) and (19) under the boundary conditions (12) and (13) will be obtained in the form of polynomials in  $r$ . Indeed, since by symmetry  $t$  and  $u$  are evidently even functions of  $r$ , they will be taken as polynomials in  $r^2$  (including terms up to  $r^6$ ). This probably increases accuracy by assigning weight to different annuli according to their cross-sectional area.

In section 4, where the 'first régime' of flow is studied, a solution with a variable boundary layer thickness is needed and (because of this added complication) a simpler form of the profiles is used, no attempt being made to apply the more delicate of the above conditions, namely those involving the values of second derivatives at the boundaries. In this we follow Squire's work (5, p. 641) on free convection. For this purpose, an amended form of the momentum equation (18) is needed, in which  $(\partial^2 u / \partial r^2)_{r=1}$  has been eliminated between it and (19). Since in this first régime of flow  $u$  is independent of  $r$  outside the boundary layer there is no contribution to the square bracket in (19) from the upper limit, and the amended form of (18) is in consequence

$$\frac{1}{\sigma} \frac{\partial}{\partial x} \int_0^1 r u^2 dr = - \int_0^1 r t dr + \frac{1}{2} \left( \frac{1}{\sigma} u \frac{\partial u}{\partial x} + t \right)_{r=0} + \left( \frac{\partial u}{\partial r} \right)_{r=1}. \quad (20)$$

Except in calculating the similarity solution the terms in  $\sigma^{-1}$  in equations (17) to (20) will be neglected, as explained in section 2.

#### 4. Flow with laminar boundary layer not filling the tube

In this section the first régime of flow (section 2) is studied. In the extreme case of it when the boundary layer fills a negligible area of the tube, the flow is identical with the flow up a vertical plate. The full equations of this flow were solved exactly by Pohlhausen (4) with  $\sigma = 0.733$ . He obtained  $N_t = 0.517 G^{\frac{1}{4}}$  for the Nusselt number based on length  $l$  of plate, which gives the relation

$$N_a = 0.517 t_1^{\frac{1}{4}} \quad (21)$$

for the relation between Nusselt number based on tube radius and the parameter  $t_1$  defined in (13).

Squire (5, p. 641), on the other hand, gave an approximate procedure in which the velocity profile was taken as a cubic polynomial and the temperature profile as a quadratic. His result, in our notation, is

$$N_a = 0.677 \left( 1 + \frac{20}{21\sigma} \right)^{-\frac{1}{4}} t_1^{\frac{1}{4}}. \quad (22)$$

For  $\sigma = 0.733$  this formula gives  $N_a = 0.550t_1^4$ , which is only 6 per cent. in excess of the accurate value.

We conclude that the error introduced by Squire's approximate procedure is of tolerable order of magnitude. The additional error due to replacing  $\sigma^{-1}$  by 0 depends, of course, on the value of  $\sigma$ . In the above case it would be 23 per cent., but this was for a low value of  $\sigma$  typical of gases. For  $\sigma = 2$  it would be only 10 per cent. These errors will have to be borne in mind in finally evaluating the theory (section 7).

In this section the Squire procedure will be carried through with  $\sigma^{-1} = 0$  and with a vertical velocity permitted outside the boundary layer. Thus we assume that approximately

$$t = \begin{cases} t_1 & (0 < r < \beta) \\ t_1 \left[ 1 - \left( \frac{r-\beta}{1-\beta} \right)^2 \right] & (\beta < r < 1) \end{cases}, \quad (23)$$

$$u = \begin{cases} -\gamma & (0 < r < \beta) \\ -\gamma \left[ 1 - \left( \frac{r-\beta}{1-\beta} \right)^2 \{ 1 + \delta(r-1) \} \right] & (\beta < r < 1) \end{cases}, \quad (24)$$

where  $\beta, \gamma, \delta$  are functions of  $x$ . Equations (23) and (24) already satisfy the boundary conditions on  $r = 1$ . The equations (17) and (20) are now used to determine  $\beta, \gamma$ , and  $\delta$ . Thus the equation of conservation of mass in (17) gives

$$\delta = -\frac{5(3+2\beta+\beta^2)}{(3+2\beta)(1-\beta)}. \quad (25)$$

Equation (20) with  $\sigma^{-1} = 0$  then gives

$$\gamma = t_1 \frac{(3+\beta)(3+2\beta)(1-\beta)^3}{36(3+4\beta+3\beta^2)}. \quad (26)$$

Finally the equation of conservation of heat in (17) gives

$$t_1 \frac{d}{dx} \left[ \frac{(1-\beta)^3(3+\beta)(45+132\beta+181\beta^2+62\beta^3)}{30240(3+4\beta+3\beta^2)} \right] = t_1 \frac{d}{dx} [F(\beta)] = \frac{1}{1-\beta}. \quad (27)$$

The complicated fraction  $F(\beta)$  is tabulated in Table 1, together with

$$\frac{t_1}{x} = \left[ \int_1^\beta (1-\beta) dF(\beta) \right]^{-1}. \quad (28)$$

The value of expression (28) at the orifice  $x = 1$  is the parameter  $t_1$ , so the table gives a relation between  $t_1$  and the value of  $\beta$  at the orifice. The table

also gives values of the Nusselt number for given values of  $\beta$  at the orifice. This, by (15), is

$$N_a = \frac{1}{t_1} \int_0^1 \left( \frac{2t_1}{1-\beta} \right) dx = 2t_1 F(\beta). \quad (29)$$

The cross-plot of  $N_a$  against  $t_1$  obtained from Table 1 is shown in Fig. 7, where its asymptote  $N_a = 0.677t_1^4$  (the Squire solution for  $\sigma^{-1} = 0$ ) is also shown.

TABLE 1

$\beta$	$F(\beta)$	$t_1/x (= t_1 \text{ at orifice})$	$N_a$
0	.001488	1060	3.15
.1	.001309	1290	3.37
.2	.001094	1680	3.69
.3	.000858	2400	4.12
.4	.000625	3770	4.71
.5	.000413	6740	5.56
.6	.000238	14450	6.89
.7	.000112	40500	9.07
.8	.000037	182000	13.5
.9	.000005	2400000	27
1.0	0	$\infty$	$\infty$

Although the solution exists formally for values of  $t_1$  down to 1,060, the actual critical value of  $t_1$  at which such a solution ceases to apply will be somewhat greater (see section 2), being determined by the condition that the flux of fluid outside the boundary layer ceases to be a maximum at the orifice. This flux by (24) and (26) is proportional to

$$\frac{\beta^2(3+\beta)(3+2\beta)(1-\beta)^3}{3+4\beta+3\beta^2}, \quad (30)$$

which is a maximum for  $\beta = 0.38$ , corresponding to about  $t_1 = 3,400$  and  $N = 4.6$ . This point is marked in Fig. 7 with a cross. If  $t_1$  is significantly less than this value, then the solution requires that cold fluid should enter the boundary layer from outside and then leave it again without having been in the least affected. This is impossible and the solution must become increasingly inaccurate for  $t_1 < 3,400$ .

### 5. The similarity régime (laminar flow)

We pass now to the other extreme case and consider a solution of equations (17), (18) and (19), under the boundary conditions (12), such that  $u$  and  $t$  are proportional always to the same two functions of  $r$ , the factors of proportionality varying with  $x$ . A brief examination shows that the only possible form of variation with  $x$  is that  $u$  and  $t$  are both proportional to  $x$ , measured from some origin. (For that they would have the same variation with  $x$  follows from (18), whence one concludes from either (17) or (19) that

it is linear. The conclusion is equally easily drawn from equations (10) and (11).)

At the second critical value of  $t_1 = G_a(a/l)$  described in section 2 this similarity solution must hold with  $x$  measured from the closed end of the tube (in order that  $u$  and  $t$  shall vanish there). This solution will now be determined, including the value of  $t_1$  for which it holds. For smaller values of  $t_1$  the solution holds without change if  $x$  is measured from the point at which flow ceases (Fig. 3).

Now the boundary conditions and equations (19) and the first of equations (17) are satisfied by

$$\left. \begin{aligned} t &= t_1 x \left( 1 - \beta r^2 + \frac{8\beta - 9}{5} r^4 + \frac{4 - 3\beta}{5} r^6 \right), \\ u &= -4\beta x (1 - 6r^2 + 9r^4 - 4r^6) - \frac{1}{24} \left( t_1 + \frac{16\beta^2}{\sigma} \right) x (r^2 - 3r^4 + 2r^6). \end{aligned} \right\} \quad (31)$$

The parameters  $\beta$  (*not to be confused with the  $\beta$  of section 4, which will not occur again*) and  $t_1$  are then determined from the second of equations (17), which becomes

$$t_1 + \frac{16\beta^2}{\sigma} = \frac{320(126 - 51\beta - 2\beta^2)}{13 - \beta}, \quad (32)$$

and from equation (18), which becomes

$$\begin{aligned} \frac{1}{\sigma} \left( \frac{48}{35} \beta^2 + \frac{1}{420} \beta \left( t_1 + \frac{16\beta^2}{\sigma} \right) + \frac{1}{120960} \left( t_1 + \frac{16\beta^2}{\sigma} \right)^2 \right) \\ = \frac{24 + 7\beta}{120} t_1 - 48\beta + \frac{8\beta^2}{\sigma}. \end{aligned} \quad (33)$$

The solution of (32) and (33) is most easily obtained for  $\sigma = \infty$ , when there are three roots (indeed the equation in terms of  $\beta$  is a cubic), namely

$$\begin{aligned} \beta &= 2.091, \quad t_1 = 311; \quad \beta = -4.017, \quad t_1 = 5006; \\ \beta &= -25.705, \quad t_1 = 949. \end{aligned} \quad (34)$$

Of these only the first corresponds to a similarity solution achievable in practice. The evidence for this is somewhat complex, but note first that the *other* two solutions have  $u > 0$  on the axis of the tube as well as near the walls, with therefore a region of negative  $u$  somewhere in between. Thus the velocity profile has at least three 'waves' in it, as against two for the first profile.

Now in reality there are probably infinitely many similarity solutions of equations (10) and (11) under the boundary conditions (12), with velocity profiles having every number of waves in them from 2 to  $\infty$ . The method of obtaining approximate solutions which has been used is only suitable

for profiles with very few waves, say 2 or 3. Hence only these emerge from it. (The third solution already is probably hopelessly inaccurate.)

The existence of this infinity of similarity solutions is typical of almost any physical problem under homogeneous boundary conditions like (12). (Mathematically we have an eigenvalue problem.) In problems with damping, the one corresponding to reality is the one with least damping, which here is evidently the one with fewest waves (since the damping is viscous). For a linear problem the general solution would be a linear combination of the different similarity solutions,<sup>†</sup> and the steady solution is that similarity solution which damps out least rapidly, being attained when the others have become small compared with it. For the present problem, which is non-linear, the solutions other than the similarity solutions are related in a more complicated way (see section 6), but it is reasonable to suppose that of the similarity solutions it is still only the solution with fewest waves which is reached as a steady state in practice. This conclusion is supported by the plausibility of the resulting complete  $(N_a, t_1)$  curve (Fig. 7).

Since only the positive root of (33) is relevant, it is the only root whose variation with  $\sigma$  need be considered. When this is calculated the variation of  $\beta$  with  $\sigma$  is found to be quite negligible;  $t_1$ , however, varies considerably. For  $\sigma = 1$ , for example, the root is

$$\beta = 2.099, \quad t_1 = 227. \quad (35)$$

This value of  $t_1$  is 27 per cent. below the value for  $\sigma = \infty$ .

Since by (15) and (31)

$$N_a = \frac{1}{t_1} \int_0^1 \left( t_1 x \frac{12 - 4\beta}{5} \right) dx = \frac{6 - 2\beta}{5}, \quad (36)$$

the Nusselt numbers for  $\sigma = \infty$  and  $\sigma = 1$  respectively, by (34) and (35), are

$$N_a = 0.364 \quad (\sigma = \infty, t_1 = 311), \quad N_a = 0.360 \quad (\sigma = 1, t_1 = 227). \quad (37)$$

These points can be marked in on the  $(N_a, t_1)$  curve (Fig. 7).

Note that, whereas in the present extreme case of the problem  $t_1$  is overestimated (for given  $N_a$ ) by putting  $\sigma = \infty$ , the reverse is true in the other extreme case, as (22) shows. For some intermediate case, the  $(N_a, t_1)$  curves for  $\sigma = \infty$  and  $\sigma = 1$  must cross, and in this region the approximation obtained by putting  $\sigma = \infty$  must be particularly good.

For smaller values of  $t_1$  than that (say  $t_s$ ) which is characteristic of the similarity solution when it fills the whole tube,  $t$  and  $u$  are given by equations (31) with  $t_1$  replaced by  $t_s$  and  $x$  by  $x - l(1 - t_1/t_s)$ . For  $x < l(1 - t_1/t_s)$  there

<sup>†</sup> For an example of this in heat-transfer theory, consider the temperature distribution in laminar flow through pipes (5, p. 616).

is no motion and no variation of temperature (Fig. 3), and the top of this region plays exactly the same role relative to the similarity flow above it as does the closed end of the tube in the case discussed above. The Nusselt

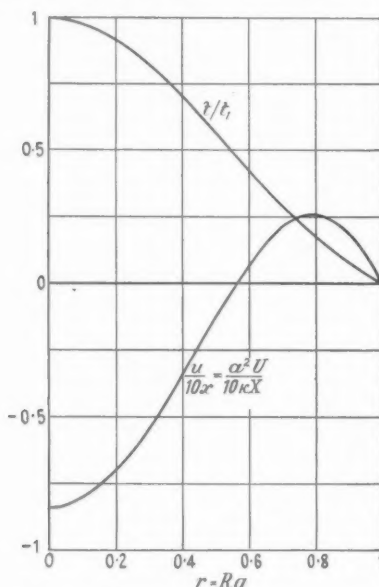


FIG. 4. Velocity and temperature profiles for the laminar similarity solution.

number is therefore unchanged if in it  $l$  be replaced by the 'effective length' of tube  $lt_1/t_s$ . If this is not done, therefore, we have

$$N_a = N_{as} \frac{t_1}{t_s} \quad \text{for } t_1 < t_s, \quad (38)$$

where the suffix  $s$  refers to the similarity values (37). On the  $(N_a, t_1)$  diagram (Fig. 7) the relation (38) gives straight lines pointing downwards and to the left from the points representing the similarity solutions.

It is interesting that the velocity distribution (measured relative to  $\kappa l/a^2$ , see (9)) is practically unaffected by the value of  $\sigma$  (since by (31) and (32) it depends only on  $\beta$ ). Only the axial temperature gradient (proportional to  $t_1$ ) is so affected, owing to the additional thermal buoyancy effect needed to overcome the inertia of the fluid. The velocity and temperature profiles are shown in Fig. 4. The negative velocity in the middle is greater than the positive velocity at the outside because the larger values of  $r$  correspond to a larger area of tube. Similarly the temperature gradient increases at first,

as  $r$  decreases from 1, because it is causing heat transfer over a decreasing area at a rate initially changing little.

### 6. Laminar flow filling the tube without similarity

We shall now seek to satisfy the equations (17), (18) and (19) in the limiting case  $\sigma = \infty$  by means of velocity and temperature profiles which fill the tube but whose shapes vary with  $x$ . The form of the profiles is very similar to (31). In fact we take

$$t = t_c \left( 1 - \beta r^2 + \frac{8\beta - 9}{5} r^4 + \frac{4 - 3\beta}{5} r^6 \right), \quad (39)$$

$$u = - \frac{4\beta t_c}{dt_c/dx} (1 - 6r^2 + 9r^4 - 4r^6) - \frac{1}{24} t_c (r^2 - 3r^4 + 2r^6). \quad (40)$$

These satisfy the boundary conditions on  $r = 1$  and equations (19) and the first of equations (17). In (39) and (40) both  $t_c$  and  $\beta$  are functions of  $x$ .

Substituting (39) and (40) in equation (18), with  $\sigma = \infty$ , we find that

$$\frac{dt_c}{dx} = \frac{5760\beta}{24 + 7\beta}, \quad (41)$$

while the second of equations (17) becomes

$$\frac{d}{dx} \left[ t_c^2 \frac{450 + 93\beta + 14\beta^2}{604800} \right] = t_c \frac{12 - 4\beta}{5}. \quad (42)$$

Eliminating  $x$  between (41) and (42), an equation relating  $t_c$  to  $\beta$  results, namely

$$t_c \frac{dt_c}{d\beta} = \frac{\frac{1}{2}\beta(93 + 28\beta)}{3024 - 576\beta - 387\beta^2 - 14\beta^3}. \quad (43)$$

The cubic in (43) has the roots given by the values of  $\beta$  in (34) for which a similarity solution (with  $\beta = \text{constant}$ ) exists. The solution of (43) involves these roots in the form

$$t_c = \text{const} (2.091 - \beta)^{-0.0667} (4.017 + \beta)^{+0.0211} (25.705 + \beta)^{-0.9544}. \quad (44)$$

Since  $t_c$  must be 0 at the closed end  $x = 0$ , this value of  $x$  corresponds to  $\beta = -4.017$ . As  $x$  and  $t_c$  increase  $\beta$  must increase towards the value 2.091 corresponding to the similarity profiles.

Hence, by (41),

$$x = \int_{-4.017}^{\beta} \frac{24 + 7\beta}{5760\beta} dt_c(\beta), \quad t_1 = \frac{t_c(\beta_1)}{\int_{-4.017}^{\beta_1} \frac{24 + 7\beta}{5760\beta} dt_c(\beta)}, \quad (45)$$

if  $\beta_1$  is the value of  $\beta$  at the orifice  $x = 1$ , and by (15)

$$N_a = \frac{\int_{\beta_1}^{\beta_1} t_c(\beta) \frac{12-4\beta}{5} \frac{24+7\beta}{5760\beta} dt_c(\beta)}{t_c(\beta_1) \int_{-4.017}^{\beta_1} \frac{24+7\beta}{5760\beta} dt_c(\beta)}. \quad (46)$$

These forms of  $t_c$  and  $N_a$  have been written in such a form as to be functions of  $\beta_1$  independent of the constant in (44). They were computed by numerical integration, in which special account had to be taken of the singularities of the integrand. The adjacent shortened table indicates their behaviour. The peculiarities near the top of the table are due to the zeros of (43) and of the integrand of (45) at  $\beta = -3.321$  and  $\beta = -3.429$  respectively. A more extended table was used to plot the graph of  $N_a$  against  $t_1$  shown in Fig. 7 (in which the looping of the curve corresponding to the above-mentioned peculiarities is invisible to the naked eye). This graph runs continuously into the point  $t_1 = 311$ ,  $N_a = 0.364$  given by the similarity solution for  $\sigma = \infty$ . This limiting case occurs as  $\beta_1 \rightarrow 2.091$ , when almost all the change in  $x$  (see (45)) occurs for  $\beta$  near 2.091, so that the similarity profile fills almost all the tube.

TABLE 2

$\beta_1$	$t_1$	$N_a$
-4.017	5620	2.81
-3.267	5680	2.77
-2.517	5580	2.81
-1.767	5310	2.89
-1.017	4840	2.96
-0.267	4210	2.97
+0.483	3440	2.84
+1.233	2560	2.48
+1.983	1351	1.54

But in all cases of the present solution the quite different velocity and temperature profiles represented by  $\beta = -4.017$  are attained at the closed end  $x = 0$ . These profiles are illustrated in Fig. 5. The rising velocity and local *maximum* of temperature at the centre are due to convection from the horizontal end of the tube. The transition from this form of profile to one with  $u \leq 0$  in the centre (which occurs for  $\beta \geq -3.429$ ) corresponds to a flow like that illustrated in Fig. 6, with a standing ring vortex at the bottom of the tube, round which the main flow passes.†

† It is probable that something similar actually occurs in the boundary-layer flow of section 4, being also due to free convection from the horizontal closed end. But even if it does, it can have little quantitative effect on the boundary layer flow.

The  
in th

2

1

0

-1

-

0

Fig

7. S

T

 $t_1 >$ 

unhe

volu

the

heat

 $t_1$  in

plat

stra

solu

can

incre

scal

A

min

to T

low

its n

50

The joining up of the present solution with that of section 5 is effected in the next section.

(46)

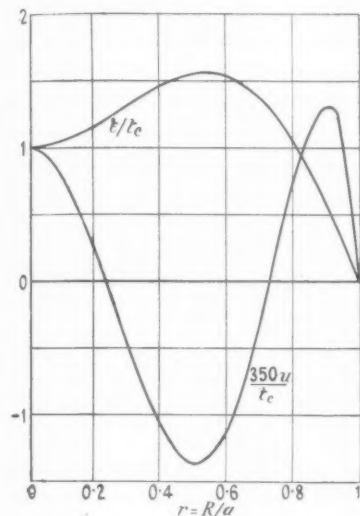


FIG. 5. Velocity and temperature profiles very near the closed end.

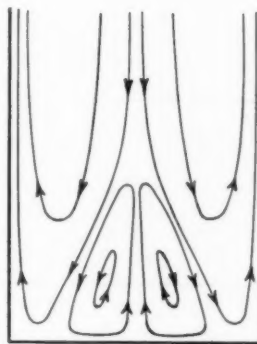


FIG. 6. Sketch of ring-vortex at closed end.

## 7. Synopsis of the laminar flow régimes

The calculations of sections 4, 5, and 6 are summarized in Fig. 7. For  $t_1 > 3400$  (if  $\sigma = \infty$ ) a flow is possible in which there is a central core of unheated fluid. The diameter of this core is least at the orifice, but the volume flow of fluid is greatest there. This is because, all the way down, the fluid in question is being drawn into the boundary layer, where it is heated and forced to change direction. The logarithmic graph of  $N_a$  against  $t_1$  in this region has the straight asymptote (corresponding to the vertical plate solution) shown, but it is noticeable that the deviation from this straight line is almost negligible even at the crossed point, where the solution ceases to have validity. This is because of the approximate cancelling out of two effects. The flow of cold fluid down the centre would increase the heat transfer (forced convection) if it were not that the whole scale of the motion is reduced by the increased viscous stresses.

Again, for  $t_1 < 5600$  (also if  $\sigma = \infty$ ), a flow is possible in which the minimum temperature over a cross-section increases from  $T_1$  at the orifice to  $T_0$  at the closed end. Naturally the heat-transfer rate is substantially lower. (Indeed, for  $t_1 < 311$ , the fluid in part of the tube is at rest, or at least its motion is negligible.) What is perhaps even more serious from a practical

point of view is its distribution along the tube; the local heat-transfer rate decreases steadily from the orifice to the closed end (except for a negligibly slight increase just before the end associated with the ring vortex of Fig. 6).

It is not clear from the figure at precisely what value of  $t_1$  the transition between the two régimes occurs, and it may be indefinite in the sense that there is a small range of values such that the steady state reached depends

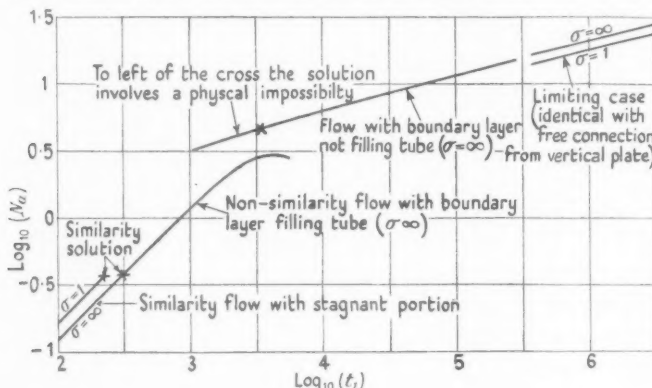


FIG. 7.

on the initial conditions. The heat-transfer rate might then exhibit hysteresis as the temperature  $T_0$  was increased or decreased with  $t_1$  in this range. But on the whole, from the form of the curves in Fig. 7, one would expect the transition to occur at the lower end of the range, near the crossed point.<sup>†</sup> If this is so, then one might recommend the tube as a heat transfer device for say  $t_1 > 4000$ , and adopt the 'fourth root' law (22) in this range.

With the aid of the limiting case curves for  $\sigma = 1$  one can visualize how the general shape of the intermediate curves discussed above might be altered for varying  $\sigma$ . Generally speaking, conditions change linearly with respect to  $\sigma^{-1}$ .

The rough rule emerging from the foregoing, that there is a critical value, equal to about 4000, of  $t_1 = G_a(a/l) = G_l(a/l)^4$ , above which  $N_a$  varies as

<sup>†</sup> It is interesting to inquire what property of the non-similarity flow characterizes this point at which the transition to the boundary layer régime is made. Actually the most striking such property is that about half the tube has a temperature profile with a local maximum at the axis, and half (the upper half) has one with a minimum there. Thus, the non-similarity solution persists until the average profile is just about to cease to have a minimum at the axis, and then the transition is made from this profile (already considerably flat at the axis) to a profile with a completely flat portion in the middle (outside the boundary layer). This observation will be found to be of suggestive value in the turbulent theory (section 11).

$t_1^{\frac{1}{2}}$ , and below which it varies as  $t_1$ , is evidently of great significance. For example if all quantities are fixed, including  $l$  but not  $a$ , then there is a critical radius  $a$  (for laminar flow), equal to about  $l(4000/G_l)^{\frac{1}{4}}$ , such that for greater radii the total heat transferred is proportional to  $a$ , and for smaller radii to  $a^4$ . Now one can imagine applications in which the *number* of holes used would depend on the radius, and might perhaps vary somewhat like  $a^{-2}$  (which would keep the porosity constant). Then the critical radius mentioned above would be the radius for maximum heat transfer. Actually, of course, a larger value than 4,000 in the formula for critical radius would preferably be used, owing to the approximate nature of these calculations, until they had been more closely checked experimentally.

Again, for fluid with given  $\rho$ ,  $c_p$ , and  $\sigma$ , the heat transfer will *increase* with viscosity in the upper range of values of  $t_1$  (because  $t_1 \propto v^{-2}$  and so  $Q \propto kN_a = \rho c_p \sigma^{-1} v N_a \propto v t_1^{\frac{1}{2}} \propto v^{\frac{1}{2}}$ ) and decrease with viscosity (like  $v^{-1}$ ) in the lower range. This means that there is an optimum viscosity, given everything else. It also means (what is more important) that the general effect of turbulence (which to the roughest approximation is like an increase of  $v$  without change of  $\rho$ ,  $c_p$  or  $\sigma$ ) will be to *decrease* heat transfer in the lower range of  $t_1$  from what it would be in laminar flow, and increase it in the upper range. Physically, this is because in the lower range the impeding of the flow is more important than the increased efficacy of the flow in transferring heat, and in the upper range the relative importance of these effects of turbulence is reversed. The quantitative extent of this distortion of the curve will be seen in section 11.

## 8. Turbulent flow: general considerations

There are two factors, in the laminar flow which has been described, which tend to make it become turbulent. First, the cross-sectional distribution of shear has a maximum in the fluid. Secondly, the temperature gradient upwards is negative. Also there are two factors resisting transition to turbulence, namely, viscous damping and the proximity of the walls. But these latter factors are present in straight pipe flow, where there is no shear maximum (except at the walls) and no temperature gradient. Hence in the present problem the transition Reynolds number may be expected to be considerably less than in straight pipe flow, and indeed Hermann (9) found that for free convection from both vertical plates and horizontal circular cylinders transition occurred when a Reynolds number based on maximum velocity and on boundary-layer thickness was about 300.

Wall roughness is unlikely to be important, because the velocities are only moderate in free convection flow. According to the predictions below, even for the largest modified Grashof numbers contemplated in the

engineering application, the velocities are such that walls on which there were no pimples of height exceeding 1 per cent. of the pipe diameter would be aerodynamically smooth. But conditions at entry to the tube will be considerably disturbed, whether the fluid enters from a large closed reservoir (continually stirred up by the discharge of heated fluid), or from a circulating system, or (as in the system of Fig. 1) from a region of mixing of the hot and cold fluids which have come together at the circumference and then flow away again down the middle. Thus it is advisable to assume low values of transition Reynolds numbers, corresponding to large entry disturbances.

The existence of three régimes of flow, corresponding to those of section 2 in laminar flow, and appearing in different ranges of values of  $G_a$  and  $l/a$ , is to be expected. But the range of  $l/a$  corresponding to the first régime, with the boundary layer not filling the tube, is doubtless reduced considerably owing to the more rapid thickening of turbulent layers. Conditions in the limiting case of this régime, when it is equivalent to convection from a vertical plate, can be obtained from Saunders's experiments (2) for  $G_l < 10^{11}$ , and by extrapolation for values of  $G_l$  beyond this. These yield the empirical formula†

$$N_a = 0.11 G_a^4. \quad (47)$$

But also, by analogy with the results of section 4, one may suppose that this is a good approximation throughout the limited range in which the first régime obtains, since the additional forcing of the convection by flow down the centre is balanced by a general reduction of velocity due to increased relative shear. But the cessation of this régime when the flux outside the boundary layer ceases to be a maximum at the orifice is made even more certain now that any fluid which has ever been in the boundary layer must continue to be turbulent.

It is the second and third régimes (which, as is clear from the above, have additional importance in turbulent flow) that present the most novel features to the fluid motion scientist and call for the formulation of new hypotheses if they are to be elucidated. The turbulence fills the whole tube, but the velocity distribution is very different from that of turbulent pipe flow, since it changes sign in the middle.

In these régimes, doubtless, the general scale of both the mean motion and the turbulence will decrease between the orifice and the closed end, just as it does for laminar flow. Probably, indeed, there is a short length

† Saunders gives this formula with both  $N$  and  $G$  based on the plate height  $l$ , but since  $l$  appears to the same (first) power on both sides of the equation it may be replaced by any other length, here the radius  $a$ . There is, of course, no *a priori* reason why heat transfer per unit area shall not be independent of the plate height. For, higher up the plate, the heat-transfer rate is increased owing to the higher velocities reached and decreased owing to the larger boundary-layer thickness, and these may cancel out.

of tube near the closed end where the local Reynolds number is so small (say about 100) that turbulence is rapidly damped out and the flow is effectively laminar. At least it will be convenient, in the theory to be developed, to take this transition to laminar flow as a sort of boundary condition at the closed end.

Now before developing any special hypotheses regarding turbulent exchange coefficients, we can at once observe an important difference between the properties of the similarity solution in laminar and turbulent flow, by writing down the equations of the mean motion and remembering that broadly the turbulent shearing stress varies as the square of a typical velocity. We may write the equations of the mean motion (compare (3) and (4)) in the form

$$\frac{\partial U}{\partial X} + \frac{\partial V}{\partial R} + \frac{V}{R} = 0, \quad U \frac{\partial T}{\partial X} + V \frac{\partial T}{\partial R} = \frac{1}{R} \frac{\partial}{\partial R} (Rq), \quad (48)$$

$$U \frac{\partial U}{\partial X} + V \frac{\partial U}{\partial R} = -f - \frac{1}{\rho} \frac{\partial p}{\partial X} + \frac{1}{R} \frac{\partial}{\partial R} (R\tau), \quad \frac{\partial p}{\partial R} = 0. \quad (49)$$

Here  $U$ ,  $V$ ,  $T$ ,  $p$  signify local mean values of the quantities so denoted previously;  $q$  signifies the mean rate of radial heat flow per unit area per unit time, divided by  $\rho c_p$  (the heat capacity per unit volume); and  $\tau$  signifies the mean shearing stress divided by the density  $\rho$ .

To eliminate the unknown pressure gradient  $\partial p / \partial X$  in (49), the device used in section 3 (subtracting the equation in the form it takes at the wall) is not really suitable because the gradient of shear stress at the wall is not a significant quantity in turbulent flow. It is better to subtract the mean value of the equation over the whole cross-sectional area (obtained by multiplying by  $R$ , integrating from  $R = 0$  to  $R = a$ , and dividing by  $\frac{1}{2}a^2$ ), giving

$$U \frac{\partial U}{\partial X} + V \frac{\partial U}{\partial R} - \frac{2}{a^2} \frac{\partial}{\partial X} \int_0^a RU^2 dR = \alpha f(T - T_m) + \frac{1}{R} \frac{\partial}{\partial R} (R\tau) + \frac{2\tau_0}{a}, \quad (50)$$

where  $\tau_0$  is the skin friction (namely minus the value of  $\tau$  at the wall) and  $T_m$  is the mean temperature across a cross-section, namely

$$T_m = \frac{2}{a^2} \int_0^a RT dR. \quad (51)$$

It might as well be said at once that the left-hand side of (50), representing the inertia of the mean flow, will always be neglected compared with the right-hand side, which represents the effect of buoyancy and shearing stress. This was found to be a reasonably good approximation in laminar flow, and is presumably better still in turbulent flow when shearing

stress is relatively more important. Thus the final form of the momentum equation, which with (48) governs the motion, is

$$\alpha f(T - T_m) + \frac{1}{R} \frac{\partial}{\partial R} (R\tau) + \frac{2\tau_0}{a} = 0. \quad (52)$$

Now in turbulent flow, to a very rough approximation, the order of magnitude of  $\tau$  at a cross-section varies as the square of the order of magnitude of  $U$ , while that of  $q$  varies as the product of those of  $U$  and  $T$ . It follows, by (52), that in a similarity solution the scale of  $T - T_0$  must vary with  $X$  like the square of the scale of  $U$ ; and by (48) that the scale of  $\partial T / \partial X$  must be the same as that of  $T$ . This means that the variation with  $X$  is exponential, not linear as with laminar flows. In fact to the rough approximation mentioned  $T - T_0$  varies like  $e^{\lambda X}$  and  $U$  like  $e^{\lambda X}$ , for some  $\lambda$ .

More exactly, there are two departures from the truth of this conclusion. First, since the simple laws for shearing stress and heat flow are only approximate,  $\lambda$  varies somewhat down the tube. In other words, if we replace  $\partial T / \partial X$  and  $\partial U / \partial X$  in the equations by  $\lambda(T - T_0)$  and  $\frac{1}{2}\lambda U$ , and solve them (see section 10), we shall find that  $\lambda$  varies. Secondly, the exponential mode of variation must cease somewhere or the tube would be infinitely long, and evidently this occurs at the transition to the laminar region, in which the variation with  $x$  becomes linear.

After a hypothesis regarding the turbulent exchange has been formulated in section 9, the similarity solution will be calculated in section 10. This will be found to hold for a particular value of  $l/a$ , which is a function of  $G_a$  but not as in laminar flow directly proportional to it. For larger values of  $l/a$  the additional length is expected to be stagnant. For smaller values of  $l/a$  a solution without similarity properties will be obtained in section 11.

As in the case of laminar flow the equations will be used only (i) at particular points and (ii) in an integrated form. The integrated forms of equations (48) are

$$\int_0^a RU dR = 0, \quad \frac{\partial}{\partial X} \int_0^a RUT dR = aq_0, \quad (53)$$

where  $q_0$  is the value of  $q$  at the wall. On the other hand, this integration gives no additional information in the case of equation (52), as is clear from the manner in which it was obtained. The equations of heat and momentum on the axis take the form

$$\left( U \frac{\partial T}{\partial X} \right)_{R=0} = 2 \left( \frac{\partial q}{\partial R} \right)_{R=0}, \quad \alpha f(T - T_m)_{R=0} + 2 \left( \frac{\partial \tau}{\partial R} \right)_{R=0} + \frac{2\tau_0}{a} = 0. \quad (54)$$

They will also be applied at the outer boundary of the so-called laminar and transition sub-layers (see section 9).

### 9. Hypothesis concerning exchange coefficients in confined turbulence

It is necessary to have a theory of the influence of the turbulence on the mean flow sufficiently detailed for skin friction and heat-transfer rate to be predicted; the kind of theory which assumes the values of these and then uses the integrated equations of motion to determine other properties of flow is useless here because of the depth of our ignorance. Now detailed theories of the influence of turbulence on the mean flow have always been based on hypotheses concerning the distribution of the 'exchange coefficient' or 'eddy kinematic viscosity'  $\epsilon$  defined by the equation

$$\tau = \epsilon \frac{\partial U}{\partial R} + \nu \frac{\partial^2 U}{\partial R^2}. \quad (55)$$

Here the turbulent component  $\epsilon \partial U / \partial R$  is less than the laminar component  $\nu \partial U / \partial R$  only near the wall; but there it becomes very small indeed. This is clear from Reynolds's expression for it as  $\bar{u}'\bar{v}'$  (the covariance of axial and radial flow velocities) which, as Reichardt (6) points out, falls to zero like  $(a-R)^3$ , since  $u'$  is proportional to  $a-R$  and  $v'$  to  $(a-R)^2$ . Away from the wall  $\epsilon$  greatly exceeds  $\nu$ . In this region it was for many years usual to apply mixing-length theories, which relate  $\epsilon$  to the local mean shear. These are now discredited and their success in certain problems ascribed to particular coincidental circumstances. In the present problem, where the velocity profile has three stationary values, the exchange coefficient would on momentum transfer theory have three corresponding zeros, which is absurd. Far from the turbulence being so small in scale that it reaches an equilibrium intensity depending only on local flow parameters, it rather seeks to fill the whole tube, at the walls of which the eddies have been described (7) as being 'anchored'. Near the wall the size and intensity of those eddies responsible for exchange is limited by the proximity of the wall, and it appears likely that this rather than the local mean shear is responsible for the well-known logarithmic profile.

These considerations lead to the hypothesis that the distribution of exchange coefficient in confined turbulent flows may depend solely on position and on some factor representing the scale of the turbulence; a reasonable such factor is the shear stress it produces at the wall. According to this hypothesis the distribution across a cross-section of factors tending to create turbulence is of no importance; only the average is of importance, as determining the scale of turbulent exchange. This is reasonable if turbulent energy is created in the form of large eddies. The mechanism by which

the turbulence transfers quantities in proportion both to their local gradient, and to a function characteristic of the local scale of the smaller eddies (the exchange coefficient), could then be that suggested by Townsend (8): the smaller eddies are rendered more nearly isotropic by energy transfer down the scale of eddy sizes, and at the same time oriented by the local shear (so that they cause a shearing stress), and a balance between these two effects determines the exchange coefficient.

Now in one problem of confined turbulence with smooth walls (flow through a straight pipe under a pressure gradient) the exchange coefficient has been determined from measurements of velocity distribution (with the help of theoretical considerations), for a wide range of values of the skin friction, by Reichardt (6). This can be taken over, according to the above hypothesis, for any flow in a circular pipe, including that at present discussed.

Reichardt's argument will be briefly recapitulated. In the flow through a straight pipe

$$(\epsilon + \nu) \frac{dU}{dR} = -\tau_0 \frac{R}{a}. \quad (56)$$

Now it is known that outside the 'laminar' and 'transition' sub-layers the velocity distribution is given to a good approximation by the formula

$$U = \frac{\sqrt{\tau_0}}{K} \log \left( A \sqrt{\tau_0} \frac{a-R}{\nu} \right), \quad K \approx 0.4, \quad A \approx 9. \quad (57)$$

Reichardt finds departure from this in the experimental values only very near  $R = 0$ , where the velocity gradient does not change sign quite discontinuously. Now, in the region outside the sub-layers,  $\epsilon \gg \nu$ , so that equations (56) and (57) give

$$\epsilon = K \sqrt{\tau_0} \frac{R(a-R)}{a}. \quad (58)$$

In particular when  $(a-R)/a$  is small (near the wall), we have approximately

$$\epsilon = K \sqrt{\tau_0} (a-R), \quad (59)$$

corresponding to the profile (57) holding in the region (sufficiently near the wall but outside the sub-layers) in which the shearing stress is effectively constant, i.e. in which

$$(\epsilon + \nu) \frac{dU}{dR} \approx -\tau_0. \quad (59a)$$

This profile has been verified for a variety of flows near a wall.

However, at the wall itself  $\epsilon$  must fall off like  $(a-R)^3$ , as observed above. And, indeed, if equation (59) held right up to the wall, the solution of equation (59a) with  $U = 0$  at  $R = a$  would be of the form (57) outside the sub-layers but with  $A = K$  instead of  $A > 20K$ . Reichardt finds that a

simple smooth curve for  $\epsilon$ , which starts to grow from the wall very slowly like  $(a-R)^3$  and then becomes asymptotic to (59) at about

$$(a-R)\sqrt{\tau_0/\nu} = 20$$

(corresponding to the boundary of the sub-layers), gives a formula (57) for  $U$  outside the sub-layers with the correct value of  $A$ . This gives a simple view of the laminar sub-layer as the region in which  $\epsilon$  is negligible and the transition sub-layer as the region in which it is changing from proportionality to  $(a-R)^3$  to proportionality to  $(a-R)$ .

Now it is important to notice that when this theory is applied the exact form of  $\epsilon$  in the sub-layers need not be used. For, provided that the shearing stress is effectively constant in the sub-layers, the velocity distribution in them must be the solution of (56) which vanishes at the wall. In particular, just outside the sub-layers it must take the form (57). The proviso is reasonable because even if some lateral gradient of shearing stress is required in the sub-layers to balance other axial forces, the sub-layers are so thin that the shearing stress in them cannot vary much from  $\tau_0$ .

Hence a satisfactory treatment of problems of flow in pipes should result from using a form of  $\epsilon$  appropriate to flow outside the sub-layers (and neglecting viscous stress there), and applying the wall-boundary condition

$$U - \frac{\sqrt{\tau_0}}{K} \log\left(A\sqrt{\tau_0}\frac{a-R}{\nu}\right) \rightarrow 0 \quad \text{as } R \rightarrow a. \quad (60)$$

The velocity distribution so determined will depart from the true one only in the sub-layers, where its detailed distribution has no effect on integrated quantities such as those in (53). The boundary condition (60) corresponds, therefore, to expressing the correctness of the momentum equation in the sub-layers, instead of at the wall as in the laminar theory.

It will be assumed that the same exchange coefficient governs the flow of heat as of axial momentum (the Reynolds analogy). This reasonable hypothesis has never been disproved. Note that it does not (as is sometimes believed) imply the equality of skin friction and heat transfer from the wall (when measured in suitable units), even for  $\sigma = 1$ , but rather causes departures from equality in the right direction (as Taylor (10) showed). On the hypothesis

$$q = (\epsilon + \kappa) \frac{\partial T}{\partial R}. \quad (61)$$

The boundary condition on  $T$  corresponding to (60) can be determined by solving the equation  $q = q_0$  in the sub-layers. The solution will take a particularly simple form,  $T - T_0 = -(q_0/\tau_0)U$ , if  $\nu = \kappa$ , i.e. if  $\sigma = 1$ . Since dependence on  $\sigma$ , for a given value of the modified Grashof number, is not

expected to be very great (judging from the results for laminar flow) the assumption  $\sigma = 1$  will be made henceforth. The boundary condition is then

$$T - T_0 + \frac{q_0}{K\sqrt{\tau_0}} \log\left(A\sqrt{\tau_0} \frac{a-R}{v}\right) \rightarrow 0 \quad \text{as } R \rightarrow a. \quad (62)$$

It is worth remarking that for any  $\sigma$  (62) would still be true if the value of  $A$  were modified; and that the true  $A$  lies between  $A$  and  $A\sigma$ .†

When the boundary conditions (60) and (62) are used the only remaining problem is the choice of  $\epsilon$  in the region outside the sub-layers. As remarked above, Reichardt finds that the equation (58), which with the boundary condition (60) is equivalent to the velocity distribution (57), produces velocities differing slightly from those observed; in fact the discontinuity in velocity gradient is slightly smoothed off in the observed distribution. This corresponds to a value of  $\epsilon$  which does not fall to zero at  $R = 0$  but rather flattens out to a central value of about half the maximum of (58).

However, in the present problem we are not interested in the fine structure of the velocity distribution. In fact it is *necessary* that we neglect it, since to apply a Pohlhausen-type method of calculation it is necessary to use velocity profiles of simple analytic character, whose shape does not suddenly alter near the centre. Also, since the centre is a point at which the equations will be forced to hold, it is desirable that it should be made typical of neighbouring points.

Hence, finally, the equations of section 8 will be used with

$$\tau = K\sqrt{\tau_0} \frac{R(a-R)}{a} \frac{\partial U}{\partial R}, \quad q = K\sqrt{\tau_0} \frac{R(a-R)}{a} \frac{\partial T}{\partial R}, \quad (63)$$

and the boundary conditions (60) and (62) at the wall. Here,  $\tau_0$  and  $q_0$  are functions of  $x$ , which are ultimately to be determined. Because the exchange coefficient vanishes at the centre the condition of evenness of  $U$ ,  $T$  (in the sense that  $\partial U/\partial R$  and  $\partial T/\partial R$  vanish at  $R = 0$ ) has to be abandoned, being replaced by a condition that  $U$  and  $T$  are finite at  $R = 0$ , which under this circumstance is just as restrictive as is the condition of evenness for non-zero exchange coefficient.

The equations (53) and (54), with (63), can be put into non-dimensional form by the substitutions

$$U = \frac{v}{aK} u, \quad T - T_0 = -\frac{v^2}{\alpha f a^3} t, \quad X = \frac{a}{K^2} x, \quad R = ar, \quad (64)$$

† The Grashof numbers and modified Grashof numbers coincide for  $\sigma = 1$ . Hence the results will be given in terms of Grashof number. But it remains true that for fluids with  $\sigma \neq 1$  the results probably have slightly more value when the Grashof number is interpreted as a modified Grashof number, and the above remark provides a reason for this.

the  
hen  
62)  
of A  
ing  
oked  
ary  
ences  
uity  
on.  
but  
8).  
ruc-  
it,  
y to  
not  
ich  
ade  
  
(63)  
are  
nge  
the  
ing  
this  
zero  
  
nal  
  
64)  
the  
with  
eted

$$\int_0^1 ru \, dr = 0, \quad \frac{\partial}{\partial x} \int_0^1 rut \, dr = -QR, \quad (65)$$

$$\text{with } u \frac{\partial t}{\partial x} = 2R \frac{\partial t}{\partial r}, \quad t - \frac{1}{2} \int_0^1 rt \, dr = 2R \frac{\partial u}{\partial r} + 2R^2 \quad (66)$$

holding on  $r = 0$ . Here  $R$  is  $\alpha \sqrt{\tau_0 / \nu}$ , the Reynolds number based on the local wall shearing stress, and

$$Q = \frac{\alpha f a^3 q_0}{K \nu^2 \sqrt{\tau_0}}. \quad (67)$$

With the new variables the boundary conditions (60) and (62) become

$$u - R \log\{AR(1-r)\} \rightarrow 0, \quad t - Q \log\{AR(1-r)\} \rightarrow 0 \quad \text{as } r \rightarrow 1. \quad (68)$$

An advantage of the equations in the form (65), (66), and (68) is that the empirical constant  $K$  has been eliminated.

### 10. The similarity régime (turbulent flow)

As stated in section 8, the similarity régime with  $T - T_0 \propto e^{\lambda x}$ ,  $U \propto e^{\lambda x}$  is only approximately achieved in turbulent flow. However, if in (65) and (66) we replace  $\partial(ut)/\partial x$  by  $\frac{3}{2}\lambda ut$  and  $\partial t/\partial x$  by  $\lambda t$ , then we find solutions for which both the shape of the velocity and temperature profiles vary only slowly with  $x$ . The substitutions are therefore permissible, similarity being approximately achieved in the sense that the profiles change shape with  $x$  much more slowly than they change scale.

As profiles satisfying (68) we choose

$$u = R[\log(1-r) + B - C(1-r)], \quad t = Q[\log(1-r) + B + D(1-r)], \quad (69)$$

where  $B = \log(AR)$ . Then the first of equations (65) gives

$$C = 3B - \frac{9}{2}, \quad (70)$$

and the second of equations (66) gives then

$$Q\left(\frac{9}{2} + \frac{2}{3}D\right) = 2R^2(3B - \frac{9}{2}). \quad (71)$$

The first of equations (66), with  $d/dx$  replaced by  $\lambda$ , gives (after substituting for  $C$  from (70))

$$R\left(\frac{9}{2} - 2B\right)\lambda Q(B+D) = -2RQ(1+D) \quad (72)$$

and the second of equations (65), with  $d/dx$  replaced by  $\frac{3}{2}\lambda$ , gives

$$\frac{3}{2}\lambda RQ\left(\frac{9}{8} - \frac{1}{3}B + \frac{17}{12}D - \frac{1}{12}BD\right) = -QR. \quad (73)$$

Eliminating  $\lambda$  from (72) and (73) we obtain

$$(81 - 24B + 17D - 6BD)(D+1) = 12(9 - 4B)(B+D). \quad (74)$$

The solution of (74) for  $D$  is given as a function of  $B$  in Table 3. It is interesting that in the range of values of  $B$  which is of greatest practical interest (which will be found to be the range  $5 < B < 8$ ) the coefficient  $D$  is practically constant at 10.5. The associated values of  $\mathbf{R} = e^B/A$  (with  $A$  taken as 9),  $\mathbf{Q}$  from (71), and  $t_c = \mathbf{Q}(B+D)$ , the value of  $t$  at  $r=0$ , which is a sort of local Grashof number, are also given. It is worth noticing that  $t_c$  is approximately  $10^{B-1}$  in each case. The product  $\mathbf{QR}$  is a non-dimensional form

$$\mathbf{QR} = \frac{\alpha g a^4}{K \nu^3} q_0 \quad (75)$$

of the local heat transfer rate.  $N_X$  is the Nusselt number based on the total heat transfer from the part of the tube below the cross-section  $X$ , and on the length  $X$ . Thus

$$\begin{aligned} N_X &= \frac{1}{k(T_0 - T_c) 2\pi X a / X} \int_0^X \rho c_p q_0 2\pi a dX = \frac{1}{\kappa(T_0 - T_c)} \int_0^X q_0 dX \\ &= \frac{1}{K t_c} \int_0^x \mathbf{QR} dx = \frac{\mathbf{QR} (\frac{1}{12} BD - \frac{17}{72} D + \frac{1}{3} B - \frac{9}{8})}{K \mathbf{Q}(B+D)}. \end{aligned} \quad (76)$$

It has been computed below taking  $K = 0.4$ .

TABLE 3

$B$	$D$	$\mathbf{R}$	$\mathbf{Q}$	$t_c$	$\mathbf{QR}$	$N_X$	$\lambda$
4	12.5	6.07	56	$9.9 \cdot 10^3$	$3.4 \cdot 10^2$	1.31	.468
5	10.6	16.5	$6.6 \cdot 10^2$	$1.04 \cdot 10^4$	$1.1 \cdot 10^4$	7.8	.271
6	10.3	44.8	$6.5 \cdot 10^3$	$1.05 \cdot 10^5$	$2.9 \cdot 10^5$	24.7	.185
7	10.4	122	$5.8 \cdot 10^4$	$1.01 \cdot 10^6$	$7.1 \cdot 10^6$	84.3	.138
8	10.7	331	$5.0 \cdot 10^5$	$9.3 \cdot 10^6$	$1.64 \cdot 10^8$	272	.109
9	11.1	900	$4.1 \cdot 10^6$	$8.2 \cdot 10^7$	$3.7 \cdot 10^9$	850	.089

Finally  $\lambda$  (obtained from (72) or (73)) tells us how the quantities vary with  $x$ , in virtue of the relations

$$\frac{dt_c}{dx} = \lambda t_c, \quad x = \int \frac{d(\log t_c)}{\lambda}. \quad (77)$$

The integral (77) for  $x$  is made definite by considering the transition to laminar flow, which, as explained in section 8, must occur near the closed end when the Reynolds number falls to such a value that disturbances are rapidly damped out. If the transition value of  $B$  is  $B_T$ , then by a combined use of (77) and the result of section 5 for  $\sigma = 1$  we have

$$x = K^2 \frac{t_c(B_T)}{227} + \int_{B_T}^B \frac{d(\log t_c)}{\lambda}, \quad (78)$$

bearing in mind that  $t_c(B_T)$  is the Grashof number based on the radius and on the central temperature at the transition point, and that  $x = k^2 X/a$ .

The value of  $B_T$  is rather difficult to forecast at all precisely, but fortunately equation (78) is very little sensitive to it. It is almost certainly between 4 and 5. Thus for  $B = 4$  the Reynolds numbers based on the radius and on the maximum upward and downward velocities respectively are 15 and 50; while for  $B = 5$  they are 70 and 250. Taking into account Hermann's observation of 300 as a typical Reynolds number based on maximum upward velocity and on boundary-layer thickness at which turbulence set in for free convection flow up a vertical plate, but remembering that a much lower value is required if existing large disturbances are to be speedily damped out, and remembering also that the net difference of velocity across the inner shear layer gives a Reynolds number obtained by adding those mentioned—but, on the other hand, that the complete confinement of the flow by walls must assist the damping-out process—we may reasonably fix on a value  $B_T = 4.5$ , at which (by logarithmic interpolation in the above table)

$$(76) \quad R = 10.0, \quad Q = 200, \quad t_c = 3.2 \cdot 10^3, \quad QR = 2000, \quad N_x = 3.45, \\ \lambda = 0.340. \quad (79)$$

Then the length of tube with laminar flow is  $3.2 \cdot 10^3 / 227 = 14$  radii. This assumes that the similarity régime occurs also in the laminar region. This can be checked by comparing the value of  $N_x$  in the laminar and turbulent flows at the join. This is the only parameter (representing total rate of heat transfer across the join) which must remain continuous however complicated the mixing process at the transition point. But for the laminar similarity solution with  $l/a = 14$  and  $\sigma = 1$  we have

$$N_l = 14N_a = 14(0.360) = 5.0,$$

which is of the right order of magnitude. (Actually any of the non-similarity flows filling the tube give also the right order of magnitude for  $N_x$ , and some of them give much smaller lengths of tube with laminar flow; it is quite likely that one of these actually occurs. But in any case, even the 14 radii are small compared with the total length of tube required for the similarity régime.)

It should be noted that the whole theoretical basis of the method of calculation is at fault for values of  $R$  as low as 10. In fact for  $B < 6$  ( $R < 45$ ) the assumption that the sub-layers fill only a small part of the tube is incorrect; and at the transition value  $B = 4.5$  the laminar sub-layer  $(a-R)\sqrt{\tau_0/\nu} < 10$  actually fills the whole tube. Thus for  $B < 6$  the formulae can be regarded only as interpolations between the laminar and fully developed turbulent flow régimes.

The integration in (78) was carried out graphically, giving a relationship between  $X/a$  and  $B$ . This is also the relationship between  $l/a$  and the orifice value of  $B$ , which determines, by Table 3, the orifice values of  $t_c$  and  $N_x$ , which are  $G_a$  and  $N_l$ . The results are finally obtained in the form of graphs of  $G_a$  and  $G_l = (l/a)^3 G_a$  and  $N_l$  and  $N_a = N_l a/l$  against  $l/a$  for the turbulent similarity régime. The results were also determined by an approximate method which will be developed in section 11, and there was good agreement. These results are shown in Fig. 9 below as the curves marked  $D = 10.5$ . It is seen that for the larger Grashof numbers the length of tube required to attain the similarity solution is very great, and also that the heat transfer remains only very moderate, as in the laminar similarity régime.

### 11. Turbulent flow filling the tube without similarity

Now also in the non-similarity régime we shall seek solutions of (65) and (66) in the form (69), and then the condition of conservation of mass and the momentum equation at the axis again give (70) and (71). But in the other two conditions  $d/dx$  can no longer be replaced by a constant, and accordingly they are

$$(4B-9) \frac{d}{dx} [Q(B+D)] = 4Q(1+D), \quad (80)$$

and

$$\frac{d}{dx} [RQ\{(6B-17)D+3(8B-27)\}] = 72RQ, \quad (81)$$

instead of (72) and (73).

Now it would be quite possible to solve (80) and (81) numerically, subject to  $B = \log(AR)$  and (71), as simultaneous differential equations. However, it would be very laborious, and the author accordingly took a simpler course, suggested by a property of the similarity solution. This was the property that  $D$  was practically independent of  $x$ . This makes it likely that, to a sufficient approximation, in the solutions appropriate for tubes which are shorter (for a given Grashof number),  $D$  is also a constant, but not the same one. This assumption makes it possible to discard one of the equations (80) and (81), and it is reasonable to discard the former, which expresses conservation of heat at the axis (and is in any case somewhat doubtful because of uncertainty regarding the form of  $\epsilon$  on the axis), in favour of the latter, which expresses a net balance of heat transfer for a whole cross-section. Then three equations have been retained, expressing conservation of heat, mass, and momentum respectively. The additional parameter  $D$  (a constant, but different for different solutions) permits the application of the theory to tubes of various length-radius ratios.

Now by (71), on this hypothesis,

$$\frac{1}{Q} \frac{d\mathbf{Q}}{dx} = \frac{2}{R} \frac{dR}{dx} + \frac{2}{2B-3} \frac{dB}{dx} = \frac{4(B-1)}{2B-3} \frac{dB}{dx}, \quad (82)$$

since  $\log(AR) = B$ . Hence, by (81),

$$\begin{aligned} \frac{dB}{dx} & \left( 1 + \frac{4(B-1)}{2B-3} + \frac{6D+24}{(6B-17)D+3(8B-27)} \right) \\ & = \frac{72}{(6B-17)D+3(8B-27)}, \end{aligned} \quad (83)$$

and so

$$\frac{dx}{dB} = x'_0(B) + Dx'_1(B), \quad (84)$$

where one finds after some reduction that

$$\begin{aligned} x_0(B) &= \frac{1}{2}B^2 - \frac{65}{24}B - \frac{5}{8}\log(2B-3) + \text{const} \\ x_1(B) &= \frac{1}{8}B^2 - \frac{13}{24}B - \frac{1}{9}\log(2B-3) + \text{const}. \end{aligned} \quad (85)$$

The constants are chosen to make  $x_0$  and  $x_1$  vanish for the 'transition' value  $B = B_T = 4.5$ . The functions so obtained are tabulated in Table 4.

TABLE 4

$B$	4.5	5	6	7	8	9
$x_0(B)$	0	-92	3.56	7.22	11.91	17.61
$x_1(B)$	0	-306	1.112	2.173	3.487	5.055

This table shows clearly the influence of varying  $D$ . The similarity solution with large  $D = 10.5$  (corresponding, by (69), to a highly peaked temperature distribution) is only possible for a very long tube, owing to the term  $Dx_1(B)$  in  $x$ . As  $D$  decreases we have solutions corresponding to shorter and shorter tubes, with the temperature distribution flatter and flatter in the middle. This is illustrated in Fig. 8. The limit of this state of affairs is given by  $D = -1$ , when the temperature gradient at the middle vanishes, and therefore a transition to a flow régime with a boundary layer not filling the tube may reasonably be expected. (Note that for  $D < -1$  the axis would become a local *maximum* of temperature.) This is precisely analogous to the state of affairs exhibited in the laminar case (section 6), when the transition from the non-similarity flow filling the tube to the boundary layer type of flow occurred (section 7) very near the value at which the average temperature distribution ceased to have a minimum value on the axis.

For each of the possible flow régimes in the range  $-1 \leq D \leq 10.5$  we need to know not only  $x$  but also

$$t_c = Q(B+D) = \frac{18e^{2B}(2B-3)(B+D)}{A^2(9+4D)} \quad (86)$$

and

$$N_x = \frac{e^B(\frac{1}{12}BD - \frac{17}{72}D + \frac{1}{3}B - \frac{9}{8})}{AK(B+D)} \quad (87)$$

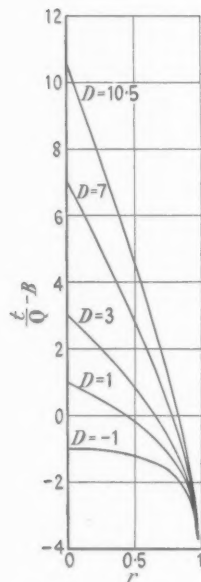


FIG. 8. The shapes of temperature profile in the turbulent flow.

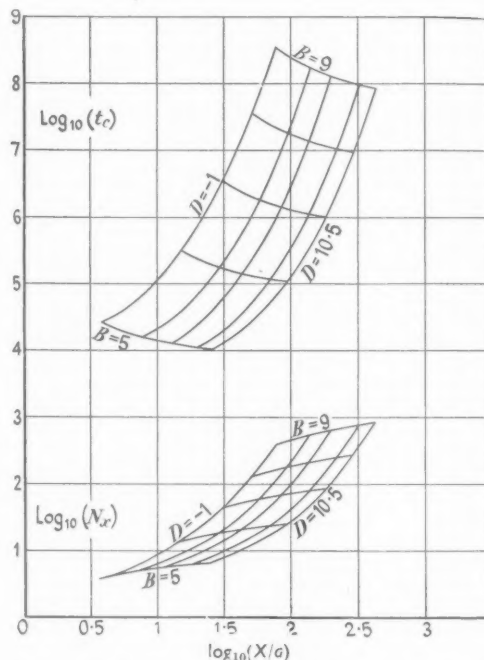


FIG. 9. Variation of  $t_c$  (Grashof number based on radius and on temperature difference between wall and axis) and  $N_x$  (Nusselt number based on length of tube) with  $X/a$ , keeping (i)  $B$  equal to 5, 6, 7, 8, 9 (ii)  $D$  equal to  $-1, 1, 3, 7, 10.5$ .

as functions of  $B$ . From calculations of these  $t_c$  and  $N_x$  have been plotted against  $X/a$  (calculated as  $k^{-2}x = 6.25x$ ) for  $B = 5, 6, 7, 8, 9$  and for  $D = -1, 1, 3, 7, 10.5$  in Fig. 9. Here no allowance has been made for the length of the laminar region. This is because the values of  $N_x$  and  $t_c$  at the transition value of  $B$  (namely 4.5) indicated a solution with large  $t_1$  as most likely in the laminar range, so that the length  $at_c/t_1$  of the laminar range is probably negligible. In fact  $N_x/t_c$  takes values which range from  $9.6 \cdot 10^{-4}$

(for the similarity solution  $D = 10 \cdot 5$ ) to  $2 \cdot 2 \cdot 10^{-4}$  (for  $D = -1$ ). Regarding these as end values for a laminar flow,  $N_X/t_c$  is the same as  $N_a/t_1$ , which takes the above values for values of  $t_1$  of the order of  $10^4$ , leading (since  $t_c$  is if anything smaller than  $10^4$ ) to lengths of laminar flow of less than one radius.

The variation of heat transfer along the tube for a given flow  $D = \text{constant}$  can be observed from Fig. 9. For the local heat-transfer rate is proportional to  $d(N_X t_c)/dx$ . It is seen that even for  $D = -1$  it varies very rapidly, like the fourth or fifth power of  $X/a$ . In a practical application the resulting reduced heat transfer rate near the closed end would be most unfavourable.

## 12. Synopsis of the turbulent and laminar flow régimes

In Fig. 10 a cross-plot is made from Fig. 8 for six values of  $l/a$ , after  $X$  has been put equal to  $l$  so that  $N_X = N_l$  and  $t_c = G_a$ . The cross-plot is of  $N_a = N_l(a/l)$  against  $G_a$ , for  $l/a = 5, 10, 20, 50, 100$ , and  $200$ , and is indicated by the dash-dotted lines in Fig. 10. In each case the curve is joined smoothly by a broken line to the laminar solution (shown as a full line), at the value of  $G_a$  corresponding to  $B = 5$ . (A slightly higher value of  $B$  is used for the spontaneous appearance of turbulence, even under large entry disturbances, than was used above for the disappearance of fully developed turbulence.) Also, at the upper end of the curve, corresponding to  $D = -1$ , a dotted line is shown to indicate the transition (see above) to the régime in which the boundary layer does not fill the whole tube. In this régime  $N_a$  and  $G_a$  are related according to equation (47).

The position of the similarity régime is indicated on each curve by a cross. For  $l/a = 5, 10$  and  $20$  this occurs in the laminar part, but for  $l/a = 50, 100$  and  $200$  there is a turbulent similarity régime instead. The dash-dotted curves below the crosses were obtained by supposing that the tube is filled by the similarity flow plus a stagnant region. None of these curves has been allowed to fall quite as low as the value of  $N_a$  predicted by theory for  $B = 5$ , for which value (as explained in section 10) the theory has little foundation; they have been permitted to begin departing from the theoretical curve from about  $B = 5 \cdot 5$ , although only rising sharply at the value of  $G_a$  corresponding to  $B = 5$ .

It is seen that transition is predicted when  $G_a$  is between  $10^4$  and  $2 \cdot 10^4$ . But it should be emphasized that this prediction, which makes the laminar régime play only a small part, is based on the hypothesis of large entry disturbances (of scale comparable with the tube diameter and typical velocities in the flow). With care taken to obtain smooth entry conditions it should be possible in the laboratory to reproduce most of Fig. 7. But in engineering applications the author expects Fig. 10 to be nearer the truth.

The (at first sight surprising) 'bucket' in each curve is due to the fact explained at the end of section 7, that transition to turbulence in the régime in which heated fluid fills the whole tube causes reduced heat transfer, because the impeding of the flow is then more serious than the increased effectiveness of the flow in transferring heat, while on the other hand the position is reversed once a boundary-layer régime has been set up. This explains the very large rise in heat transfer (by a factor exceeding 10) when

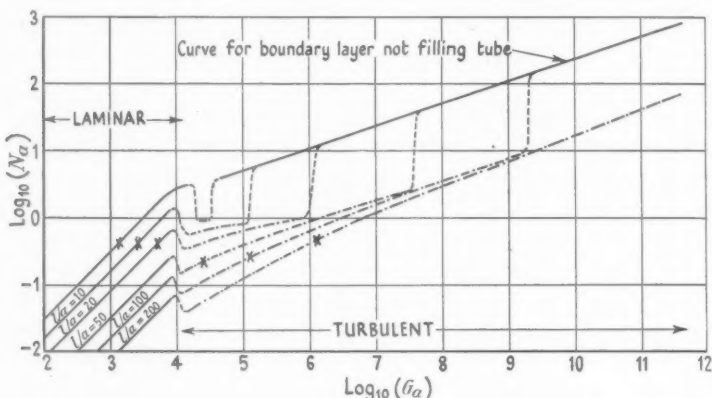


FIG. 10. Relationship between  $N_a$  and  $G_a$  for six values of the length-radius ratio, with position of transition to turbulence chosen on the assumption of large entry disturbances. Similarity solutions shown with a cross.

the boundary-layer régime appears. The author believes that this rise has at any rate not been overestimated owing to the extrapolation of Saunders's results far beyond the range in which they were observed, because according to general experience with boundary layers one would expect the variation of  $N_t$  with  $G_t$  to be as the  $\frac{2}{5}$ th rather than the  $\frac{1}{3}$ rd power, for large  $G_t$ , so that the upper curve in Fig. 10 may be placed too low.

In Fig. 11 the critical Grashof number, based on *length*, at which the large rise in heat transfer occurs, is plotted against the length-radius ratio as a full-line curve, the broken lines giving the results of the laminar and turbulent theories separately. The transition between the curves has been made to take place between  $B = 5$  and  $B = 6$ . This curve (or, later, one corrected in the light of experiment) would be used most often to determine the tube radii in terms of their length and the other constants of the problem. It is clear from all that has been said that to get best results the point  $(l/a, G_t)$  should lie on the left-hand side of the curve.

Another mode of presentation of the results, particularly useful in section 13, is given in Fig. 12. Here a special non-dimensional form

$$N_t G_a = \frac{\alpha f a^2}{2\pi k \nu \kappa} Q \quad (88)$$

of the heat transfer rate  $Q$ , not bringing in the tube length or temperature difference, is plotted against  $G_a$  for various values of  $l/a$ . This displays the effect of length (for given radius) and temperature difference separately.

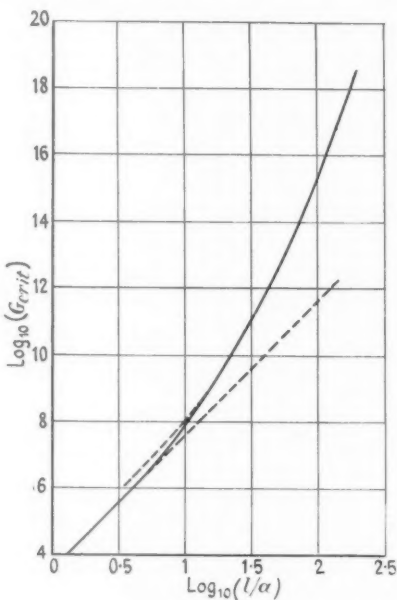


FIG. 11. The critical Grashof number (based on length), at which flow with boundary layer not filling tube is predicted to set in, as a function of the length-radius ratio.

It is seen that conditions in which an increase in length reduces heat transfer (by breaking up the flow in which the boundary layer does not fill the tube) are common, but that cases in which an increase in temperature difference has this effect are negligibly rare.

To conclude this section it must be repeated that all the results of this paper, and especially those relating to turbulent flow (as being based on more doubtful hypotheses) must be regarded as purely tentative in the

absence of experimental confirmation. They probably have little more than suggestive value, in guiding experimental workers in what to look for.

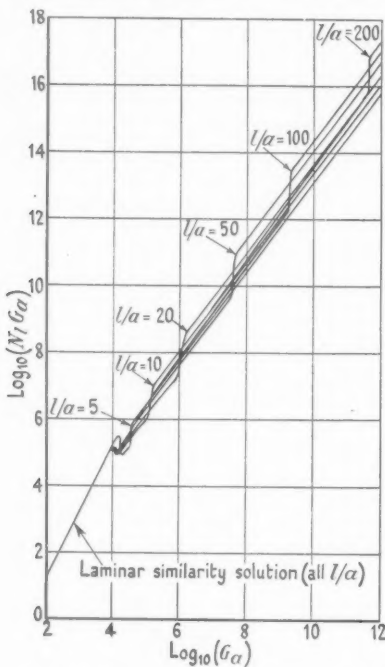


FIG. 12. Curves of the non-dimensional form of the heat transfer rate which does not involve the tube length or the temperature difference, namely  $N_t G_a = (\alpha f a^2 / 2\pi k \nu) Q$ , against  $G_a$  for various values of  $l/a$ .

### 13. Flow in a completely closed tube, part heated and part cooled

An attempt is now made to apply the above theory to the conditions illustrated in Fig. 1. Here the difficulty arises in the treatment of the complicated mixing process which occurs at the join between the heated and cooled portions of the tube, where the two circumferential flows come into direct collision. It is natural to try to treat this region by supposing that it is of limited extent and approximating it by a discontinuous join between two solutions of the type discussed in sections 2–12. But if the flow is to be completely determined it is necessary that two conditions can be applied at the join, relating the flows which mix there.

Two conditions which are evidently applicable are that the total flow

across a cross-section of both mass and heat are continuous at the join. But only the second of these is a condition that gives any information, equating the total rates of heat transfer in the two portions of the tube. For of course in all solutions the total mass flow across any cross-section is zero.

It would be natural, as a second condition, to express continuity of total momentum flux at the join. But this condition need not be satisfied, because there is nothing to prevent a substantial pressure difference between the two portions of the tube from building up; and in any case the condition would be unsuitable since inertial forces have been neglected.

Instead we apply a condition that the mixing is 'complete', in the sense that at least the fluid that flows away from the mixing region down the axis has the same temperature on both sides. This condition is probably somewhere near the truth since the mixing is highly forced.

The problem then reduces to determining two flows of the type of sections 2-12, with the same values of  $T_1$  and  $Q$ , but with different values (in general) of all other constants. These different sets of values will be denoted by the symbols  $H$  for the heated portion (with walls at temperature  $T_{0H}$ ) and  $C$  for the cooled portion ( $T_{0C}$ ). The physical constants of the fluid will be given values appropriate to temperatures near these values in the two portions. The external acceleration  $f$  (if centrifugal) may similarly have different average values  $f_H$  and  $f_C$  therein. Then

$$G_{aH} = \frac{\alpha_H f_H a^3}{\nu_H \kappa_H} (T_{0H} - T_1), \quad G_{0C} = \frac{\alpha_C f_C a^3}{\nu_C \kappa_C} (T_1 - T_{0C}). \quad (89)$$

Hence, introducing the two known constants

$$G_{aH}^C = \frac{\alpha_H f_H a^3}{\nu_H \kappa_H} (T_{0H} - T_{0C}), \quad G_{aC}^H = \frac{\alpha_C f_C a^3}{\nu_C \kappa_C} (T_{0H} - T_{0C}), \quad (90)$$

we have

$$\frac{G_{aH}}{G_{aH}^C} + \frac{G_{aC}}{G_{aC}^H} = 1 \quad (91)$$

as a relation between the unknowns  $G_{aH}$  and  $G_{aC}$ . Expressing also that the heat-transfer rate

$$Q = 2\pi a k_H (T_{0H} - T_1) N_{aH} = 2\pi a k_C (T_1 - T_{0C}) N_{aC} \quad (92)$$

is continuous, and using (89), we have

$$\frac{N_{aC} G_{aC}}{N_{aH} G_{aH}} = \frac{\alpha_C f_C / k_C \nu_C \kappa_C}{\alpha_H f_H / k_H \nu_H \kappa_H}. \quad (93)$$

The product  $N_a G_a$ , whose values in the two portions of the tube, by (93), have a ratio predictable in advance, is that plotted against  $G_a$  for different values of  $l/a$  in Fig. 12.

Now, given the constants of the problem, assume  $G_{aH}$  as some suitable

value about half as much as  $G_{aH}^C$  and deduce  $N_H G_{aH}$  from Fig. 12 (using  $l/a = l_H/a$ ). Deduce  $N_C G_{aC}$  by (93), and infer  $G_{aC}$  from the graph (using  $l/a = l_C/a$ ). Now recalculate  $G_{aH}$  from (91). Using this second approximation to  $G_{aH}$  repeat the process. The usual methods for speeding solution by successive approximations may be used to reach finally a set of values which satisfies all the equations.

Without doing this calculation, we may predict that it is unwise to use values of  $l_C$  and  $l_H$  which differ too much, since the heat-transfer rates from the two portions must be equal.

Here the calculations will be done only for the case when both portions of the tube have Grashof numbers above the critical, so that  $N_a \propto G_a^{\frac{1}{4}}$ ,  $N_l \propto (l/a)G_a^{\frac{1}{4}}$ . Then, by (93),

$$\frac{G_{aC}}{G_{aH}} = \left( \frac{\alpha_C f_C / k_C v_C \kappa_C l_C}{\alpha_H f_H / k_H v_H \kappa_H l_H} \right)^{\frac{3}{4}}, \quad (94)$$

and it follows by (91) that

$$\frac{G_{aH}}{G_{aH}^C} = \frac{T_{0H} - T_1}{T_{0H} - T_{0C}} = \left[ 1 + \left( \frac{\alpha_H f_H k_H^3 l_H^3 / v_H \kappa_H}{\alpha_C f_C k_C^3 l_C^3 / v_C \kappa_C} \right)^{\frac{1}{4}} \right]^{-1}. \quad (95)$$

(As suggested in section 1, this is  $\frac{1}{2}$  when all constants are uniform.)

Hence the Nusselt number based on the total temperature difference,

$$\begin{aligned} N_{IH}^C &= \frac{Q}{2\pi a k_H (T_{0H} - T_{0C})} = N_{IH} \frac{G_{aH}}{G_{aH}^C} = \frac{l_H}{a} 0.11 G_{aH}^{\frac{1}{4}} \frac{G_{aH}}{G_{aH}^C} \\ &= 0.11 \frac{l_H}{a} (G_{aH}^C)^{\frac{1}{4}} \left[ 1 + \left( \frac{\alpha_H f_H k_H^3 l_H^3 / v_H \kappa_H}{\alpha_C f_C k_C^3 l_C^3 / v_C \kappa_C} \right)^{\frac{1}{4}} \right]^{-\frac{4}{3}}. \end{aligned} \quad (96)$$

If all constants are given, including  $l_H + l_C$  but not the ratio  $l_H/l_C$  then (96) is a maximum if

$$\frac{l_H}{l_C} = \left( \frac{\alpha_C f_C k_C^3 / v_C \kappa_C}{\alpha_H f_H k_H^3 / v_H \kappa_H} \right)^{\frac{1}{7}}, \quad (97)$$

which will not be very far from 1 in practice.

There will also be a condition on  $l_H/l_C$  in order that  $G_{aH}$  and  $G_{aC}$  shall be supercritical with as much as possible to spare. This means that the smaller of  $G_{aH}(l_H/a)^{-M}$  and  $G_{aC}(l_C/a)^{-M}$  shall be as large as possible, where  $M$  is the slope of  $\log(G_{a\text{crit}})$  against  $\log(l/a)$ , for values of  $l/a$  near half the total length-radius ratio; thus  $M$  is three less than the slope of the curve of Fig. 10 at this point. Now it is fairly clear that the two quantities alter in opposite directions as  $l_H/l_C$  is altered, so that the maximum minimum is achieved when they are equal, which gives

$$\frac{l_H}{l_C} = \left( \frac{\alpha_H f_H / k_H v_H \kappa_H}{\alpha_C f_C / k_C v_C \kappa_C} \right)^{3/(4M+3)}. \quad (98)$$

Since  $M$  lies between 1 and 8, (98) also means a value of near 1, especially for large total lengths. Thus although (97) and (98) would normally be incompatible, one could satisfy the more important one, namely (98), without departing very far from the maximum heat transfer condition given by the other.

## REFERENCES

1. *General Discussion on Heat Transfer*, sec. IV (Institution of Mechanical Engineers, 1951).
2. O. A. SAUNDERS, *Proc. Roy. Soc. A*, **157** (1936), 278-91.
3. W. H. MCADAMS, *Heat Transmission*, 2nd edn. (McGraw-Hill, 1942).
4. E. SCHMIDT and W. BECKMAN, *Tech. Mech. Thermo*. **1** (1930), 341-9 and 391-406.
5. S. GOLDSTEIN (Edit.) *Modern Developments in Fluid Dynamics* (Oxford, 1938).
6. H. REICHARDT, *Z.A.M.M.* **31** (1951), 171-84.
7. A. A. TOWNSEND, *Proc. Camb. Phil. Soc.* **47** (1950), 375-95.
8. —— *Phil. Mag.* **41** (1950), 890-906.
9. R. HERMANN, *Ver. deutsch. Ing. Forschungsheft*, **379** (1936), 1-24.
10. G. I. TAYLOR, *Proc. Roy. Soc. A*, **129** (1930), 25-30.

## NOTE ADDED IN PROOF

Since the above was written Mr. B. W. Martin, Lecturer in Mechanical Engineering at King's College, Newcastle, has done some experiments on the system studied in sections 2-12, with glycerine as the working fluid and  $l/a = 47.5$ . The modified Grashof number  $G_a$ , based on tube radius and on the values of the fluid properties at the temperature of the wall, ranged from about 600 to  $3 \cdot 10^6$ . Turbulence is believed to have begun to appear only at the highest values of  $G_a$  that were attained, and to have been absent at  $G_a = 1.5 \cdot 10^6$ . This seems to indicate that transition values of  $G_a$  are a lot higher than has been assumed in the paper, although it should be noticed that these values of  $G_a$  are based on the viscosity of the very hot glycerine at the wall, and that the cold glycerine at the centre of the tube had a much higher viscosity, which will have tended to damp turbulence starting up there.

The lower curve in Fig. 7 is confirmed in shape for  $1.0 < \log_{10} t_1 < 3.4$ , but the experimental points lie above the curve by about 0.25. The upper curve is well confirmed for  $4.3 < \log_{10} t_1 < 4.7$ . Between these ranges the flow exhibited regular periodic oscillations which are believed to be associated with the existence of the two possible steady flow régimes (according as the boundary layer does or does not fill the tube) of sections 4 and 6; these oscillations sometimes occurred for  $\log_{10} t_1$  as low as 3. The amplitude was greatest around  $\log_{10} t_1 = 3.5$ , beyond which it decreased as  $t_1$  increased, until at  $\log_{10} t_1 = 4.3$  (that is, at  $G_a = 10^6$ ) the oscillations had disappeared, although it is believed that turbulence had not yet set in.

Thus the presence of two curves in Fig. 7 appears to represent not a mathematical error but a genuine physical uncertainty, which is resolved in practice by the appearance of an oscillatory flow. However, it remains to be seen whether the above interpretation of Mr. Martin's experiments is confirmed by further study. His investigations will be published when they have reached a more advanced and conclusive stage; the author is grateful for being permitted to include the above brief reference to them.

# THE PROPAGATION OF SHOCK WAVES IN A CHANNEL OF NON-UNIFORM WIDTH

By W. CHESTER (*Dept. of Mathematics, The University, Bristol*)

[Received 17 July 1952]

## SUMMARY

The disturbance produced behind a plane shock wave of arbitrary strength, travelling down a channel of non-uniform width, is investigated. The problem is linearized on the basis of small variations in the width of the channel.

It is found that, if the initial and final widths of the channel are  $2b$ ,  $2c$ , respectively, the ultimate effect in the neighbourhood of the incident shock is simply a change in the shock strength with a consequent change in pressure behind the shock of amount

$$K(p_1 - p_0)(1 - c/b),$$

where  $(p_1 - p_0)$  is the initial pressure discontinuity across the shock. The parameter  $K$  decreases monotonically with the shock strength and  $0.5 \geq K \geq 0.394$ .

When the flow behind the shock is subsonic an acoustic pulse also travels back along the channel with sonic velocity relative to the fluid. If  $2g(x) (= 0, \text{ if } x < 0)$  is the variation in the width of the channel, the pressure in this pulse is ultimately

$$-Nb^{-1}(p_1 - p_0)g(\tau s),$$

where  $s$  is the distance from the front of the pulse. The parameter  $\tau$  decreases monotonically with the shock strength and  $2 \geq \tau \geq 0.608$ ;  $N$  takes the value 0.5 for weak shocks and is singular when the flow behind the shock is sonic.

When the flow behind the shock is supersonic a similar pulse is produced ( $N$  becomes negative) now travelling downstream, and this is superimposed on the solution for steady flow in the channel.

The singularity in  $N$  for sonic flow behind the incident shock would suggest the possibility of strong secondary shocks occurring.

## 1. Introduction

THE object of this paper is to investigate the flow which results when a shock wave travels along a two-dimensional channel of non-uniform width. The variations in width are assumed to take place within a finite length of the channel, and this region of transition separates two portions of infinite length and uniform, but not necessarily equal, widths. The problem is linearized on the basis of small variations in the channel width, but there is no restriction on the shock strength. The pressure field behind the shock front is built up from the known solution of the diffraction of a shock wave travelling along a wall when the direction of the latter changes discontinuously, so presenting a corner to the flow (see Fig. 1 and (1)). From this is deduced a basic solution for the flow in a channel formed by two such walls, that is, a channel of uniform width connected to a channel of uniformly increasing width (see Fig. 2). Because of the linear character of the solution, the flow in the case when the cross-section varies in an

arbitrary manner can be obtained by superposition. This solution is then used to investigate the ultimate nature of the flow at large distances from the transition section.

## 2. Diffraction by a corner

We consider first the two-dimensional problem envisaged in Fig. 1. A plane shock moves with uniform velocity  $U$  into still air and is bounded by a plane wall perpendicular to the shock front. A second plane wall meets the

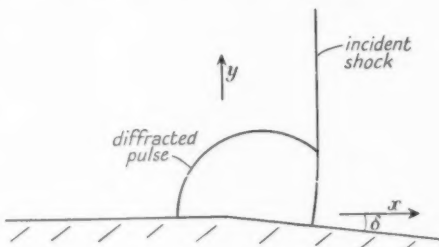


FIG. 1 (a)

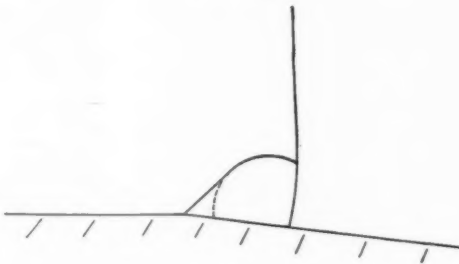


FIG. 1 (b)

first along a line parallel to the shock front, the resulting corner presenting an angle  $(\pi + \delta)$  to the flow. When the shock front has progressed beyond the corner it will be diffracted by the inclined wall, and an expanding region of non-uniform flow will be formed behind the shock front.

Let the fluid velocity, pressure, density, and sonic velocity in the region of uniform flow behind the shock front be denoted by  $q_1, p_1, \rho_1, a_1$  respectively, and let the corresponding quantities ahead of the shock be  $0, p_0, \rho_0, a_0$ . Choose coordinate axes  $O(x, y)$  with origin at the corner and the  $x$ -axis along the original wall produced, and let the shock reach the corner at time  $t = 0$ . If  $q_1 < a_1$ , then at any later time the perturbed flow is bounded by the incident shock and a circle of radius  $a_1 t$  with its centre at the point  $(q_1 t, 0)$ . If the uniform flow behind the shock is supersonic,  $q_1 > a_1$ , then the corner

lies outside the sonic circle and the boundary must be augmented by the tangent to the circle from the corner. In either case, since there is no fundamental length in the data defining the problem, the flow variables are expressible as functions of  $x/t, y/t$  only.

If the angle  $\delta$  is small, the pressure in the region of perturbed flow will differ from  $p_1$  by a term proportional to  $\delta$  on a linear theory; this excess pressure is conveniently denoted by

$$(p_1 - p_0)p \left( \frac{x - q_1 t}{a_1 t}, \frac{y}{a_1 t} \right) \delta = (p_1 - p_0)p(X, Y) \delta \quad (\text{say}). \quad (1)$$

The linearized problem has been solved by Lighthill (1), and the following is a summary of his results.

Let  $M (= U/a_0 > 1)$  be the Mach number of the shock, and let  $M_1 (= q_1/a_1)$  denote the Mach number of the uniform flow behind the shock. Then

$$M_1 = \frac{5(M^2 - 1)}{[(7M^2 - 1)(M^2 + 5)]^{\frac{1}{2}}} \quad (2)$$

(L. (3)<sup>†</sup>; the adiabatic index is given the value 1.4 appropriate to a diatomic gas).

In the  $(X, Y)$ -plane the circular part of the boundary has unit radius and centre at the origin. The corner is at the point  $(-M_1, 0)$ , and the straight part of the incident shock is the line

$$X = \frac{U - q_1}{a_1} = \left\{ \frac{M^2 + 5}{7M^2 - 1} \right\}^{\frac{1}{2}} = \cos \chi \quad (3)$$

(L. (9)).

The excess pressure coefficient  $p$  satisfies the relation

$$\frac{\partial p}{\partial y_1} + i \frac{\partial p}{\partial x_1} = \frac{C[D(z_1 - 1 + \gamma^2) - 1] \sec \chi}{(z_1^2 - 1)^{\frac{1}{2}}(z_1 - 1 + \gamma^2)[\alpha - i(z_1 - 1)^{\frac{1}{2}}][\beta - i(z_1 - 1)^{\frac{1}{2}}]} \quad (4)$$

(L. (45)), where

$$z_1 = x_1 + iy_1 = -\frac{1}{2} \left[ \left\{ \frac{\rho \exp\{i(\theta + \chi)\} - 1}{\rho \exp i\theta - \exp i\chi} \right\}^2 + \left\{ \frac{\rho \exp i\theta - \exp i\chi}{\rho \exp\{i(\theta + \chi)\} - 1} \right\}^2 \right], \quad (5)$$

$$X + iY = \frac{2\rho \exp i\theta}{1 + \rho^2} \quad (6)$$

<sup>†</sup> This denotes equation (3) of Lighthill's paper (1). To facilitate comparison, Lighthill's notation has been used in the main, but the following changes should be noted:

$(x, y)$ ,  $(X, Y)$ ,  $k$  and  $p$  now become  $(X, Y)$ ,  $(x, y)$ ,  $\cos \chi$  and  $\delta p \cos \chi$ , respectively.

(L. p. 459 et seq. and (31), (35)),

$$\alpha\beta = 2M^2, \quad \alpha + \beta = 2M^2 \cos \chi, \quad \gamma^2 = 2(M_1 + \cos \chi)^2(M_1 \cos \chi + 1)^{-2}, \quad (7)$$

$$C = \frac{2M_1(M_1 + \cos \chi)(\beta + \gamma)(\gamma + \alpha) \sin \chi}{\pi(M_1 \cos \chi + 1)^2}, \quad (8)$$

$$\frac{5(M_1 \cos \chi + 1)^2 \cos \chi}{6M_1^2(M_1 + \cos \chi)} = \frac{D(\gamma + \alpha)(\alpha + \beta)}{\alpha\beta} - \frac{\alpha + \beta + \gamma}{\alpha\beta\gamma}. \quad (9)$$

(L. (3), (9), (15), (50), (51).)

### 3. Application to flow in a channel

We now consider the propagation of a shock between two walls of infinite extent forming a channel of uniform width  $2b$  (say) connected to a channel of uniformly increasing width (Fig. 2). In the initial stages the solution of

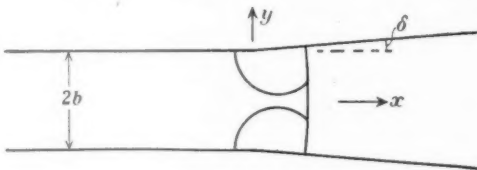


FIG. 2.

section 2 is still valid, the diffraction pattern produced by a single corner being repeated at the upper and lower walls of the channel. This will be the complete solution until the circular waves have expanded sufficiently to encounter the opposite walls, when further modification is required to satisfy the boundary condition there. If, for the moment, we ignore the divergence of the channel walls (in so far as the reflecting property of the latter is concerned) and imagine them to be straight and parallel along the whole length of the channel, then the modification would be a simple reflection at each wall simulated by appropriate images. This is also correct to the first order if the divergence of the walls is small, for the flow quantities in the perturbation waves are already small quantities of the first order.

The image waves will themselves be reflected eventually; thus the complete linear solution is obtained from an infinite image series expanding in time with sonic velocity, their centres moving downstream with the velocity of the fluid behind the original shock.

Let the  $x$ -axis now be taken along the centre-line of the channel, and let the  $y$ -axis separate the two sections of uniform and non-uniform width.

In terms of the basic solution of section 2, the excess pressure inside the channel is then given by

$$\delta(p_1 - p_0)P(x, y, t) = \delta(p_1 - p_0) \sum_n p \left\{ \frac{x - q_1 t}{a_1 t}, \frac{(2n+1)b-y}{a_1 t} \right\} + \\ + p \left\{ \frac{x - q_1 t}{a_1 t}, \frac{(2n+1)b+y}{a_1 t} \right\}, \quad (10)$$

where the summation is taken over all the images which have expanded sufficiently to influence the pressure at the point considered.

To generalize this for an arbitrary variation in channel width, we first consider the effect of moving the origin of coordinates upstream a distance  $\xi$ , so that the channel has constant width for  $-\infty < x < \xi$ . If the origin of time is suitably altered so that the shock reaches  $x = 0$  at  $t = 0$ , the excess pressure inside the channel will be

$$\delta(p_1 - p_0)P(x - \xi, y, t - \xi/U). \quad (11)$$

Now let the upper wall of the channel be defined by

$$y = b + g(x) \quad (12)$$

(the channel itself being symmetrical about the centre line), and choose the origin so that all variations in width occur for  $x > 0$ , so that  $g(x) \equiv 0$  for  $x < 0$ .

Equation (12) is equivalent to

$$dy/dx = \int_0^\infty H(x - \xi) dg'(\xi) = g'(x), \quad (13)$$

where

$$H(x) = \begin{cases} 1 & (x > 0) \\ 0 & (x < 0) \end{cases} \quad (14)$$

and is the Heaviside unit function.

Since the expression (11) is the excess pressure appropriate to a channel for which

$$dy/dx = \delta H(x - \xi), \quad (15)$$

we identify  $dg'(\xi)$  of (13) with  $\delta$  of (15), and sum for all the elementary variations in slope to get the following expression for the excess pressure,

$$(p_1 - p_0) \int_0^\infty P(x - \xi, y, t - \xi/U) dg'(\xi). \quad (16)$$

#### 4. Asymptotic behaviour near the shock front

The main purpose of this paper is a study of the asymptotic behaviour of (16) at large distances from the origin when the variations in the width of the channel occur within a transition section of finite length joining two sections of uniform (though not necessarily equal) width.

Equation (10) is first transformed by means of *Dirichlet's summation formula*, namely

$$\sum''_{\nu_1 < n < \nu_2} f(n) = \lim_{\lambda \rightarrow \infty} \sum_{n=-\lambda}^{\lambda} \int_{\nu_1}^{\nu_2} f(z) e^{2\pi i n z} dz, \quad (17)$$

where  $\Sigma''$  denotes that the first term is  $\frac{1}{2}f(\nu_1)$  if  $\nu_1$  is an integer, and the last term  $\frac{1}{2}f(\nu_2)$  if  $\nu_2$  is an integer (3).

We then have

$$\begin{aligned} P = & \frac{1}{2}p\left(\frac{x-q_1 t}{a_1 t}, \frac{b-y}{a_1 t}\right) + \frac{1}{2}p\left(\frac{x-q_1 t}{a_1 t}, \frac{b+y}{a_1 t}\right) + \\ & + \frac{a_1 t}{2b} \sum_{n=-\infty}^{\infty} \left[ \int_{(b-y)/a_1 t}^{1 - ((x-q_1 t)/a_1 t)^2} (-1)^n p\left(\frac{x-q_1 t}{a_1 t}, Y\right) \exp\left(\frac{n\pi i}{b}(atY+y)\right) dY + \right. \\ & \left. + \int_{(b+y)/a_1 t}^{1 - ((x-q_1 t)/a_1 t)^2} (-1)^n p\left(\frac{x-q_1 t}{a_1 t}, Y\right) \exp\left(\frac{n\pi i}{b}(a_1 tY-y)\right) dY \right]. \quad (18) \end{aligned}$$

We consider the behaviour of (18) at a fixed distance behind the main shock, so that

$$x = Ut - \text{constant}. \quad (19)$$

Then, when  $t$  is large,

$$P = \frac{a_1 t}{b} \sum_{n=-\infty}^{\infty} \int_0^{\sin \chi} (-1)^n p[\cos \chi, Y] \exp\left(-\frac{n\pi i a_1 t Y}{b} \cos \frac{n\pi y}{b}\right) dY + A + O\left(\frac{1}{t}\right) \quad (20)$$

where  $A$  is some constant independent of  $t$ .

Comparison with the result for diffraction by a single corner (section 2) shows that the integral occurring in (20) is taken along the shock from the wall to the sonic circle. (This follows from (3) and the fact that in the  $(X, Y)$ -plane the sonic circle has unit radius.) At the upper limit  $p = 0$ , the pressure being continuous at the sonic circle to the present approximation. Equation (20) thus becomes, after an integration by parts,

$$P = -\frac{a_1 t}{b} \int_0^{\sin \chi} Y dp - 2 \sum_{n=1}^{\infty} \frac{(-1)^n}{n\pi} \cos \frac{n\pi y}{b} \int_0^{\sin \chi} \sin \frac{n\pi a_1 t}{b} dp + A + O(t^{-1}). \quad (21)$$

Now on the shock

$$y_1 = 0,$$

$$Y = \left(\frac{x_1 - 1}{x_1 + 1}\right)^{\frac{1}{2}} \sin \chi \quad (22)$$

(equations (5) and (6) or L. (47)), thus  $x_1$  runs from 1 to  $\infty$ . Further, from (4),

$$\frac{\partial p}{\partial x_1} = \frac{O[D(x_1 - 1 + \gamma^2) - 1](\alpha + \beta) \sec \chi}{(x_1 + 1)^{\frac{1}{2}}(x_1 - 1 + \gamma^2)(x_1 - 1 + \alpha^2)(x_1 - 1 + \beta^2)}. \quad (23)$$

Thus, since the second term in (21) is  $O(t^{-1})$ , it follows that

$$\begin{aligned}
 P &= -a_1 tb^{-1} \int_1^\infty \sin \chi \left( \frac{x_1 - 1}{x_1 + 1} \right)^{\frac{1}{2}} \frac{\partial p}{\partial x_1} dx_1 + A + O\left(\frac{1}{t}\right) \\
 &= -2Ca_1 tb^{-1}(\alpha + \beta) \tan \chi \int_0^\infty \frac{[D(x^2 + \gamma^2) - 1]x^2 dx}{(x^2 + 2)(x^2 + \alpha^2)(x^2 + \beta^2)(x^2 + \gamma^2)} + \\
 &\quad + A + O\left(\frac{1}{t}\right) \\
 &= -KUt/b + A + O(t^{-1}) \text{ (say),}
 \end{aligned} \tag{24}$$

where

$$K = \frac{C\pi(\alpha + \beta)\tan \chi \{(D\gamma^2 - 1)(2^{\frac{1}{2}} + \alpha + \beta + \gamma) + D(2^{\frac{1}{2}}\alpha\beta + 2^{\frac{1}{2}}\alpha\gamma + 2^{\frac{1}{2}}\beta\gamma + \alpha\beta\gamma)\}}{(M_1 + \cos \chi)(2^{\frac{1}{2}} + \alpha)(2^{\frac{1}{2}} + \beta)(2^{\frac{1}{2}} + \gamma)(\alpha + \beta)(\alpha + \gamma)(\beta + \gamma)}. \tag{25}$$

Finally, when the variation in cross-section is arbitrary, the pressure change behind the shock wave is obtained by substituting (24) in (16). The range of integration is effectively finite in (16) because of the assumption that  $g'(x)$  is identically zero outside a finite interval in the neighbourhood of the origin. The pressure change is thus

$$-(p_1 - p_0) \int \left\{ \frac{KU}{b} (t - \xi/U) - A + O(t^{-1}) \right\} dg'(\xi), \tag{26}$$

and, since  $g'(\xi)$  is zero at the end points, this is

$$-\frac{K(p_1 - p_0)}{b} [g] + O(t^{-1}), \tag{27}$$

where  $[g]$  denotes the net change in  $g$ . If the final width of the channel is  $2c$ , then (18) may be written as

$$K(p_1 - p_0)(1 - cb^{-1}) + O(t^{-1}). \tag{28}$$

Thus, ultimately, the effect of the change in cross-section amounts to a change in the shock strength. The flow behind the shock again becomes uniform, the pressure (in excess of  $p_1$ ) being given by (28).

The parameter  $K$  is a monotonic decreasing function of the shock strength. The limiting values for a shock of zero strength and a shock of infinite strength are 0.5 and 0.394... respectively. The detailed variation of  $K$  is shown in Fig. 3, where it is graphed against  $p_1/p_0$ .

A simple verification of the result for the limiting case of an acoustic pulse ( $K = \frac{1}{2}$ ) is possible (2). For the energy in a progressive wave, per unit cross-section of the channel, is proportional to the square of the amplitude. Since the amplitude of the reflected pulse will be  $O(1 - cb^{-1})$  it follows that the energy in the transmitted pulse will be unchanged to the first order in  $(1 - cb^{-1})$ , and this will be the case if the amplitude varies inversely as the square root of the width of the channel. The excess pressure in the pulse is a convenient measure of the amplitude, and initially this is

$(p_1 - p_0)$ . The ultimate value is thus

$$(p_1 - p_0)(b/c)^{\frac{1}{2}} = (p_1 - p_0) + \frac{1}{2}(p_1 - p_0)(1 - c/b) + O(1 - c/b)^2.$$

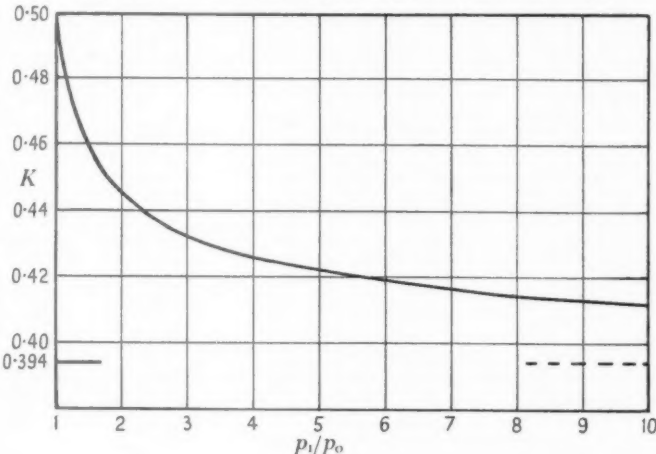


FIG. 3.

### 5. Asymptotic behaviour of the returning pulse

When the flow behind the incident shock is subsonic, a disturbance will also be propagated into the upstream section of the channel. At a large distance from the origin the wave-fronts of the original diffracted waves and their subsequent reflections will have an envelope consisting of a plane wavefront travelling with sonic velocity relative to the fluid. At any given time the position of the envelope will be given by

$$x = -(a_1 - q_1)t, \quad (29)$$

and behind it the flow will tend to become uniform across the width of the channel.

We find the pressure variation in this returning wave by considering the behaviour of (18) at a fixed distance ( $d$ , say) downstream of the envelope which constitutes the front of the wave, so that

$$x = -(a_1 - q_1)t + d. \quad (30)$$

Then

$$\begin{aligned} P = & \frac{1}{2}p\left(-1 + \frac{d}{a_1 t}, \frac{b-y}{a_1 t}\right) + \frac{1}{2}p\left(-1 + \frac{d}{a_1 t}, \frac{b+y}{a_1 t}\right) + \\ & + \frac{a_1 t}{2b} \sum_{n=-\infty}^{\infty} \left[ \int_{(b-y)/a_1 t}^{(1-(1-d/a_1 t)^2)^{\frac{1}{2}}} (-1)^n p\left(-1 + \frac{d}{a_1 t}, Y\right) \exp\left(\frac{n\pi i}{b}(a_1 t Y + y)\right) dY + \right. \\ & \left. + \int_{(b+y)/a_1 t}^{(1-(1-d/a_1 t)^2)^{\frac{1}{2}}} (-1)^n p\left(-1 + \frac{d}{a_1 t}, Y\right) \exp\left(\frac{n\pi i}{b}(a_1 t Y - y)\right) dY \right]. \end{aligned} \quad (31)$$

We therefore require the behaviour of  $p(X, Y)$  when

$$\begin{aligned} X &= -1 + O(t^{-1}), \\ Y &= O(t^{-\frac{1}{2}}). \end{aligned} \quad (32)$$

It may be deduced from (5) and (6) that, when  $X$  and  $Y$  satisfy these conditions,

$$\left. \begin{aligned} x_1 &= -1 + 4\{X+1-Y^2\}\{1+O(t^{-\frac{1}{2}})\}\tan^2\chi/2 \\ y_1 &= 4Y\{2X+2-Y^2\}\{1+O(t^{-\frac{1}{2}})\}\tan^2\chi/2 \end{aligned} \right\}. \quad (33)$$

Further, in the neighbourhood of  $z_1 = -1$ ,

$$p = \frac{-C[D(2-\gamma^2)+1][1+x_1+(1+x_1)^2+y^2]^{\frac{1}{2}}[1+O((1+x_1)^2+y^2)^{\frac{1}{2}}]}{\cos\chi(2-\gamma^2)(\alpha+2^{\frac{1}{2}})(\beta+2^{\frac{1}{2}})} \quad (34)$$

This follows at once from (4) and the fact that  $p = 0$  at  $z_1 = -1$  since this point is on the boundary of the diffracted pulse. A combination of (33) and (34) gives

$$p = -L[1+O(t^{-\frac{1}{2}})][2(X+1)-Y^2]^{\frac{1}{2}} \quad (35)$$

$$\text{with } L = \frac{2C[D(2-\gamma^2)+1]\tan\chi/2}{\cos\chi(2-\gamma^2)(\alpha+2^{\frac{1}{2}})(\beta+2^{\frac{1}{2}})}, \quad (36)$$

when  $X$  and  $Y$  satisfy (32).

Equation (35) for  $p$  is now substituted in (31) to give

$$\begin{aligned} P &= -\frac{La_1t}{b}[1+O(t^{-\frac{1}{2}})] \times \\ &\quad \times \sum_{n=-\infty}^{\infty} \int_0^{(2d/a_1t)^{\frac{1}{2}}} (-1)^n \left(\frac{2d}{a_1t} - Y^2\right)^{\frac{1}{2}} \exp\left(\frac{n\pi ia_1tY}{b}\right) \cos\left(\frac{n\pi y}{b}\right) dY + O(t^{-\frac{1}{2}}) \\ &= -L\pi d/2b + O(t^{-\frac{1}{2}}) \\ &= -L\pi[x+(a_1-q_1)t](2b)^{-1} + O(t^{-\frac{1}{2}}) \end{aligned} \quad (37)$$

in virtue of equation (30).

Finally we substitute (37) in (16) to find the pressure variation in the returning pulse when there is an arbitrary variation in the cross-section of the channel. Since  $P$  is clearly zero ahead of the returning pulse ( $\{x+(a_1-q_1)t\} < 0$ ) it follows that (16) becomes

$$\begin{aligned} -\frac{L\pi}{2b}(p_1-p_0) \int_0^{U(x_1+(a_1-q_1)t)/(U+a_1-q_1)} &\{x-\xi+(a_1-q_1)(t-\xi/U)\} dg'(\xi) + O(t^{-\frac{1}{2}}) \\ &= -(Nb^{-1})(p_1-p_0)g[\tau\{x+(a_1-q_1)t\}] + O(t^{-\frac{1}{2}}), \end{aligned} \quad (38)$$

where

$$\tau = \frac{U}{a_1-q_1+U} = \frac{M_1+\cos\chi}{1+\cos\chi} \quad (39)$$

and  $N = L\pi/2\tau = \frac{\pi C[D(2-\gamma^2)+1]\tan\chi}{(2-\gamma^2)(\alpha+2^{\frac{1}{2}})(\beta+2^{\frac{1}{2}})(M_1+\cos\chi)}.$  (40)

Thus a graphical picture of the ultimate nature of the pressure variations in this rearward pulse is obtained by imagining the upper wall of the channel stretched in the  $x$ -direction by a factor  $\tau$ , magnified in the  $y$ -direction by a factor  $-N(p_1-p_0)/b$  and moving upstream with a velocity  $(a_1-q_1).$

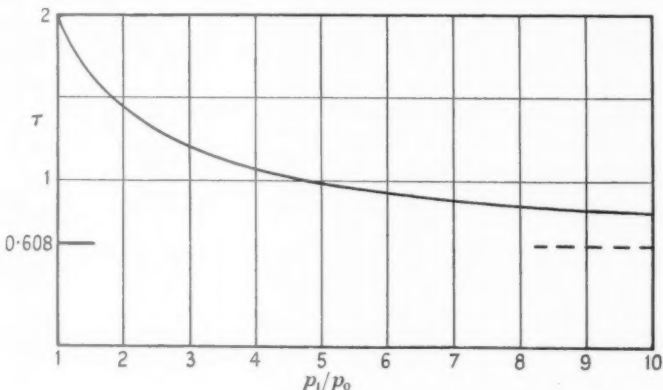


FIG. 4.

The values of  $\tau$  and  $N$  for various shock strengths are shown in Figs. 4 and 5. The parameter  $\tau$  is monotonic decreasing and takes the values 2, 1, and 0.6076... respectively when the incident shock has zero strength, when the flow velocity behind the shock is sonic, and when the shock strength becomes infinite.

The parameter  $N$  is not so well behaved. For subsonic flow behind the incident shock it increases rapidly from a value of 0.5 for a shock of zero strength, and becomes singular when the flow behind the shock is sonic. Near  $M_1 = 1$  the behaviour of  $N$  is, in fact, described by the asymptotic relation

$$N \sim \frac{1}{(1-M_1^2)\cos\chi}. \quad (41)$$

The solution, of course, breaks down near  $M_1 = 1$ . However, experience of other linearized solutions suggests that large non-linear disturbances are often concealed by such singularities. If this is a correct inference in the present case, then a strong secondary shock wave ought to be formed if there is a contraction in the channel and the flow behind the incident shock is just subsonic. Thus we obtain a mathematical expression for the process of 'choking'.

For supersonic flow behind the shock  $N$  becomes negative (and singular, according to (41), near  $M_1 = 1$ ). As the shock strength tends to infinity the value of  $N$  tends to  $-1.550\dots$ .

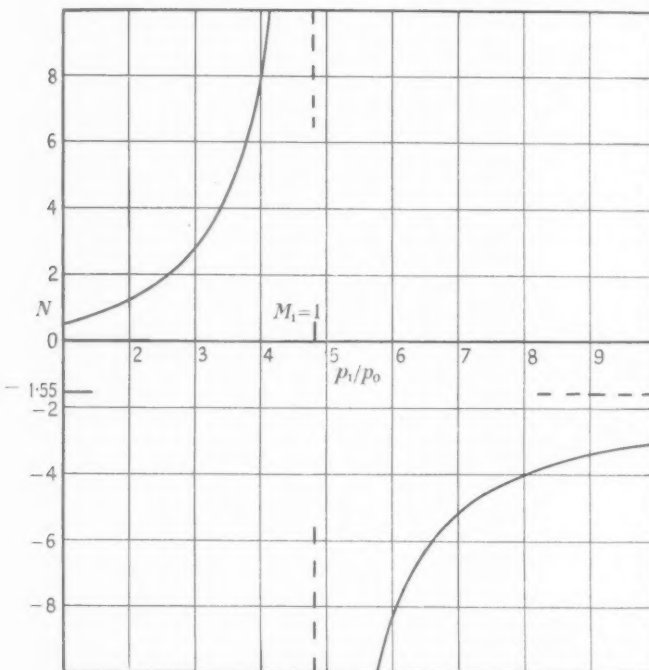


FIG. 5.

In the supersonic case it must be remembered that although (38) can still be interpreted as an acoustic pulse (now travelling downstream with velocity  $(q_1 - a_1)$ ), it no longer represents the whole of the disturbance. In the case of a uniformly expanding channel there is the additional effect of the linear approximation to the two Prandtl-Meyer expansions at the corners (see Fig. 1(b)), and these are themselves continually reflected by the channel walls. In the general case when the variation in the channel width is arbitrary, the additional disturbance can be thought of as the integrated effect of these Prandtl-Meyer expansions (or weak compression waves) and their reflections, which originate at each elementary increment of slope in the walls of the channel. Evidently the mathematical solution representing the combination of all these must be simply that of

steady flow along the channel, and if the velocity vector is defined in terms of a velocity potential  $\phi$  as  $q_1 \left( 1 + \frac{\partial \phi}{\partial x}, \frac{\partial \phi}{\partial y} \right)$ , then  $\phi$  satisfies the equation

$$\frac{\partial^2 \phi}{\partial y^2} = (M_1^2 - 1) \frac{\partial^2 \phi}{\partial x^2} \quad (42)$$

and a boundary condition  $\frac{\partial \phi}{\partial y} = \frac{dg}{dx}$  (43)

on  $y = b$ .

In the Heaviside operational calculus, (42) and (43) become (with  $s$  as the operator)

$$\frac{\partial^2 \phi}{\partial y^2} = (M_1^2 - 1)s^2 \phi = B^2 s^2 \phi \quad (44)$$

(say), and  $\frac{\partial \phi}{\partial y} = s \int_0^\infty e^{-sx} \frac{dg}{dx} dx = \eta$  (say) on  $y = b$ . (45)

The solution, symmetrical about  $y = 0$ , is

$$\phi = (\eta/Bs) \cosh Bsy \operatorname{sech} Bsb. \quad (46)$$

Also, by Bernoulli's theorem, the excess pressure is, to the first order

$$\Delta = -\rho_1 q_1^2 \frac{\partial \phi}{\partial x} = -\rho_1 q_1^2 s \phi, \quad (47)$$

and so, by interpreting (47), we have

$$\Delta = -\frac{\rho_1 q_1^2}{2\pi i} \int_{\gamma-i\infty}^{\gamma+i\infty} \frac{\eta}{Bs} \frac{\cosh Bsy}{\sinh Bsb} e^{sx} ds. \quad (48)$$

Now  $dg/dx$  is zero except in the neighbourhood of the origin. Thus the upper limit in the integral occurring in (45) is effectively finite and, for small  $s$ ,

$$\eta = [g]s + O(s^2). \quad (49)$$

It follows that, if  $\eta$  is not singular to the left of the contour of integration in (48),

$$\Delta = -\frac{\rho_1 q_1^2}{B^2 b} [g] + \sum_n A_n \cos\left(\frac{n\pi y}{b}\right) \cos\left(\frac{n\pi x}{B}\right) \quad (50)$$

for some constants  $A_n$ . The series in (50) represents a fluctuating contribution to the pressure, and this fluctuation does not die out even at large distances from the origin of the disturbance.

It can easily be shown (with the help of L. (1)) that, in terms of the pressure discontinuity across the incident shock, the first term in (50) can be written

$$-\frac{M_1(p_1 - p_0)}{(M_1^2 - 1)b \cos \chi} [g], \quad (51)$$

and this, in combination with (38), represents the ultimate *average* pressure increment in the pulse. This term is also singular at  $M_1 = 1$ , and comparison with (38) and (41) shows that it is asymptotically equal and opposite to the value taken by (38) in the heart of the rearward pulse (when  $g[\tau\{x + (a_1 - q_1)t\}]$  takes its final and constant value, here denoted by  $[g]$ ). Thus, in combination, the singular terms tend to cancel out in the heart of the wave, but the linear theory still indicates rapid increase of pressure (if  $[g] > 0$ ) as the pulse is penetrated from its front. Hence, for reasons similar to those invoked in the subsonic case, there should be a secondary shock produced when there is an expansion in the channel and the flow is just supersonic behind the incident shock (secondary shocks in expanding channels have, in fact, been observed—see (4)).

It should be mentioned that the above reasoning does not apply to the flow immediately behind the incident shock, where the steady flow field has not penetrated. Equation (28) is carried over to the supersonic case without qualification.

#### REFERENCES

1. M. J. Lighthill, *Proc. Roy. Soc. A*, **198** (1948), 454.
2. LORD RAYLEIGH, *Theory of Sound*, 2nd ed., vol. ii, p. 68 (London, 1896).
3. L. DIRICHLET and R. DEDEKIND, *Zahlentheorie*, 3rd ed., pp. 283-4 (Berlin, 1871).
4. A. HERTZBERG, *J. Aero. Sci.* **18** (1951), 803.

# ON SOME EIGENVALUE PROBLEMS OF EXCEPTIONAL DIFFICULTY, EXEMPLIFIED BY A CASE OF ELASTIC INSTABILITY

By R. V. SOUTHWELL (*Cambridge*) and  
GILLIAN VAISEY (*Imperial College, London*)

[Received 22 August 1952]

## SUMMARY

Relaxation methods were employed in 1941 (2) to estimate the critical load and the mode of distortion ('waving') for a flat plate representative of a cantilever I-beam. The value thus obtained for the critical load was believed to be correct within 1 per cent.; but the mode was less accurately determined, and attempts to improve it have resulted in the present paper. (Though less important, practically, than the critical load, it has interest as determining the arrangement of stiffeners.)

Normally (e.g. for struts or 'whirling' shafts) the eigenvalues are widely separated and all positive, and the gravest mode can be guessed with fairly close accuracy since it is devoid of nodal lines. But in general these features cannot be postulated, and then approximate treatment is much harder. All three appear to be lacking in the cantilever problem, which thus exemplifies problems of a wider class. The consequent difficulties, being mainly computational, are not met by discussions which presume that equations can be solved exactly.

## Introduction

1. THE complete solution of an eigenvalue problem (giving every eigenvalue and its associated mode) is seldom obtainable and from a practical standpoint is seldom needed. In a case of elastic instability, for example, what matter are the load which first induces instability and the mode of distortion ('waving') which results. The first is usually estimated on the basis of 'Rayleigh's principle', the second by a process (here termed 'intensification') which is commonly attributed to Vianello and/or Stodola.<sup>†</sup>

Applied to systems like struts or 'whirling' shafts, these methods quickly yield the wanted information: Rayleigh's, because the deflexion in the gravest mode is known to be one-signed and as such can be guessed closely; 'intensification', because the eigenvalues (critical loads or speeds) all have the same sign and are, moreover, widely separated. But in general these conditions are not realized, and on that account both methods (as normally

<sup>†</sup> Some questions of attribution are discussed in section 34.

applied) may fail. Thus the few solved cases of elastic instability in plates suffice to show that in such problems†

- (A) the gravest mode may be characterized by nodal lines, and as such be impossible to guess with any accuracy;
- (B) the eigenvalues may have both signs;
- (C) two or more of the gravest eigenvalues may be nearly or exactly equal.

Any or all of (A)–(C) may be confronted in cases which, on account of their complexity, are tractable only by numerical methods; and must be surmounted before a relaxational technique can be applied in the manner (e.g.) of Pellew and Southwell (1). This is the object of the present paper.

2. We take as a test example the system shown in Fig. 1—a problem attacked by L. Fox, J. R. Green, and F. S. Shaw in 1941 (2). A deep rectangular cantilever, with edges ‘clamped’, is stressed by uniform thrust applied to one of its longer sides. Contours in Fig. 1 exhibit the compressive principal stress which this load induces when acting *downwards*: then, the gravest mode is characterized (Fig. 2) by waving localized in the bottom right-hand corner; but clearly, if the loading were reversed, the principal stress would be compressive, and the waving localized, in the *upper* right-hand corner. The system thus exemplifies (B), section 1.

The equation defining the characteristic modes and eigenvalues can be deduced in the manner of (3) sections 494–7. It has the form

$$\vartheta w = \lambda \vartheta' w, \quad (2)^*$$
 (1)

where

$$\begin{aligned} \vartheta w &\equiv D \nabla^4 w \quad \left( \nabla^2 \equiv \frac{\partial^2}{\partial x^2} + \frac{\partial^2}{\partial y^2} \right) \\ -\lambda \vartheta' w &\equiv \frac{\partial}{\partial x} \left( P_x \frac{\partial w}{\partial x} - S \frac{\partial w}{\partial y} \right) + \frac{\partial}{\partial y} \left( P_y \frac{\partial w}{\partial y} - S \frac{\partial w}{\partial x} \right) \end{aligned} \quad (2)$$

( $D$  denoting the flexural rigidity). For the loading ( $w$ ) shown in Fig. 1 (cf. (3), section 416)

$$\begin{aligned} -P_x &= \frac{w}{d^3} [3x^2(2y-d) - 4y^3 + 6dy^2 - \frac{1}{5}d^2y + \frac{1}{5}d^3] \\ -P_y &= \frac{w}{d^3} (2y^3 - 3dy^2) \\ S &= \frac{6w}{d^3} xy(d-y) \end{aligned} \quad , \quad (3)$$

† A and C are exemplified by a rectangular plate compressed in one direction; B by a square or rectangular plate which ‘buckles’ under shear. Perhaps because only simple cases have been solved, it seems not to have been noticed that in general a plate can buckle under the load-system either as given or reversed. The theoretical significance of this fact was first remarked by D. N. de G. Allen.

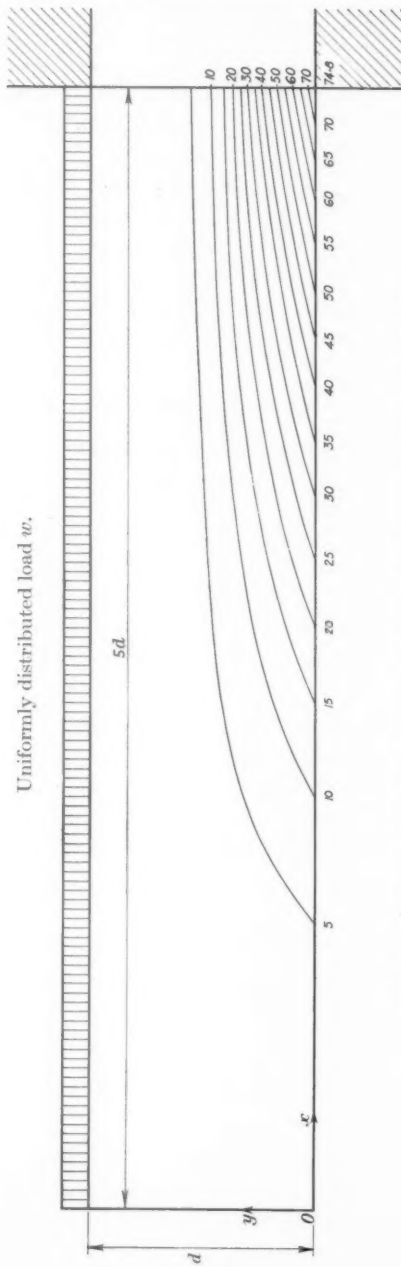


FIG. I. (Contours show the (compressive) principal stress as a multiple of  $w/2h$ .)

so the eigenvalue

$$\lambda \propto \frac{wd^2}{Eh^3} \quad (4)$$

when (1) is made 'non-dimensional' by the substitutions

$$x = dx', \quad y = dy'.$$

3. We shall suppose (1) to have been thus rendered 'non-dimensional', and in treating the test example we shall use  $\vartheta$ ,  $\vartheta'$ , indiscriminately, both for the operators specified in (2) and for their approximations in finite differences ((2), sections 24-25). But the symbols admit of a wider interpretation, and thereby the range of this paper is extended:† they may stand for any two self-adjoint operators, provided that in the 'energy equation' derived from (1)—viz.

$$I \text{ (say)} \equiv \iint w \vartheta w \, dx dy = \lambda \iint w \vartheta' w \, dx dy \equiv \lambda I'/\Lambda \text{ (say)}, \quad (5)$$

—the integral ( $I$ ) on the left is necessarily positive. This can be shown to be the fact when (as here)  $\vartheta \equiv \nabla^4$  and the edge-conditions are

$$w = \frac{\partial w}{\partial v} = 0. \quad (6)$$

No restriction is imposed on the right-hand integral ( $I'/\Lambda$ ) in (5), so the eigenvalue  $\lambda$  may have either sign.

### Assumptions

4. As always (when it is linear) the governing equation does not define the amplitudes of the characteristic modes. Typifying them by  $w_k$ , a function defined by

$$\vartheta w_k = \lambda_k \vartheta' w_k \quad (7)$$

and by the conditions (6), we 'normalize' them by imposing the relation

$$\iint w_k \vartheta w_k \, dx dy = \lambda_k \iint w_k \vartheta' w_k \, dx dy = 1, \quad (3)^*$$

and we presume them to satisfy the 'conjugate relations'

$$\left. \begin{aligned} \iint w_s \vartheta w_r \, dx dy &= \iint w_r \vartheta w_s \, dx dy = 0 \\ \iint w_s \vartheta' w_r \, dx dy &= \iint w_r \vartheta' w_s \, dx dy = 0 \end{aligned} \right\}. \quad (4)^* \quad (9)$$

Finally, we assume the validity of expansion in the characteristic modes: i.e. that, when the  $A$ 's are given appropriate values, the series expression

$$w = \sum_k [A_k w_k] \quad (5)^* \quad (10)$$

† Its application depends, of course, on whether (1) is tractable relaxationally.

4) holds in respect of any mode which does not violate the edge-conditions, and admits of operation either by  $\vartheta$  or by  $\vartheta'$ .

(Only this last assumption is open to question: strictly, it calls for examination in respect of each particular equation. But it is justified in relation to systems of finite freedom, and in effect we change the system to one of this kind when we substitute finite differences for derivatives in the governing equation, thereby reducing the number of the points that are 'relaxable'. This standpoint was adopted in a recent paper (4) which gives proofs of some theorems used here (e.g. that the assumption  $I \prec 0$  requires all the eigenvalues to be *real*). Those theorems will be cited without proof but (to facilitate reference) with their equation and section numbers in (4) distinguished by asterisks.)

### I. REVIEW OF APPROXIMATE METHODS ALREADY CURRENT

5. Taking the test example as representative of problems which may have any or all of the features 'A', 'B', and 'C', section 1, we now examine the applicability of some current methods. No hope of exact solution can be entertained, so we restrict the review to methods which in effect replace a continuous system by one having finite freedom. Equally it is evident that a mode like Fig. 2 (Fox and Green's solution (2) of the test example) will not be adequately represented—as in methods like Galerkin's—by a synthesis of a few selected functions *chosen without prior knowledge of its form*. In Fig. 2 the number of nodes that are 'relaxable', and hence the number of the characteristic modes and eigenvalues, is 273. It appears that little has been written with systems of this complexity in mind; and perhaps for that reason little attention has been given to the consequences of inescapable *computational errors* (cf. (4), section 7\*).

#### Rayleigh's method

##### 6. On the assumptions made in section 4

$$\left. \begin{aligned} I &\equiv \iint w \vartheta w \, dx dy = \sum (A_k^2) \\ I'/\Lambda &\equiv \iint w \vartheta' w \, dx dy = \sum (A_k^2/\lambda_k) \end{aligned} \right\}, \quad (6)^*$$
(11)

consequently (section 3\*)  $\lambda_R$  as defined by

$$\lambda_R = \Lambda I/I' = \sum (A_k^2)/\sum (A_k^2/\lambda_k) \quad (7)^* \quad (12)$$

has a stationary value when the mode  $w$  is 'normal' so that all of the  $A$ 's are zero except one. This is 'Rayleigh's principle'—proclaimed by him as holding when the eigenvalues are all positive. It holds also when (as here) they have both signs but (section 2\*) are all real.

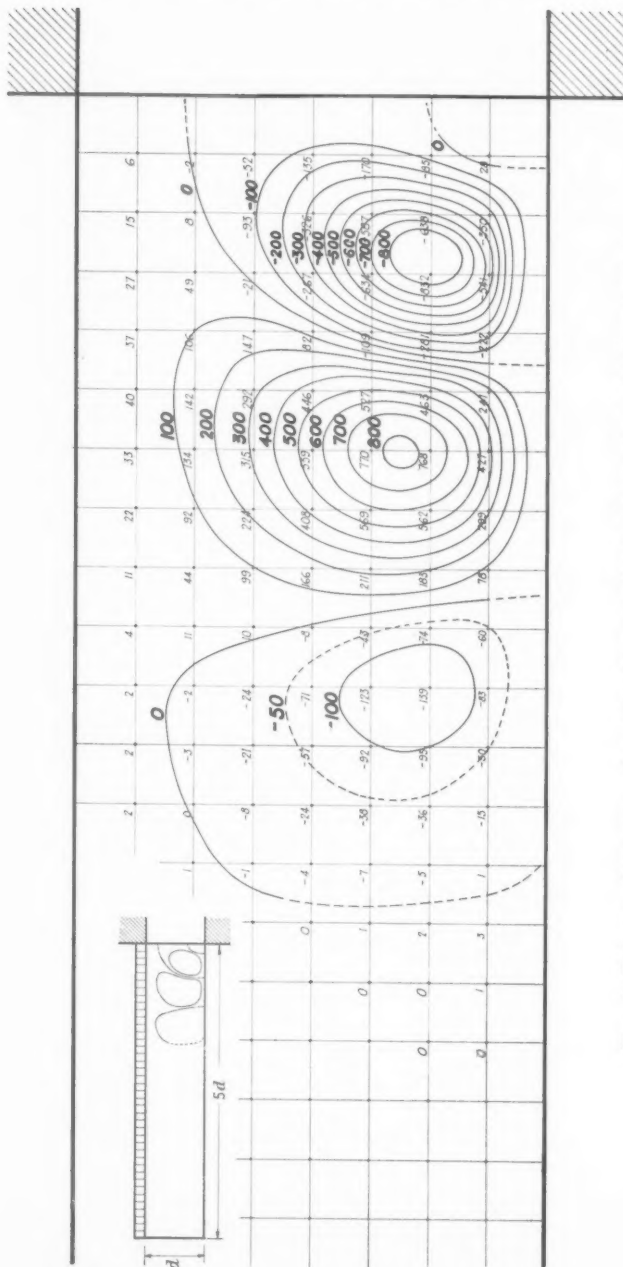


FIG. 2. Values and contours of  $w$ . (Absolute magnitude of distortion is indeterminate.)

Lord Rayleigh (5) argued, further, that  $\lambda_R$  as defined in (12) always has a value intermediate between the least and the greatest of them (or above the least, if the system has infinite freedom), consequently  $\lambda_R$  as computed from a guessed form  $w$  (here termed a 'Rayleigh estimate') may be regarded as an upper limit to  $\lambda_1$ . This theorem fails when  $I'/\Lambda$  can take either sign or vanish, for in the last event  $\lambda_R$  is infinite. But a theorem due to G. V. (section 4\*) asserts that

$$\begin{aligned} \lambda_R &\text{ cannot lie between the least positive and the least} \\ &\text{negative eigenvalue } (\lambda_1 \text{ and } \lambda_{-1}, \text{ say}). \dagger \end{aligned} \quad (13)$$

### 'Intensification'

7. The practical importance of Rayleigh's principle lies in his use of it (section 6) to obtain an upper limit to  $\lambda_1$  by simple computations based on a *guess* regarding the form of  $w_1$ . In most problems of the sort which he considered the form can be guessed with considerable accuracy, and then in virtue of the stationary property the resulting estimate of  $\lambda_1$  is extremely close. But in the wider class considered here little confidence can be put in a guess regarding  $w_1$ ; then it may be improved by a process, here termed 'intensification', which is variously ascribed to Schwarz (6), Vianello (7), and Stodola (8). This derives from  $w$ , successively, other forms  $w_I, w_{II}, \dots$ , etc., satisfying the edge-conditions together with

$$\left. \begin{aligned} \vartheta w_I &= \Lambda \vartheta' w \\ \vartheta w_{II} &= \Lambda \vartheta' w_I \\ &\dots, \text{ etc.} \end{aligned} \right\} \quad (9)^*$$

in which  $\Lambda$  is any convenient multiplier.

*Provided that  $w_1$  is a component of the guessed form  $w$ , when every eigenvalue  $> 0$  then  $w_I, w_{II}, \dots$ , etc., will approximate more and more closely to  $w_1$ ; when the eigenvalues have both signs they will approximate to  $w_1$  or  $w_{-1}$  according as  $\lambda_1$  or  $\lambda_{-1}$  is the smaller.* For if  $w$  is expressible in the series

$$w = \sum (A_k w_k), \quad (10)\text{bis}$$

then

$$\left. \begin{aligned} w_I &= \Lambda \sum (A_k w_k / \lambda_k) \\ w_{II} &= \Lambda^2 \sum (A_k w_k / \lambda_k^2) \\ &\dots, \text{ etc.} \end{aligned} \right\} \quad (10)^*$$

so the gravest mode becomes successively more predominant in  $w_I, w_{II}, \dots$ , etc.

† A normal mode will be termed positive or negative in conformity with the sign of its associated  $\lambda$ .  $\sum_k$  will denote a summation extending only to positive modes, typified by  $w_k$ ;

$\sum_{-l}$  a summation extending only to negative modes, typified by  $w_{-l}$ ;  $\Sigma$  a summation extending to every normal mode.

8. Another interpretation is admissible. The response ( $w$ ) to a transverse loading  $Z_0$  is governed by

$$[\vartheta - \lambda \vartheta']w = Z_0 \equiv \vartheta w_0 \text{ (say),} \quad (16)$$

when the edge-loading has an intensity defined by  $\lambda$ ; and a formal solution of (16) is

$$w = \sum [A_k w_k / (1 - \lambda/\lambda_k)] \quad (17)$$

when

$$w_0 = \sum [A_k w_k]$$

Alternatively, assuming  $w$  to be representable by the series

$$w = P_0 + P_1 \lambda + \dots + P_n \lambda^n + \dots, \text{ etc.,} \quad (18)$$

we obtain

$$\sum_n [\lambda^n (\vartheta P_n - \vartheta' P_{n-1})] \equiv \vartheta w_0$$

on substitution in (16); and hence

$$\vartheta P_n = \vartheta' P_{n-1}, \quad \vartheta P_0 \equiv \vartheta w_0. \quad (19)$$

From these last relations and from the edge-conditions it follows that

$$P_0 = w_0 = \sum [A_k w_k], \quad P_n = \sum [A_k w_k / \lambda_k^n],$$

so that when  $n$  is large (and if every  $|\lambda_k| > \lambda_1$ ),

$$P_n \rightarrow A_1 w_1 / \lambda_1^n \text{ (therefore } \lambda_1 P_n \rightarrow P_{n-1} \text{) as } \lambda \rightarrow \lambda_1.$$

Then the series (18)  $\rightarrow A_1 w_1 / (1 - \lambda / \lambda_1)$ —in conformity with (17).

Thus successive intensifications of  $w_0$  yield cofactors of  $\lambda, \lambda^2, \dots$ , etc., in a power-series (18) valid when  $\lambda < \lambda_1$ , and as such they have the nature of successive corrections. (In section 7 they appeared as successive approximations.)

#### 'Partial transfer'

9. That  $\lambda_1 < |\lambda_{-1}|$  in the test example can be shown by resolving the load-system of Fig. 1 into two components, (a) and (b), Fig. 3. If (a) were

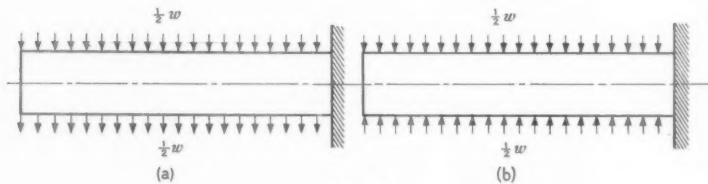


FIG. 3.

to act alone, the eigenvalues would form equal and opposite pairs; but superposition of (b), a destabilizing system, will alter each of them by a positive quantity, thus increasing  $|\lambda_1|$  and decreasing  $|\lambda_{-1}|$ .

Here, then, 'intensification' may be expected to furnish an estimate of the wanted mode  $w_1$ . But 'B', section 1, will frustrate that purpose if  $|\lambda_{-1}| < \lambda_1$ , so may be a cause of difficulty. In that event a device which we here term 'partial transfer' may have value, as giving a bias towards components of the wanted sign. (An equivalent device was proposed by L. F. Richardson (9) in 1910.) *Its success requires the proviso of section 7.*

$\lambda_0$  denoting some chosen number, and  $\lambda'$  standing for  $(\lambda - \lambda_0)$ , then (1) may be written in the equivalent form

$$[\vartheta - \lambda_0 \vartheta']w = \lambda' \vartheta' w. \quad (1A)$$

Let the operator on the left of (1A) be substituted for  $\vartheta$  in (14), so that  $w_I, w_{II}, \dots$ , etc., are now related with  $w$  by

$$\left. \begin{aligned} [\vartheta - \lambda_0 \vartheta']w_I &= \Lambda \vartheta' w \\ \dots, \text{etc.} & \end{aligned} \right\}. \quad (20)$$

Then an argument on the lines of section 7 shows that

$$\left. \begin{aligned} w_I &= \Lambda \sum [A_k w_k / (\lambda_k - \lambda_0)] \\ w_{II} &= \Lambda^2 \sum [A_k w_k / (\lambda_k - \lambda_0)^2] \\ \dots, \text{etc.} & \end{aligned} \right\}, \quad (21)$$

when  $w$  has the series expression  $\sum [A_k w_k]$ : i.e.  $\lambda_k$  in (15) is now replaced by  $(\lambda_k - \lambda_0)$ , so now the measure of the relative contributions of  $w_k$  and  $w_1$  is reduced in each intensification by a factor  $(\lambda_1 - \lambda_0) / (\lambda_k - \lambda_0)$  instead of  $\lambda_1 / \lambda_k$ , and convergence will be much accelerated if  $\lambda_0 \neq \lambda_1$ . In particular negative components will be eliminated, because  $|(\lambda_k - \lambda_0)| > |\lambda_k|$  when  $\lambda_k < 0$ .

#### 'Elimination of the dominant component'

10. A practical disadvantage of 'partial transfer' is that (20), normally, entail far more labour than (14). That objection does not apply to a procedure which Fox and Green employed in 1941 (2) in combination with another device which is explained below. Starting from any guessed mode  $w_A$  (say), they derived from this another mode  $w_B$  by solving—in conjunction with the edge-conditions—the equation

$$\vartheta w_B = \Lambda [\vartheta - (\lambda_R)_A \vartheta'] w_A, \quad (22)$$

in which  $\Lambda$  as before denotes some convenient multiplier and  $(\lambda_R)_A$  is the 'Rayleigh estimate' deduced from (11) and (12) with  $w$  replaced by  $w_A$ . An argument on the lines of section 7 shows that, when

$$w_A = \sum [A_k w_k],$$

then, as deduced from (22),

$$\begin{aligned} w_B &= \Lambda \sum [A_k w_k (1 - (\lambda_R)_A / \lambda_k)] \\ &= w_A - (\lambda_R)_A w_1, \quad \text{when } \partial w_1 = \Lambda \partial' w_A. \end{aligned} \quad (23)$$

Thus  $w_B$  can be regarded as the difference between  $w_A$  and the result of one intensification. (This significance was not remarked in (2).)

Here we shall term the procedure 'elimination of the dominant component'. That it achieves this end is apparent from the first expression for  $w_B$  in (23); for if  $A_s w_s$  (say) is the predominant component of  $w_A$ , then (by 'Rayleigh's principle')  $1 - (\lambda_R)_A / \lambda_s \neq 0$ .

### 'Optimal synthesis'

11. In (2) it was used in conjunction with a device which we now explain. (It should be emphasized that such combination is not obligatory. Either method can be employed without the other.)

$w_A, w_B$  now denoting any two modes which satisfy the edge-conditions, if

$$w = w_A + \gamma w_B \quad (\gamma \text{ real})$$

the 'Rayleigh estimate' derived from  $w$  is

$$\lambda_R = \frac{\mathbf{a} + 2\gamma\mathbf{b} + \gamma^2\mathbf{c}}{\mathbf{d} + 2\gamma\mathbf{f} + \gamma^2\mathbf{g}} \equiv \frac{N}{D} \text{ (say)},$$

where

$$\left. \begin{aligned} \mathbf{a} &\equiv \iint w_A \partial w_A \, dx dy \\ \mathbf{b} &\equiv \iint w_A \partial w_B \, dx dy \equiv \iint w_B \partial w_A \, dx dy \\ \mathbf{c} &\equiv \iint w_B \partial w_B \, dx dy \\ \mathbf{d} &\equiv \iint w_A \partial' w_A \, dx dy \\ \mathbf{f} &\equiv \iint w_A \partial' w_B \, dx dy \equiv \iint w_B \partial' w_A \, dx dy \\ \mathbf{g} &\equiv \iint w_B \partial' w_B \, dx dy \end{aligned} \right\} \quad (24)$$

From this expression it follows that  $\lambda_R$  is stationary both when  $\gamma^2 = \infty$  and when

$$(\mathbf{bd} - \mathbf{af}) + (\mathbf{cd} - \mathbf{ag})\gamma + (\mathbf{cf} - \mathbf{bg})\gamma^2 = 0, \quad (25)$$

and that in the latter event it is given by

$$\lambda_R = (\mathbf{a} + \mathbf{b}\gamma)/(\mathbf{d} + \mathbf{f}\gamma) = (\mathbf{b} + \mathbf{c}\gamma)/(\mathbf{f} + \mathbf{g}\gamma). \quad (26)$$

When  $\gamma = 0$ ,

$$\lambda_R = \mathbf{a}/\mathbf{d} = (\lambda_R)_A, \text{ say, and } \frac{1}{2}\partial\lambda_R/\partial\gamma = (\lambda_R)_A\{\mathbf{b} - \mathbf{f}(\lambda_R)_A\}/\mathbf{a},$$

so unless  $\mathbf{b} = \mathbf{f}(\lambda_R)_A$  the gradient of  $\lambda_R$  will not be zero; consequently (if  $(\lambda_R)_A > 0$ ) some real value of  $\gamma$  will give to  $\lambda_R$  a positive value nearer than  $(\lambda_R)_A$  to  $\lambda_1$ . If  $(\lambda_R)_A > 0$  it entails no restriction to assume that either  $(\lambda_R)_B > (\lambda_R)_A$  or  $(\lambda_R)_B < \lambda_{-1}$  (cf. section 6). In either event a closer estimate of  $\lambda_1$  than either  $(\lambda_R)_A$  or  $(\lambda_R)_B$  will be obtained by 'optimal synthesis'.

12. Both roots of (25) are real when (as here: cf. section 3)  $N$  in (24) is necessarily positive; for on that understanding

$$\mathbf{a} > 0, \quad \mathbf{c} > 0, \quad \mathbf{ac} \geq \mathbf{b}^2,$$

therefore

$$\mathbf{a}^2\mathbf{c}^2 > \mathbf{ab}^2\mathbf{c}, \quad (i)$$

also

$$\begin{aligned} (\mathbf{d}/\mathbf{a} - \mathbf{g}/\mathbf{c})^2 &= (\mathbf{d}/\mathbf{a} + \mathbf{g}/\mathbf{c})^2 - 4\mathbf{dg}/\mathbf{ac} \\ &\geq 4\{\mathbf{f}/\mathbf{b}(\mathbf{d}/\mathbf{a} + \mathbf{g}/\mathbf{c} - \mathbf{f}/\mathbf{b}) - \mathbf{dg}/\mathbf{ac}\} \end{aligned} \quad (ii)$$

because

$$(\mathbf{d}/\mathbf{a} + \mathbf{g}/\mathbf{c} - 2\mathbf{f}/\mathbf{b})^2 \geq 0;$$

and on multiplying corresponding sides of (i) and (ii) we have

$$(\mathbf{cd} - \mathbf{ag})^2 \geq 4\{\mathbf{bf}(cd + ag) - \mathbf{f}^2\mathbf{ac} - \mathbf{b}^2\mathbf{dg}\} = 4(\mathbf{bd} - \mathbf{af})(\mathbf{cf} - \mathbf{bg}).$$

The modes derived from (25) are conjugate, viz.

$$w_I \text{ (say)} = w_A + \gamma_1 w_B, \quad w_{II} \text{ (say)} = w_A + \gamma_2 w_B;$$

for the conditions of such conjugacy are (cf. (9), section 4)

$$\left. \begin{aligned} 0 &= \iint w_I \vartheta w_{II} dx dy = \mathbf{a} + \mathbf{b}(\gamma_1 + \gamma_2) + \mathbf{c}\gamma_1\gamma_2 \\ 0 &= \iint w_I \vartheta' w_{II} dx dy = \mathbf{d} + \mathbf{f}(\gamma_1 + \gamma_2) + \mathbf{g}\gamma_1\gamma_2 \end{aligned} \right\}, \quad \text{according to (24)},$$

and according to (25)

$$(\mathbf{cf} - \mathbf{bg})(\gamma_1 + \gamma_2) = \mathbf{ag} - \mathbf{cd}, \quad (\mathbf{cf} - \mathbf{bg})\gamma_1\gamma_2 = \mathbf{bd} - \mathbf{af}. \quad (27)$$

### Rayleigh's method in conjunction with intensification

13. G. Temple (10) and Temple and Bickley (11), also J. J. Koch (12) in effect, have used intensification in conjunction with Rayleigh's method. By this procedure, when the eigenvalues are all positive, the accuracy of his estimate is improved: for as derived from  $w$  it is given by (12), and as derived from  $w_I$  it is given by

$$\left. \begin{aligned} (\lambda_R)_I &\equiv \Lambda I''/I'', \text{ say,} \\ \text{where } I'' &\equiv \iint w_I \vartheta w_I dx dy = \Lambda^2 \sum (A_k^2/\lambda_k^2) \\ I''' &\equiv \iint w_I \vartheta w_{II} dx dy = \Lambda^3 \sum (A_k^2/\lambda_k^3) \end{aligned} \right\}. \quad (11)^* \quad (28)$$

Hence (section 6\*)

$$(\lambda_R)_I/\lambda_R \leq 1 \text{ when every } \lambda \text{ is positive but not (necessarily) otherwise.}$$

### An alternative to the 'Rayleigh estimate'

14. But all of Rayleigh's arguments apply to

$$\mu_S^2 \text{ (say)} \equiv \Lambda^2 I/I'' = \sum (A_k^2)/\sum (A_k^2/\lambda_k^2), \quad (13)^* \quad (29)$$

whether all of the eigenvalues have one sign or no, because every  $\lambda^2 > 0$ . That is to say (section 7\*)

$$\mu_S^2 \geq \text{the smaller of } \lambda_1^2 \text{ and } \lambda_{-1}^2,$$

$$(\mu_S^2)_I \leq \mu_S^2, \text{ when } (\mu_S^2)_I \text{ is derived from } w_I.$$

Finally, by (12) and (29),

$$\begin{aligned} \mu_S^2/(\lambda_R)^2 &\equiv I'^2/II'' = [\sum (A_k^2/\lambda_k^2)]^2 / \sum (A_k^2/\lambda_k^2) \cdot \sum (A_k^2) \\ &= 1 - \sum_{r,s} [A_r^2 A_s^2 (\lambda_r^{-1} - \lambda_s^{-1})^2] / \sum (A_k^2/\lambda_k^2) \cdot \sum (A_k^2) \quad (30) \\ &\leq 1, \text{ whatever the signs of the eigenvalues.} \end{aligned}$$

Thus  $\mu_S^2$  (which of course entails 'intensification') has advantages over the Rayleigh estimate  $\lambda_R$ —more especially in relation to systems like our test example.

15. 'Optimal synthesis' (section 11) can be performed on the basis of (29). That expression gives for  $w = w_A + \gamma w_B$  ( $\gamma$  real)

$$(\mu_S^2/\Lambda^2)_w = \frac{\mathbf{a} + 2\gamma\mathbf{b} + \gamma^2\mathbf{c}}{\mathbf{D} + 2\gamma\mathbf{F} + \gamma^2\mathbf{G}}$$

where  $\mathbf{a}, \mathbf{b}, \mathbf{c}$  have their expressions (24) and where

$$\Lambda^2 \mathbf{D} = \iint w'_A \partial w'_A \, dx dy, \quad (24)\text{A}$$

$$\Lambda^2 \mathbf{F} = \iint w'_A \partial w'_B \, dx dy$$

$$\Lambda^2 \mathbf{G} = \iint w'_B \partial w'_B \, dx dy$$

$w'_A$  and  $w'_B$  denoting functions obtained by intensification of  $w_A$  and  $w_B$  on the basis of equations like (14).

Every consequence drawn from (24) has a parallel which can be drawn from (24)A, except that (cf. section 10\* of (4)) the first but not the second of (9) is satisfied by the modes which make  $\mu_S^2$  stationary, whereas both of (9) are satisfied (cf. section 12) by the modes which make  $\lambda_R$  stationary.

## II. REVIEW OF EARLIER WORK ON THE TEST EXAMPLE

16. In the earlier attack on our test example (2), reliance was placed on a use of 'Rayleigh's method' in combination with 'optimal synthesis' as described in section 11. There, no restriction is imposed on  $w_A$  or  $w_B$  except that both must satisfy the edge-conditions: in (2), 'point-relaxation' was employed to relate  $w_B$  with  $w_A$  by (22)—no attempt being made to solve

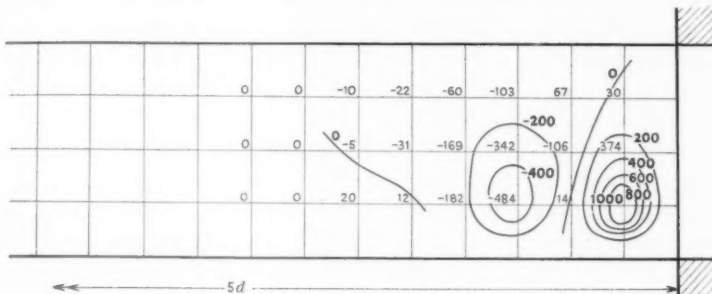


FIG. 4.

(22) exactly, since the aim was merely to obtain a second component differing widely from  $w_A$ . The objective was strictly practical—to compute  $\lambda_1$  in a case where the gravest mode could not be guessed. 'Intensification' was not utilized, or 'partial transfer'; and the alternative ( $\mu_S^2$ ) to Rayleigh's estimate ( $\lambda_R$ ) had not at that time been recognized.

To make the example a drastic test of method, the initial estimate of the gravest mode was deliberately made wide of the mark (viz. symmetrical both in  $x$  and  $y$ , and of one sign throughout). The first and final nets had mesh-side  $d/4$  and  $d/8$  (Fig. 2). On the first, by 12 optimal syntheses the mode was greatly altered and the Rayleigh estimate was brought down to a nearly stationary value. Fig. 4 (a rough plot of hitherto unpublished computations) shows the results of this stage of the work.

Further syntheses on the finer net brought  $\lambda_R$  down from 7.904 to 5.949, a value 'believed to be correct within about 1 per cent.' Less exactitude was attempted in the determination of the mode (Fig. 12 of (2)—here reproduced as Fig. 2); and no proof was adduced to show that this approximates to  $w_1$  (not to some other characteristic mode).

17. Other theoretical questions were left unanswered: e.g., could the accuracy of Fig. 2 have been improved without excessive computational labour? is 'C', section 1, a feature of this system; and if so, what mode is associated with  $\lambda_2$ ? This last question has some practical interest: first, since if  $\lambda_1 \div \lambda_2$  the figure given above (5.949) overestimates  $\lambda_1$ ; secondly, because the mode conditions the best arrangement of 'stiffeners'.

These questions prompted an investigation which has resulted both in this paper and in (4). At the outset it was evident that any or all of 'A', 'B', and 'C', section 1, might be features of the test example; that 'A' would invalidate use of 'Rayleigh's method' except in conjunction with some means to an accurate estimation of  $w_1$ ; and that as a consequence of 'B' either sign might be taken by a 'Rayleigh estimate'. At first this was taken as an indication that Rayleigh's method must be discarded; but subsequently our recognition of an 'excluded range' (section 6) showed that every positive estimate  $\geq \lambda_1$  and so made it likely that the estimate 5.949 is close, since  $\lambda_R$  became nearly stationary in the later syntheses performed by Fox and Green.

To this extent their Fig. 4 gained plausibility, despite the italicized proviso of section 7. It did not seem possible to prove that  $w_1$  was a component in their initial guess—and only so, in theory, would it contribute to the modes which they derived from it by a method shown (section 10) *in effect* to be 'intensification'; but the likelihood of such failure is reduced by the fact that (22) was not solved exactly. None the less it was felt that other methods should be tried, to attain their results, if possible, by a different route.

### III. NEW METHODS APPLIED TO THE TEST EXAMPLE

#### (1) 'Exploration' with an applied point-loading

18. This method rests on the theoretical expression for the response ( $w$ ) to a concentrated force applied at some chosen point  $P$  when the intensity of the destabilizing forces (edge-thrusts) is specified by  $\lambda$ . In (16), section 8, let  $Z_0$  be zero except within an elemental area at  $P$ , and let

$$\iint Z_0 \, dx \, dy \text{ for the elemental area} = 1.$$

Then, on multiplying (16) by  $w_k$  and integrating over the whole area of the plate, we obtain

$$(w_k)_P = \iint w_k Z_0 \, dx \, dy = \iint w_k \vartheta w_0 \, dx \, dy = A_k, \text{ simply,}$$

when its series  $\sum [A_k w_k]$  is written for  $w_0$ . Accordingly in this instance (17) become

$$\left. \begin{aligned} w_0 &= \sum [(w_k)_P w_k], \\ w &= \sum [(w_k)_P w_k / (1 - \lambda/\lambda_k)] \end{aligned} \right\}, \quad (31)$$

and show that the response at the 'load-point'  $P$  is

$$\left. \begin{aligned} (w)_P &= \sum [(w_k)_P^2 / (1 - \lambda/\lambda_k)] \\ &= \sum [(w_k)_P^2], \quad \text{when } \lambda = 0 \end{aligned} \right\}. \quad (32)$$

19. It follows from (32) that when  $\lambda = \lambda_k$  (that is, when one of the eigenvalues is attained) a zero force at  $P$  will make  $(w)_P$  unity. The second of (32) shows this force to be positive and finite when  $\lambda = 0$ ; so, on the side  $\lambda > 0$  it first becomes zero when  $\lambda = \lambda_1$ , on the side  $\lambda < 0$  it first becomes zero when  $\lambda = \lambda_{-1}$ . If, then,  $w$  can be determined for chosen values of  $\lambda$ ,

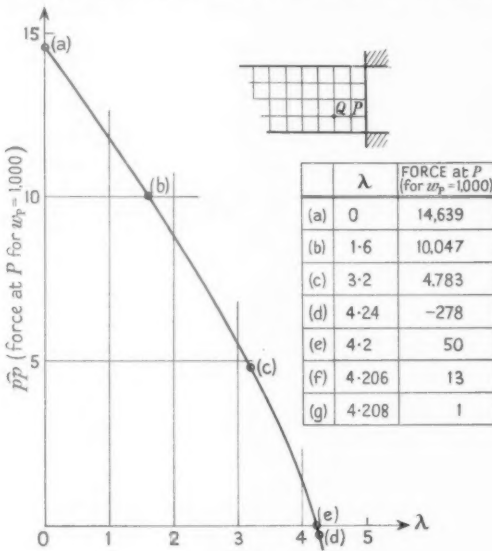


FIG. 5.

by plotting the force required when  $(w)_P = 1$  (a quantity which we here denote by  $\hat{p}p$ ) we can derive  $\lambda_1$  as the smallest positive  $\lambda$  for which  $\hat{p}p = 0$ . Like 'partial transfer' the method effects a bias towards modes and eigenvalues of the wanted sign.

Here too, however, theory imposes a proviso: *in order that the method may yield  $w_1$ ,  $(w_1)_P$  must not be zero*. Thus here too, in theory, 'A' may be a cause of failure; but the chance of this is small—and will be made still smaller if 'exploration' is repeated with the unit force applied at a different point. Whether the method is feasible can of course be settled only by trial. It entails use of a different 'pattern' at every nodal point; but precision is needed only in the final stages, when  $\lambda$  has a value close to  $\lambda_1$  and  $\hat{p}p \neq 0$ .

#### Application to the test example (Figure 1)

20. Fig. 5 illustrates the procedure as applied to the coarse-net system. Each point represents a relaxational solution in which, with the same displacement imposed at  $P$ , residuals were brought sensibly to zero except at the boundary and at the 'load-point'  $P$ . On that understanding

(cf. section 19) the residual at  $P$  is a measure of  $-\hat{p}\hat{p}$ . Only relative values are required to determine  $\lambda_+$ .

- (i) A curve drawn through (a), (b), and (c) suggested a zero force for  $\lambda = 4.24$ ;
  - (ii) trial of this value led to solution (d);
  - (iii) a new curve drawn through points (a), (b), (c), and (d) suggested a zero for  $\lambda = 4.20$ ;
  - (iv) trial of this value led to solution (e).

Thereafter, linear interpolation could be used: between (d) and (e) to suggest a value (4.206) which led to (f), and between (e) and (f) to suggest a value (4.208) which led to (g). This last solution entailed a force at  $P$  which was comparable with the other neglected residuals: consequently the mode obtained in (g) could be accepted, and this gave 4.2073 as the estimate of  $\lambda_1$ .

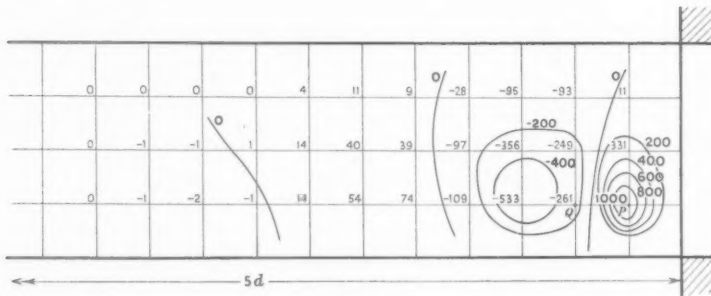


FIG. 6.

21. Fig. 6, which shows the mode as thus deduced, may be compared with Fig. 4, which gives the mode obtained by Fox and Green. The general similarity of the diagrams, and the agreement of the corresponding Rayleigh estimates (4.288 and 4.2073), suggest that both relate to the gravest mode; but the net is too coarse to define this with precision, or to justify replacement of the integrals by summations. (Fox, using standard formulae of integration, found on halving the mesh-side that  $\lambda$  rose at once from 4.288 to 7.904.)

## Extension of the method

22. In the unlikely event (section 19) of  $P$ 's being nodal for  $w_1$ ,  $\lambda_1$  will not be altered by the imposition of a constraint at  $P$ , so an exploration made with  $P$  restrained and another point  $Q$  loaded will yield the same eigenvalues as before; but if  $(w_1)_P \neq 0$  then, by a theorem due to Rayleigh ((5), section 88), a constraint at  $P$  will cause  $\lambda_1$  to rise. We may exclude as almost

unthinkable the possibility that both  $P$  and  $Q$  are nodal for  $w_1$ ; and on that understanding two explorations (one as above; the other with  $P$  loaded and  $Q$  restrained) will indicate whether 'C', section 1, is a feature of the system.

For suppose that  $\lambda_2 = \lambda_1$  exactly. Then two distinct modes are associated with  $\lambda_1$ , and in some combination of them  $Q$  is nodal; therefore if (as in section 19)  $\hat{pp}$  denotes the force required to make  $(w)_P$  unity, and if  $\hat{pq}$

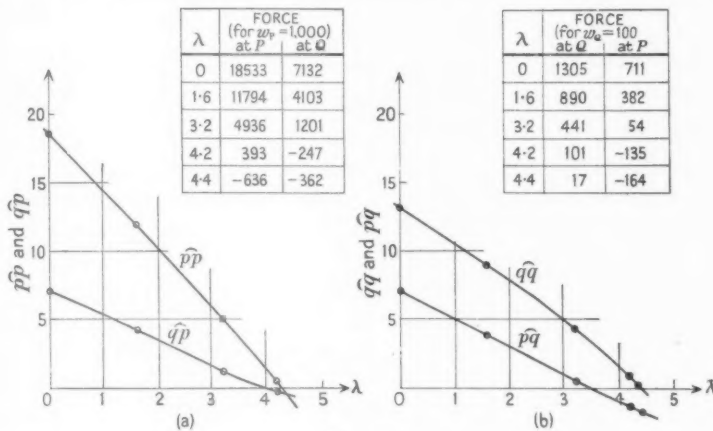


FIG. 7.

stands for the corresponding force of restraint at  $Q$ ,  $\hat{qp}$  as well as  $\hat{pp}$  will be zero when  $\lambda = \lambda_1$  as obtained before. If  $\lambda_2 > \lambda_1$  but only by a small quantity, the constraint at  $Q$  (which we have assumed not to be nodal for  $w_1$ ) will cause  $\hat{pp}$  to vanish for a slightly higher  $\lambda$ , and  $\hat{qp}$  will not vanish simultaneously.

### Application to the test example

23. Figs. 7 present the results of a double exploration on the same net ( $a = \frac{1}{4}$ ) as before. In (a), with  $Q$  (Fig. 5) restrained a fixed displacement was imposed at  $P$ , and  $\hat{pp} = 0$  when  $\lambda \neq 4.27$ . Comparing this value with 4.208 as deduced from Fig. 5 (cf. section 20), we conclude that (for this net)

- (i)  $\lambda_2 \neq \lambda_1$ —otherwise the estimate of  $\lambda_1$  would not have been raised (cf. section 22);
- (ii)  $P$  is not nodal in  $w_1$ —otherwise (unless  $Q$  too is nodal in that mode) Figs. 5 and 7(a) would have yielded widely different estimates of  $\lambda_1$ ;
- (iii)  $Q$  is not nodal in  $w_1$  (since the estimate of  $\lambda_1$  is raised as a consequence of the restraint at  $Q$ ); but lies close to a nodal line (since the rise of  $\lambda_1$  is less than 2 per cent.).

Both (ii) and (iii) are confirmed by Fig. 6 if (as in section 21) that diagram is assumed to approximate to  $w_1$ .

In (b), with point  $P$  restrained a fixed displacement is imposed at  $Q$ , and  $\hat{q}q = 0$  when  $\lambda \doteq 4.44$ . This increased rise gives further support to (iii).

**24.** In theory a 'Maxwell relation' should be satisfied—namely

$$\hat{p}q = \hat{q}p \quad (33)$$

and Fig. 5 should be deducible from Figs. 7 by the formula

$$\hat{p}p \text{ in Fig. 5} = (\hat{p}p - \hat{q}q^2/\hat{q}q) \text{ as computed from Figs. 7.} \quad (34)$$

(33) is confirmed less exactly than was expected; but (34) is very closely realized when the product  $\hat{q}q \cdot \hat{q}p$  is taken in place of  $\hat{q}q^2$ . Both  $\hat{q}q$  and  $\hat{q}p$  come to zero before either  $\hat{p}p$  or  $\hat{q}q$ .

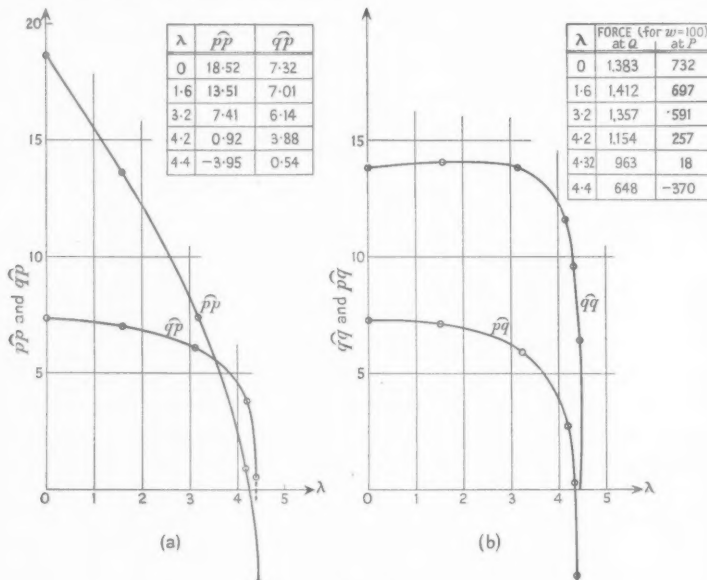


FIG. 8.

That the curves of  $\hat{p}p$  and  $\hat{q}q$  in Figs. 5 and 7 are nearly linear is evidence that  $w_1$  predominates in (32). It does so because  $P$  and  $Q$  lie (Fig. 5) in the region where the destabilizing forces are large: if either or both had lain near the top right-hand corner in Fig. 1, then initially 'negative' modes would have predominated and  $\hat{p}p$  and  $\hat{q}q$  would have increased with  $\lambda$ , falling only (and then rapidly) to zero as  $\lambda \rightarrow \lambda_1$ . Results of this kind were obtained in an earlier exploration, when  $P$  had the same position as before but  $Q$  was on the centre-line: then (cf. Figs. 8), though  $\hat{p}p$  still fell

fairly steadily, the variation of  $\hat{q}\hat{q}$  was quite different. (The 'Maxwell relation' (33) is closely satisfied.)

### Practical aspects

25. So far as it can be tested by one example, 'exploration' seems to meet all practical requirements when (as on the coarser net) use of a different 'relaxation pattern' at every point is feasible. Each solution yields a good starting assumption for the next, and (if the point of loading is chosen suitably) no trouble comes from 'negative' components. But (section 21) a finer net is needed to define the mode and thereby to evaluate  $\lambda_1$  with precision; and no method can be recommended which entails a different pattern at each of the 273 'relaxable' nodes in Fig. 2. Thus 'exploration' has value only in the initial computations on the coarser net: there, it provides an estimate of the gravest mode which has no appreciable 'negative' component and accordingly, if made the starting assumption on the fine net, will almost certainly obviate trouble due to 'A' and/or 'B', section 1.

But nothing found on the coarse net can establish that two or more of the gravest eigenvalues will not be nearly or exactly equal in the fine-net system. If  $\lambda_2 = \lambda_1$  exactly, any combination of  $w_1$  and  $w_2$  may be taken as the gravest mode and will not be altered by intensification; but if  $\lambda_2$  is slightly greater than  $w_1$ , then in theory intensification will reduce the component  $w_2$ , but very slowly, so in practice it may fail to yield  $w_1$  on account of inescapable computational errors.

26. On the fine net Fox and Green used optimal synthesis in conjunction with the method of section 12 (there shown to be equivalent to 'intensification') and 'after point liquidation had been carried as far as was deemed practicable' ((2), section 32). Probably they would have found these methods insufficient if they had sought to determine the mode as accurately as the eigenvalue; for while one intensification of their accepted mode (Fig. 2) reduced  $\lambda_R$  by only 0·1 per cent.,<sup>†</sup> both it and subsequent intensifications entailed appreciable changes in the mode. Other attempts based on various starting assumptions agreed in suggesting that  $\lambda_1$  lies close to 5·94; but in no instance was a quite definite mode obtained, and as a rule each intensification (in the latter stages) resulted in a small but appreciable and nearly invariant alteration (in the notation of section 7,  $\Delta_I \equiv w_I - w$  and  $\Delta_{II} \equiv w_{II} - w_I$  were small and nearly identical). Moreover, occasionally  $\lambda_R$  appeared to rise.

<sup>†</sup> Namely, from 5·9464 to 5·9413. The value (5·949) which Fox and Green recorded is believed to relate to a mode slightly different from Fig. 2; but their conclusion that it is 'correct within about 1 per cent.' is supported by these figures.

It thus appeared that 'intensification'—the only method yet available on the finer net—might fail as applied to systems which have the features 'A' and 'B' and may have the feature 'C', section I. (The fact—shown by Fig. 7—that  $\lambda_1$  and  $\lambda_2$  are not equal for the coarse-net system cannot be adduced as an argument against their being equal when the number of the eigenvalues is much larger.)

## (2) Introduction of an 'ancillary restraint'

27. The possibility that  $\lambda_2 = \lambda_1$  exactly may be tested by introducing an 'ancillary restraint'. Rayleigh ((5), section 92a) has shown that application of a constraint (unless at a point which is nodal: there it has no effect)—

- (i) reduces by one the number of the eigenvalues;
- (ii) raises each eigenvalue to a new value intermediate between its old value and that of the next higher eigenvalue.

If originally the two gravest eigenvalues were exactly equal, this means that one is conserved, but only one: the second is made greater than before. If more than two are equal, by employing more than one constraint we can again make the gravest eigenvalue unique; and for the modified system it appears (from one trial) that intensification is effective.

Assuming an 'ancillary restraint' to prevent displacement of a point  $P$  in the region where the destabilizing forces are large, by intensification we can find the gravest mode and eigenvalue ( $w_C$  and  $\lambda_C$ , say) of the system as thus modified, also the force exerted by the restraint. If this is zero, then the restraint is inoperative, and  $\lambda_C$ ,  $w_C$  may be identified with the wanted  $\lambda_1$ ,  $w_1$ : if it is large, then the restraint entails a large increase of stability, therefore  $(\lambda_C - \lambda_1)$  and *a fortiori*  $(\lambda_2 - \lambda_1)$  must be considerable (for we have seen that  $\lambda_C$  lies between  $\lambda_1$  and  $\lambda_2$ ). The latter result is unlikely, since unless  $\lambda_2 \neq \lambda_1$  intensification should not have failed to yield  $w_1$ . More probably, what will result are a mode ( $w_C$ ) entailing a small force at  $P$  and an eigenvalue ( $\lambda_C$ ) slightly greater than  $\lambda_1$ .

## Theoretical aspects

28. G. V., applying this procedure to the test example, took as her starting assumption a combination, making  $w_P$  zero, of two modes found earlier and believed to be fair approximations to  $w_1$ . From this she was able by intensification to derive an acceptable solution  $w_C$  and a value 6.0032 for  $\lambda_C$ .

According to (31) of section 18,

$$\text{so } \begin{aligned} w_C &= \sum [(w_k)_P w_k / (1 - \lambda_C/\lambda_k)], & w_0 &= \sum [(w_k)_P w_k] \\ W_C \text{ (say)} &\equiv w_C - w_0 = \lambda_C \sum [(w_k)_P w_k / (\lambda_k - \lambda_C)] \end{aligned} \quad \{ \quad (35)$$

Each of  $w_C$  and  $w_0$  has a singularity due to unit forces at  $P$ , so  $W_C$  has no singularity; and the first terms dominate its series (35) by reason of the smallness of  $(\lambda_1 - \lambda_C)$  and  $(\lambda_2 - \lambda_C)$  compared with other denominators—always provided that  $(w_1)_P, (w_2)_P$  are not zero. This is made reasonably certain by  $P$ 's location in a region where the destabilizing forces are large. (In G. V.'s test,  $P$  had the position shown in Fig. 5.)

Two intensifications of  $W_C$  in accordance with

$$\vartheta \bar{W}_C = \Lambda \vartheta' W_C, \quad \vartheta' \bar{W}_C = \Lambda \vartheta' \bar{W}_C$$

yield modes

$$\begin{aligned} \bar{W}_C &\equiv \Lambda \cdot \lambda_C \sum [(w_k)_P w_k / \lambda_k (\lambda_k - \lambda_C)] \\ \bar{\bar{W}}_C &\equiv \Lambda^2 \cdot \lambda_C \sum [(w_k)_P w_k / \lambda_k^2 (\lambda_k - \lambda_C)] \end{aligned} \quad (36)$$

which also have no singularity at  $P$  and in which  $w_1, w_2$  are still more predominant. The Rayleigh estimate for  $\bar{W}_C < \lambda_C$ , the Rayleigh estimate for  $\bar{\bar{W}}_C$ ; but will not be much smaller if the force of restraint is small.

G. V.'s computations gave a value slightly less than 6.002. This being larger than some earlier estimates, it was to be expected that  $\bar{W}_C, \bar{\bar{W}}_C$  would differ sensibly—and this proved to be the fact. They had the characteristic noticed in section 26: namely, that  $\Delta_I, \Delta_{II}$  as there defined were small and nearly identical. The suspected reason was near-equality of  $\lambda_1$  and  $\lambda_2$ ; and the final problem, in the test example, was seen to be closer estimation of the gravest mode.

### The final problem: estimation of the gravest mode

29. At this point our collaboration was interrupted and it was left to the senior author to make a final assessment of results. That task led him to some theorems which were presented in (4) and, in respect of the test example (sections 17–19\*), to the conclusion that either  $\lambda_1$  is restricted by the double inequality

$$5.9648_0 \leqslant \lambda_1 \leqslant 5.9967_0 \quad (38*) \quad (37) A$$

(and in that event the earlier estimate, 5.949, of Fox and Green (section 15) is in error by not more than 0.8 per cent.) or  $\lambda_2$ , which is very nearly equal to  $\lambda_1$ , lies within the range

$$5.9648_0 \leqslant \lambda \leqslant 6.03943_4 \quad (39)*, \quad (37) B$$

and then  $\lambda_1$  may be less than the lower of those limits. In this second event the estimate of Fox and Green is likely to be still closer.

The inequalities (37), A and B, are based on values which G. V., identifying  $w, w_I, w_{II}$  with  $W_C, \bar{W}_C, \bar{\bar{W}}_C$ , and giving to  $\Lambda$  the value (6.002) which

she had found for  $\lambda_R$  (section 28), computed for the integrals

$$\left. \begin{aligned} I &\equiv \iint w \vartheta w \, dx dy = \sum [A_k^2] \\ I' &\equiv \iint w \vartheta w_I \, dx dy = \Lambda \sum [A_k^2/\lambda_k] \\ I'' &\equiv \iint w \vartheta w_{II} \, dx dy = \Lambda^2 \sum [A_k^2/\lambda_k^2] \equiv \iint w_I \vartheta w_I \, dx dy \\ I''' &\equiv \iint w_I \vartheta w_{II} \, dx dy = \Lambda^3 \sum [A_k^2/\lambda_k^3] \\ I^{IV} &\equiv \iint w_{II} \vartheta w_{II} \, dx dy = \Lambda^4 \sum [A_k^2/\lambda_k^4] \end{aligned} \right\} \quad (15)^* \quad (38)$$

(Her identification of  $\Lambda$  with  $\lambda_R$  entailed exact equality of  $I$  and  $I'$  (cf. (12), section 6), and her other estimates were

$$I''/I = 1.0012_1, \quad I'''/I = 1.0019_3, \quad I^{IV}/I = 1.0029_3 \quad (32)^* \quad (39)$$

—a dropped figure such as 3 denoting some value between 2 and 4 but possibly nearer to 2 or 4 than to 3.†) In addition to these restrictions on  $\lambda$ , (4) drew some conclusions in regard to *modes*: e.g. (section 18\*) that as computed from (12) for

$$w_\gamma \equiv w + \gamma w_I (\equiv W_C + \gamma \bar{W}_C) \quad (23)^* \quad (40)$$

$\lambda_R/\Lambda$  has a maximum value  $-2.46415039$  when  $\gamma = -0.99914$  and  
a minimum value  $0.999140032_4$  when  $\gamma = 2.47$  } (41)

and that as computed from (30) for  $w$ ,

$\mu_S^2/\Lambda^2$  has a maximum value  $(2.08130718)^2$  when  $\gamma = -0.99907$  and  
a minimum value  $(0.99911809)^2$  when  $\gamma = 3.40$ . } (33)\* (42)

30. Only the second of (42) was utilized, (4) being only concerned with eigenvalues; but all of (41) and (42) serve to elucidate the final problem (section 29) *when taken in conjunction with (37) A*. Thus  $\lambda_R$  and  $\mu_S^2$  as computed for  $w_\gamma$  take maximum values when  $\gamma = -1$  with an error of the order of 0.1 per cent.: i.e. when to this order of approximation the mode is

$$w - w_I \equiv -\Delta_I, \quad \text{as defined in section 26,}$$

$$= \sum [A_k w_k (1 - \Lambda/\lambda_k)] \quad \text{when } w = \sum (A_k w_k). \quad (43)$$

Now in (4) (37) was obtained as

$$0.99380_3 \leq \lambda_1/\Lambda \leq 0.999118 \quad (37)^* \quad (44)$$

† Strictly, the computations in (4) should have been extended to allow for this possibility. But thereby the paper would have been greatly lengthened, and it is unlikely that the limits would have been much altered.

with  $\Lambda = 6.002$  (section 29). This shows that  $w_1$  makes a negligible contribution to  $\Delta_I$ , therefore  $A_1^2$  has a negligible influence on the values which  $\lambda_R$  and  $\mu_S^2$  take for  $\Delta_I$ ; and the arguments of section 7 and section 14 then serve to deduce from (41) and (42) that

$$|\lambda_{-1}|/\Lambda \leq 2.46415, \quad \lambda_2/\Lambda \leq 2.08131. \quad (45)$$

31. We can go further if in each of the series (43) and (38) three terms, at most, are taken as significant, so that we may write

$$w = A_1 w_1 + A_r w_r + A_s w_s, \quad I = A_1^2 + A_r^2 + A_s^2, \dots, \text{etc.} \quad (46)$$

For then elimination of  $A_1^2$  between successive pairs of (38) yields four relations between  $I$ ,  $A_r^2$ , and  $A_s^2$ —namely,

$$\left. \begin{aligned} (\mathbf{A}, x\mathbf{B}, x^2\mathbf{C}, x^3\mathbf{D})I &= (1, r, r^2, r^3)(1-r)A_r^2 + (1, s, s^2, s^3)(1-s)A_s^2 \\ \text{where } x &\equiv \lambda_1/\Lambda, \quad r \equiv \lambda_1/\lambda_r, \quad s \equiv \lambda_1/\lambda_s \\ \mathbf{A} &\equiv 1-x \equiv \epsilon \text{ (say)}, \quad \mathbf{B} \equiv \epsilon - x\mathbf{a} \\ \mathbf{C} &\equiv \epsilon + \mathbf{a} - x\mathbf{b}, \quad \mathbf{D} \equiv \epsilon + \mathbf{b} - x\mathbf{c} \end{aligned} \right\}, \quad (47)$$

and when

$$\left. \begin{aligned} 1+\mathbf{a} &\equiv I''/I, \quad 1+\mathbf{b} \equiv I'''/I, \quad 1+\mathbf{c} \equiv I^{IV}/I \\ \text{so that } 10^4 \times (\mathbf{a}, \mathbf{b}, \mathbf{c}) &= 12 \cdot 1, 19 \cdot 3, 29 \cdot 3 \end{aligned} \right\}, \quad (48)$$

according to (39); and all of (47) are closely satisfied when

$$\left. \begin{aligned} r &\doteq x \equiv \lambda_1/\Lambda, \quad s = -0.4x \\ (1-r)A_r^2/I &= 1-x(1+\mathbf{a}/1.4) \doteq 1-x/0.9992 \\ A_s^2/I &= \mathbf{a}/(1.4)^2 \doteq 6.2 \times 10^{-4} \end{aligned} \right\}. \quad (49)$$

Since  $r < 1$  (by hypothesis) and  $x (= \lambda_1/\Lambda)$  is restricted by (44), (49) give real values both to  $A_r$  and to  $A_s$ .  $A_s^2$  is very small in relation to  $I$  (and to  $A_1^2$ ), but  $A_r^2$  can have a value which is comparable, since  $(1-r)$  is small like  $(1-x)$ .

Thus the values (39) afford indications that

- (a) another characteristic mode ( $w_2$ ) is associated with an eigenvalue ( $\lambda_2$ ) which is very little greater than  $\lambda_1$ .
- (b) the mode ( $W_C$ ) from which (39) were derived contains an appreciable ‘negative’ component, associated with an eigenvalue ( $\lambda_{-1}$ ) nearly equal to  $\lambda_1/(-0.4) = -2.5\lambda_1$ . The amplitude,  $A_s$ , of this negative component of  $W_C$  is small (of the order  $10^{-2}$ ) in relation to  $A_1$  and  $A_r$ ; but in  $\Delta_I$  its amplitude is sensible because the other components are reduced almost to zero.

Undue weight must not be given to the indications, since they are based on a merely plausible hypothesis and on computed values which have uncertain accuracy. But the indications are consistent with (45) and with the observations recorded in section 28, also with the second of the possibilities that were contemplated in section 29; and they give helpful guidance towards a solution of the final problem (section 29). (For example, given a close estimate of  $\lambda_s$  ( $= \lambda_1/s$ ), the negative component of  $W_C$  can be eliminated by the method of section 10.)

32. The indications, moreover, are unambiguous—to the extent that the values (39) are accurate. The first two of (47) require that

$$\begin{aligned} (r-s)(1-r)A_r^2 &= (x\mathbf{B}-s\mathbf{A})I, \\ (s-r)(1-s)A_s^2 &= (x\mathbf{B}-r\mathbf{A})I \end{aligned} \quad (50)$$

and the last two, when these expressions are substituted, give

$$\left. \begin{aligned} (r+s)x\mathbf{B}-rs\mathbf{A} &= x^2\mathbf{C} \\ (r+s)^2x\mathbf{B}-rs\{x\mathbf{B}+(r+s)\mathbf{A}\} &= x^3\mathbf{D}, \\ (\mathbf{B}^2-\mathbf{AC})(r+s) &= x(\mathbf{BC}-\mathbf{AD}) \\ (\mathbf{B}^2-\mathbf{AC})rs &= x^2(\mathbf{C}^2-\mathbf{BD}) \end{aligned} \right\} \quad (51)$$

whence

Hence  $r$  and  $s$  can be computed.

The inequality (44) implies that

$$8 \leq \epsilon \times 10^4 \leq 62,$$

so all of  $\epsilon, \mathbf{a}, \mathbf{b}, \mathbf{c}$  are of order  $10^{-3}$  or less, and terms of the third and higher order in those quantities are negligible in comparison with  $\mathbf{a}^2, \mathbf{ab}, \dots$ , etc. On that understanding, when  $\mathbf{A}, \mathbf{B}, \mathbf{C}, \mathbf{D}$  are given their expressions (47),

$$\left. \begin{aligned} \mathbf{B}^2-\mathbf{AC} &= \mathbf{a}^2-\epsilon(3\mathbf{a}-\mathbf{b}) \\ \mathbf{BC}-\mathbf{AD} &= \mathbf{a}(\mathbf{b}-\mathbf{a})+\epsilon(\mathbf{c}-2\mathbf{b}) \\ \mathbf{C}^2-\mathbf{BD} &= \mathbf{b}^2-\mathbf{a}(\mathbf{b}+\mathbf{c}-\mathbf{a})+\epsilon(\mathbf{c}+3\mathbf{a}-3\mathbf{b}) \end{aligned} \right\} \quad (52)$$

with sufficient approximation. These quantities vanish for values of  $\epsilon \times 10^4$  which differ, but which all lie between 8.5 and 9.5. In that narrow range as computed from (51) and (52),  $(r+s)$  and  $rs$  vary rapidly—and take values excluded by the requirements  $|r| < 1, |s| < 1$ : but all of  $(\mathbf{B}^2-\mathbf{AC}), \dots$ , etc., vanish for the same value of  $\epsilon^\dagger$  when changes are made in  $\mathbf{a}, \mathbf{b}$ , and  $\mathbf{c}$  which

$\dagger$  The necessary and sufficient condition is

$$\mathbf{a}(\mathbf{c}-2\mathbf{a}) = (\mathbf{b}-\mathbf{a})^2,$$

and is closely satisfied when, for example, (48) are replaced by

$$10^4 \times (\mathbf{a}, \mathbf{b}, \mathbf{c}) = 12.2, 19.5, 28.8.$$

Then  $10^4 \times \epsilon = 8.8$ , approximately, according to all of (52).

hardly go outside their margins of uncertainty (cf. section 29); and (52) then indicate that

$$\left. \begin{aligned} (r+s)/x &\doteq 0.6, & rs/x^2 &\doteq -0.4, \\ \text{therefore } r/x, s/x &\doteq 1, -0.4, \\ \text{i.e. } \lambda_r &\doteq \lambda_1/x, & \lambda_s &\doteq -2.5\lambda_1/x \end{aligned} \right\} \quad (53)$$

These are the values recorded in (49), and when  $A_r^2$  and  $A_s^2$  have the values given there the first two of (47) are satisfied exactly, the last two very nearly if  $\epsilon$  lies within the limits imposed by (44). The last two of (53) are compatible with (45); and the first of them indicates very near equality of  $\lambda_2$  and  $\lambda_1$  (thus explaining the near-identity of  $\Delta_I$  and  $\Delta_{II}$ <sup>†</sup>), the second explains the negative maximum of  $\lambda_R$  which is given in the first of (41).

### Conclusion

33. Finally—and consistently with the indications of section 31—the second of (42) shows that a better approximation to  $w_1$  than  $W_C$  is the mode

$$w = (W_C + 3.4\bar{W}_C)/4.4 \quad (54)$$

of which contours are given in Fig. 9. This differs sensibly from the mode obtained by Fox and Green (Fig. 2), nodal lines of which are reproduced in Fig. 9; yet both modes are associated with eigenvalues that differ from 5.97 by less than 1 per cent.

Thus although the ‘final problem’ has not been solved completely, what has been done is of nearly equal value from a practical standpoint. For Figs. 2 and 9 are different combinations of  $w_1$  and  $w_2$  (each containing, probably, a small admixture of  $w_{-1}$  and of other unwanted modes); and all combinations are almost equally likely to occur (since  $\lambda_1$  and  $\lambda_2$  have been shown to be nearly equal), so the conclusion in regard to stiffener (section 17) is evident: the region of maximum waving has been delimited, but the ‘phase’ of the waving is nearly indeterminate.

34. All three of the difficulties ‘A’, ‘B’, and ‘C’, section 1, have been found to characterize the test example; and all for practical purposes have been surmounted, by methods which should have very wide application. We have shown, in sections 18–24 and 27, how to ensure the presence of  $w_1$  in a ‘guess’ which is to be improved by intensification: in (4), how, at the cost of two intensifications, to impose *both upper and lower limits on  $\lambda_1$* ; in sections 31–32, how from two intensifications to draw helpful indications regarding the *three modes  $w_1, w_2, w_{-1}$* .

<sup>†</sup> The cofactor of  $A_2 w_2$  is  $-\eta$  in  $\Delta_I$ ,  $-\eta(1-\eta)$  in  $\Delta_{II}$ , where  $\eta \equiv 1 - \Lambda/\lambda_1$ ; and these quantities are nearly equal when  $\lambda_2 \doteq \lambda_1/x \equiv \Lambda$ .

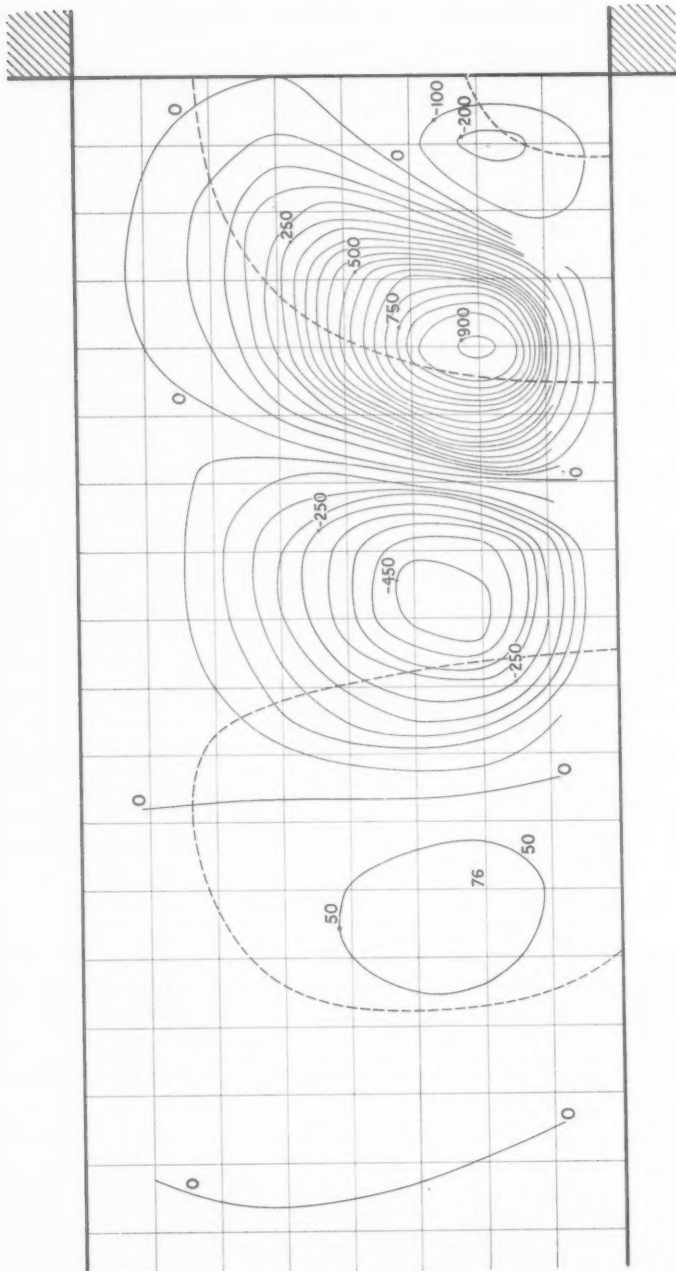


FIG. 9.

A w  
tive t  
'Rayl  
pron  
meth  
dently  
gener  
found  
'Holz  
but o  
treatm  
second  
appro  
refer  
certain  
the n

The  
positi  
with  
claim  
and :

**35**  
for a  
possi  
diagr  
need  
Miss  
of see

1. A
2. D
3. R
4. —
5. L

A word should be added concerning our reference to methods by descriptive titles instead of names. We are in no doubt about the attribution of 'Rayleigh's principle', but except in this instance we have hesitated to pronounce on questions of priority. It would seem that some of the methods we have described were devised by two or more authors independently—as a rule, for the solution of *particular* problems; and that their general applicability was recognized only later, by expositors. We have found attribution specially difficult in respect of the many methods—e.g., 'Holzer's'—which in effect satisfy the equation for normal modes at all but one point of the system considered. In our view the *purpose* of this treatment is material. It was proposed, for example, by Rayleigh in the second edition (1926) of his *Theory of Sound* (section 88) as a means of approximating to eigenvalues, and we think it unlikely (since he gave no reference) that he derived his notion from Holzer's book (13: 1921): certainly this did not influence Baird and Stedman (14), who proposed the method in 1914 (for struts).

This paper in effect employs the treatment, but with emphasis on the *position* of the loaded point, since its concern is rather with the mode than with the eigenvalue. We hesitate, in this matter as elsewhere, to make claim to any priority: all we would say is that sections 8–12, 14, 18–24, and 32, also (4), contain matter which *to the best of our belief* is new.

35. Grateful acknowledgement is due to the Clothworkers' Company, for a grant to Imperial College which made Miss Vaisey's collaboration possible; also to Miss M. Evenett, of that College, for assistance with the diagrams and in computations, requiring a desk machine, which have been needed since that collaboration ended (section 29). (Neither she nor Miss Vaisey, in the nature of the case, has responsibility for the conclusions of sections 29–33.)

## REFERENCES

1. A. PELLEW and R. V. SOUTHWELL (Part VI), *Proc. Roy. Soc. A*, **175** (1940), 262–90.
2. D. G. CHRISTOPHERSON, L. FOX, J. R. GREEN, F. S. SHAW, and R. V. SOUTHWELL, (Part VIIB), *Phil. Trans. R.S. C.*, **1** (1941), 57–83, and *A*, **239** (1945), 461–87.
3. R. V. SOUTHWELL, *An Introduction to the Theory of Elasticity* (Oxford, 1936).
4. —— 'Some extensions of Rayleigh's Principle', *Quart. J. Mech. and Applied Math.* **6** (1953), 257–72.
5. LORD RAYLEIGH, *Proc. London Math. Soc.* **4** (1873), 357–68, and *Scientific Papers*, vol. 1, no. 21. Much of the paper is reproduced in *Theory of Sound* (2nd ed. 1894, Macmillan), vol. 1, sections 88–92a: it is to this source that the present paper refers.

6. H. A. SCHWARZ, *Gesammelte Mathematische Abhandlungen* (1890), 241–65 (Berlin, Springer).
7. L. VIANELLO, *Zeitschr. Ver. deutsch. Ing.* **42** (1898), 1436–43.
8. A. STODOLA, *Steam Turbines* (2nd ed. 1905), 185–6 (London, Constable).
9. L. F. RICHARDSON, *Phil. Trans. R.S. A.*, **210** (1910), 307–57.
10. G. TEMPLE, *Proc. Roy. Soc. A*, **119** (1928), 276–93; *Proc. Lond. Math. Soc.* (2) **29** (1928), 257–80.
11. —— and W. G. BICKLEY, *Rayleigh's Principle and its Applications* (Oxford, 1933).
12. J. J. KOCH, *2nd Intern. Congress for App. Mechanics* (Zürich, 1926).
13. H. HOLZER, *Die Berechnung der Drehschwingungen* (Berlin, Springer, 1921).
14. L. BAIRSTOW and E. W. STEDMAN, *Engineering*, 2 Oct. 1914; reprinted in *Adv. Ctte. Aero Rep. and Mem.* **158** (1914).

in,

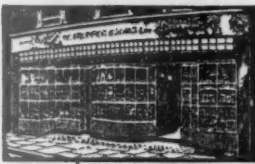
(2)

rd,

in



**HEFFER'S**



**BOOKS  
ON SCIENCE  
MATHEMATICS &  
THE HUMANITIES  
IN ALL LANGUAGES**

★

*Catalogues available free  
books & learned journals bought*

★

**W. HEFFER & Sons, Ltd.**  
Petty Cury • Cambridge

## ELECTRICAL BREAKDOWN OF GASES

By J. M. MEEK and J. D. CRAGGS (*International Series of Monographs on Physics*). Illustrated. 6os. net

The purpose of this book is to summarize present knowledge about the mechanisms of growth of electrical discharges in gases and the transitions between different forms of discharges.

While it has been written primarily for physicists and electrical engineers engaged on fundamental investigations of the nature of electrical breakdown in gases, it should be of value also to those concerned with the development and application of gas-filled electronic tubes, or with the many other technical problems associated with gaseous discharges.

OXFORD UNIVERSITY PRESS

# THE QUARTERLY JOURNAL OF MECHANICS AND APPLIED MATHEMATICS

VOLUME VI

PART 4

DECEMBER 1953

## CONTENTS

M. E. RAYNER: A Note on Uniqueness Proofs for Boundary-value Problems in Potential Theory and Steady Heat Conduction . . . . .	385
J. MORRIS and J. W. HEAD: Note on Lin's Iteration Process for the Extraction of Complex Roots of Algebraic Equations . . . . .	391
M. J. Lighthill: Theoretical Considerations on Free Convection in Tubes . . . . .	398
W. CHESTER: The Propagation of Shock Waves in a Channel of Non-uniform Width . . . . .	440
R. V. SOUTHWELL and G. VAISEY: On some Eigenvalue Problems of Exceptional Difficulty, exemplified by a case of Elastic Instability . . . . .	453

*The Editorial Board gratefully acknowledge the support given by: Boulton Paul Aircraft Ltd., Courtaulds Scientific and Educational Trust Fund; English Electric Co., Ltd.; Imperial Chemical Industries Ltd.; Institution of Mechanical Engineers; C. A. Parsons & Co., Ltd.; Unilever Ltd.*

---

*The publishers are signatories to the Fair Copying Declaration in respect of this journal. Details of the Declaration may be obtained from the offices of the Royal Society upon application.*

